Biological and molecular insights on MLA-based resistance of barley to powdery mildew derived from investigation of an in-frame Lys-Leu deletion in the essential protein SGT1

by

Antony Victor Ernest Chapman

A dissertation submitted to the graduate faculty

in partial fulfillment of the requirements for the degree of

DOCTOR OF PHILOSOPHY

Major: Genetics

Program of Study Committee:
Roger P. Wise, Co-major Professor
Steven A. Whitham, Co-major Professor
Justin Walley
Steve Rodermel
Mark Hargrove

The student author, whose presentation of the scholarship herein was approved by the program of study committee, is solely responsible for the content of this dissertation. The Graduate College will ensure this dissertation is globally accessible and will not permit alterations after a degree is conferred.

Iowa State University

Ames, Iowa

2021

DEDICATION

I would like to dedicate this dissertation to my family. I would not have made it this far without the love and support of my parents Victor and Carole, and my sister Suzy. You three supported my childhood dream of becoming a mad scientist throughout the years, allowing me to take this big step closer to making it a reality. Thank you for being patient and understanding. To my wife Rileigh, who has only just begun this crazy journey with me, I look forward to sharing the future with you. And finally, I dedicate this to my daughters Ruby and Fen who fill my heart with love and my future with hope.

TABLE OF CONTENTS

Page

LIST OF FIGURES

Page

LIST OF TABLES

Page

ACKNOWLEDGMENTS

I would like to express gratitude to my mentor Dr. Roger Wise for supporting me throughout my studies, you have taught me many lessons that I won't forget. I would also like to thank my committee members, Dr. Steve Whitham, Dr. Justin Walley, Dr. Steve Rodermel, and Dr. Mark Hargrove for their guidance and aid throughout. I give special thanks to Dr. Steve Whitham for taking me on as Facility Manager of the Enviratron when I was at risk of losing my funding, I would not have achieved as much as I did without your thoughtfulness.

To the undergraduate assistants who have been and gone during my time, Eunice Kong, Jessica Faust, Morgan Bixby, I thank for their assistance with experiments. I enjoyed mentoring you and I foresee great things from you all. To my fellow graduate students, Dalton Smedley, Maxwell McReynolds, Wesley Weirson, I thank you for the substantial conversations and drinks that helped to blow off steam. To my fellow lab members, Gregory Fuerst, Priyanka Surana, Valeria Valásquez-Zapata, Sagnik Banerjee, Weihui Xu, and Mitch Elmore, I couldn't have succeeded without you withstanding all my inane questions and quandaries. To the Iowa State Lacrosse Club, who put up with an old man with mediocre lacrosse skills for several years, I thank you for the comradery and friendships.

ABSTRACT

The molecular interactions between crops and pathogens are complex and require elucidation if we are to maintain food supplies against the ever-encroaching threat of disease. The resistance gene *Mla (Mildew resistance locus a*) and its orthologs protect barley (*Hordeum vulgare* L.) and other cereals from fungal diseases, such as barley powdery mildew caused by *Blumeria graminis* f. sp. *hordei* (*Bgh*). However, there are many missing links in our knowledge of how MLA functions. The HRS complex is necessary for MLA to function, consisting of the proteins HSP90 (Heat shock protein 90), RAR1 (Required for Mla12 Resistance 1), and SGT1 (Suppressor of G-two allele of Skp1).

To identify new mechanisms in MLA-mediated immunity, the Wise laboratory had performed fast-neutron mutagenesis of a resistant barley line to identify mutants compromised against *Bgh* infection and identified a susceptible line with a heritable recessive mutation. I then utilized this line to perform extensive genetic analysis and discovered that the mutation disrupted a subset of *Mla* alleles. I used exome-capture, bulk-segregant analysis, and fine-mapping to delineate the causal mutation to a two amino acid deletion in the SGS domain of SGT1, $Sgt1_{\Delta KL308\text{-}309}$, which does not display the lethality common to most *Sgt1* mutants.

I proceeded to characterize the $SGT1_{\Delta KL308\text{-}309}$ mutation to uncover specifics of MLA-SGT1 interactions. I generated a yeast strain with stably integrated *HvRar1* and *HvHsp90*, to show that $SGT1_{\Delta KL308\text{-}309}$ has weakened interactions with both MLA1 and MLA6 in a Y2H system. Additionally, I utilized parallel reaction monitoring mass-spectrometry to show that MLA6 peptide accumulation was significantly less in the $Sgt1_{\Delta KL308\text{-}309}$ mutant line. As the function of

Mla6 is disrupted by the $Sgt1_{\Delta KL308\text{-}309}$ mutation, whereas *Mla1* is not, the mutation appears to disproportionately affects MLA variants with inherently weaker interactions with SGT1.

To uncover specific molecular mechanisms behind their interactions, I used site-directed mutagenesis to generate specific MLA1, MLA6, and SGT1 mutant constructs and tested these in our Y2H system. I found that two specific sites in MLA1, when mutated to the MLA6 residues at the same position, abolished interaction between MLA1 and SGT1. Moreover, I show that the $Sgt1_{\Delta KL308\text{-}309}$ mutation has a less severe disruption than alanine or arginine substitutions at the same sites, which may indicate that the disorder of the SGS domain is paramount for its function. Combining my data with recent work in CC-NLRs, I propose a cyclical model of the MLA-HRS resistosome function and interaction.

CHAPTER 1. GENERAL INTRODUCTION

Overview

The control of crop diseases and pests is fundamental to modern agriculture and society. As we have spread monocultures across the land, we have unfortunately created fertile ground for which any opportunistic organism will seek to take hold. Just as crops have evolved through artificial selection, pathogens and pests have specialized to target those same crops. Currently, between 17% and 30% yield loss is estimated for the top five crops grown worldwide caused by diseases or pests (Savary *et al.*, 2019). Polycultures, which historically had given some promise for harboring a few select individuals immune to any disease, have disappeared. Therefore, it has become necessary to prioritize disease resistance traits in the breeding of elite varieties to protect their yield.

There are many kinds of organisms that cause plant diseases, each of which can require unique mechanisms of detection and resistance responses by the host. Pathogenic fungi are commonly differentiated by their lifestyles (Doehlemann *et al.*, 2017). Obligate biotrophs, such as *Cladosporium fulvum*, the cause of tomato leaf mold (Thomma *et al.*, 2005), and *Blumeria graminis*, which causes multiple cereal powdery mildews (Yamaoka *et al.*, 2006), must parasitically feed on a living cells, so they cannot be grown on media. Whereas non-obligate biotrophs, such as *Ustilago maydis,* the cause of corn smut (Brefort *et al.*, 2009), and *Piriformospora indica* (Lahrmann *et al.*, 2013), a root endophyte and potential symbiont, have both biotrophic and saprophytic life stages, allowing culture on media. In contrast, necrotrophs, such as *Botrytis cinerea*, the cause of gray mold on many dicots (Choquer *et al.*, 2007), and *Cochliobolus victoriae*, the cause of oat Victoria blight (Kessler *et al.*, 2020), must

feed on dead tissue. Interestingly, hemibiotrophs, such as *Magnaporthe oryzae*, the cause of rice blast (Ebbole, 2007), and the multitude of disease-causing *Colletotrichum* species (Gan *et al.*, 2013), initially parasitize biotrophically before switching to necrotrophic lifestyle and killing their host.

Blumeria graminis f. sp. *hordei* (*Bgh*) is a model obligate biotrophic fungus that causes powdery mildew on barley (*Hordeum vulgare* L.), leading to nearly 40% yield loss in cereals (Draz *et al.*, 2019). When a *Bgh* spore lands on a barley leaf, it first lays down a primary germ tube that adheres it to the waxy cuticle (Yamaoka *et al.*, 2006). The spore will then produce a secondary germ tube, which develops an appressorium. Instead of trying to enter the host through stomata, like some fungal pathogens do (Ye *et al.*, 2020), *Bgh* instead generates turgor pressure in the appressorium which allows the penetration peg to puncture through the waxy cuticle directly into the host epidermal cell. As the fungus penetrates it develops the haustorium, where it will secrete proteins into the host cell and uptake nutrients (Godfrey *et al.*, 2009). The haustorium is surrounded by an invaginated formation of the host plasma membrane, known as the extrahaustorial membrane, which is a key site of interactions between fungus and host (Kwaaitaal *et al.*, 2017). Whether the haustorium is able to fully mature is determined by whether the host cell is able to successfully detect the pathogen and initiate defense responses. If the pathogen is successful, it will feed off the host cell and form elongating secondary hyphae on the leaf surface, which will travel to neighboring epidermal cells and initiate secondary infections.

Extracellular Responses to pathogens

Each cell within a plant has the ability to defend itself against disease (Dodds and Rathjen, 2010). However, it is very detrimental for these defense responses to be permanently activated (van Wersch *et al.*, 2016, Genot *et al.*, 2017). Instead, plants rely on finely tuned equilibriums to maintain defense responses just below a threshold which reduces negative consequences to growth while allowing for rapid responses to pathogens (Sun *et al.*, 2020).

The numerous facets of plant immunity can be distinguished by whether they depend on extracellular or intracellular interactions. Pattern recognition receptor (PRR) -triggered immunity (PTI) is the general plant response to apoplastic microbe- or damage-associated molecular patterns (MAMPs or DAMPs respectively) (Couto and Zipfel, 2016). MAMPs consist of microbe-derived essential molecules that indicate the presence of potential pathogens, such as bacterial flagellin (Gómez-Gómez *et al.*, 2001), fungal chitin (Miya *et al.*, 2007), and oomycete β-glucans (Fliegmann *et al.*, 2004). DAMPS consist of plant-derived molecules indicative of harm caused biologically or mechanically to the plant, such as extracellular glutamate (Toyota *et al.*, 2018), ATP (Choi *et al.*, 2014), NAD (Wang *et al.*, 2017), and cell wall glycans (Bacete *et al.*, 2018). Both MAMPs and DAMPs are detected extracellularly by PRRs, which are trans-membrane proteins with extracellular sensing domains. Once a ligand is detected, PRRs will transduce a signal that causes a multitude of responses, including transcriptional changes, stomatal closure, Ca^{2+}-oscillations, reactive oxygen species production, and MAP kinase cascades (Choi *et al.*, 2016, Yamada *et al.*, 2016, Ye *et al.*, 2020, Zhou *et al.*, 2020). These responses, if left unperturbed, will generally lead to complete immunity to most potential plant pathogens.

Though PTI provides a powerful first line of defense, pathogens have evolved a variety of methods to avoid it. *C. fulvum* secretes multiple proteins that suppress PTI, such as Avr4, which shields chitin from plant chitinases, Ecp6, which sequester free chitin oligosaccharides, and Avr2, which inhibits host proteases (van den Burg *et al.*, 2006, van Esse *et al.*, 2008, de Jonge *et al.*, 2010). In similar fashion, some bacterial *Pseudomonas* strains secrete proteins, such as AprA, that degrades flagellin, and have modified their flagellin with glycans to avoid detection (Pel *et al.*, 2014, Buscaill *et al.*, 2019). Additionally, the root fungal pathogen *Verticillium dahlia* releases an apoplastic protein, VdPDA1, that protects chitin from being detected via deacetylation (Gao *et al.*, 2019).

Even non-pathogenic, symbiotic, or beneficial microbes have evolved methods to avoid PTI, sharing similar adaptations as many pathogens (Bolton *et al.*, 2008, Pel *et al.*, 2014). Symbiotic *Sinorhizobium* have adapted their flagellin to be unrecognizable by the PRR FLS2, though by amino acid sequence differences rather than the glycan modifications in *Pseudomonas* (Felix *et al.*, 1999, Buscaill *et al.*, 2019). The root endophyte *Piriformospora indica* suppresses host response with FGB1, which binds β-glucans to prevent their detection (Wawra *et al.*, 2016). Another group of endophytes, *Pestalotiopsis*, deacetylate their own chitin oligomers to chitosan, which is not recognized by CERK1, similar to *V. dahlia* (Cord-Landwehr *et al.*, 2016, Gao *et al.*, 2019).

Intracellular responses to pathogens

Once a pathogen invades a host cell, it secretes effector proteins that aim to shut down PTI and facilitate nutrient absorption (Jaswal *et al.*, 2020). However, the intracellular resistance proteins of plants are able to detect these effectors either directly or indirectly through their

actions. A majority of resistance proteins fall into the category of Nod-like resistance, aka nucleotide-binding, leucine-rich repeat proteins (NLRs) (van Wersch *et al.*, 2020). Most NLRs have been found to respond to a single ligand in a gene-for-gene relationship. Once its ligand is detected, NLRs will initiate the hypersensitive response, which shares similarity with PTI but is more severe and usually terminates in the death of the host cell (Sun *et al.*, 2020).

NLR canonical structure consists of an N-terminal signaling domain, a central nucleotide binding (NB), and a C-terminal leucine-rich repeat domain (LRR) (Jones *et al.*, 2016). NLRs are grouped overall by their N-terminal signaling domain, possessing either a coiled coil (CC) or Toll/interleukin 1 receptor (TIR) domains, into CNLs or TNLs respectively (van Wersch *et al.*, 2020). The first crystal structure obtained of an NLR domain was for the CC domain of MLA10 (Maekawa *et al.*, 2011), followed by the CC domains of potato (*Solanum tuberosum)* Rx1 and wheat (*Triticum aestivum* L.) Sr33 (Hao *et al.*, 2013, Casey *et al.*, 2016). These domains were found to be required for homo-oligomerization and self-associated autoinhibition, except for Rx1 which instead forms a complex with RanGAP2 (Tameling and Baulcombe, 2007). Furthermore, CC domains appear to be dimeric signaling components, causing autoactivation when expressed alone, and are inactivated when dimerization is prevented (Collier *et al.*, 2011, Wang *et al.*, 2015b).

The NB domain has been categorized as the molecular switch of NLRs. The NB domain binds ATP, ADP, or in some cases neither, and is able to hydrolyze ATP to ADP (Wang *et al.*, 2019b). While bound to ADP, NLRs exist in the inactive autoinhibited state caused by the NB domain interacting with and inhibiting both the CC and LRR domains (Wang *et al.*, 2015b). When ADP is swapped for ATP, the interactions between the NB and other domains are

disrupted, allowing them to interact and signal (Kourelis and van der Hoorn, 2018). The cause behind activation appears to vary between systems. In some cases the ATP/ADP pocket is deeply buried, such as ZAR1 in Arabidopsis, which requires interaction of a cognate effector with the LRR domain to cause a conformational shift, allowing ADP to be released and ATP to enter (Wang *et al.*, 2019a). In contrast, the flax L protein appears to naturally cycle between the active and inactive states in an equilibrium. This maintains a very small amount of ATP-bound L, which can then interact with the effector AvrL567 (Bernoux *et al.*, 2016). Therefore, the difference in mechanisms may be determined by many factors, including the overall structure, how buried the ATP/ADP pocket is, and whether it can interact with the effector prior to activation.

The NB domain has two additional subdomains, ARC1 (Apaf-1, Resistance proteins, CED4) and ARC2, in addition to several defined structures and motifs (van Ooijen *et al.*, 2008). The ARC2 subdomain has been observed to rotate to form an open conformation in the active ATP-bound state in mammalian Apaf-1 (Zhou *et al.*, 2015). In the NB domain, the P-loop (Walker A) motif is necessary for the binding of the β or γ phosphates of ATP or ADP, mutations of which cause loss-of-function (Bai *et al.*, 2012, Wendler *et al.*, 2012). In contrast, the kinase2 (Walker B) motif is required for the ATPase activity and causes autoactivity when mutated (Tameling *et al.*, 2002). Similarly, the MHD motif in the ARC2 subdomain is the sensor which detects whether ATP or ADP is bound, mutations of which cause autoactivity (Tameling *et al.*, 2006).

The LRR domain of NLRs are defined by their leucine-rich motifs (LxxLxLxxNxL), though other hydrophobic amino acids can replace leucine, such as valine or isoleucine (Padmanabhan

et al., 2009). The number of times this motif repeats in the LRR varies up to 25 repeats and forms a super-helix arc-like structure (Santiago *et al.*, 2016). The leucine-rich motifs form parallel β-sheets on the concave side of a super-helix, whereas the variables sites on the convex side of the arc can take a variety of structures (Matsushima and Miyashita, 2012, Sukarta *et al.*, 2016).

The LRR domain of NLRs perform dual functions of autoinhibition and ligand-specificity (Slootweg *et al.*, 2013). In the inactive ADP-bound state, the LRR domains interact with the NB domain to prevent autoactivation in the absence of the ligand (Hu *et al.*, 2013, Qi *et al.*, 2018). The LRR domains appear to be under positive selection pressure, concentrated in the LRR motifs, likely due to the need to recognize unrelated effectors under strong selective pressure themselves (Zhang *et al.*, 2006, Ruggieri *et al.*, 2014, Fischer *et al.*, 2016, Liu *et al.*, 2017). Direct interactions between LRR domains and their ligands has been observed in many different systems (Tang *et al.*, 2002, Bernoux *et al.*, 2016, Li *et al.*, 2017, Lin *et al.*, 2017, Saur *et al.*, 2019). In multiple LRR-containing proteins, the LRR domain appears to be flanked by capping domains which are suggested to maintain structural integrity (She *et al.*, 2011, Matsushima and Miyashita, 2012, Chakraborty *et al.*, 2018, Zhang *et al.*, 2018). Capping domains contain LRR repeats and cysteines that are predicted to form disulfide bonds, anti-parallel to the rest of the LRR domain. These capped areas protect the hydrophobic regions from solvent exposure.

The methods by which NLRs detect pathogen effectors are plentiful and do not appear to segregate between pathogen families. Perhaps the simplest method is where an effector directly interacts with the NLR, usually through the LRR or another C-terminal domain, which then transmits the signal itself. A recent example of a direct interaction is between several

alleles of a barley CNL, Mildew Resistance Locus A (MLA7, MLA9, MLA10, and MLA22), and unrelated effectors from *Bgh* (AVR_{A7} AVR_{A9}, AVR_{A10}, and AVR_{A22}) (Saur *et al.*, 2019). Moreover, *Mla*-orthologous wheat NLRs Sr35 and Sr50 directly detect the wheat stem rust (*Puccinia graminis* f. sp. *tritici*) effectors AvrSr35 and AvrSr50, respectively (Chen *et al.*, 2017, Salcedo *et al.*, 2017). Outside of fungal pathogens, the *Nicotiana tabacum* TNL N recognizes the tobacco mosaic virus p50 helicase domain and the potato CNL Rx recognizes the Potato Virus X (PVX) coat protein (Rairdan and Moffett, 2006, Burch-Smith *et al.*, 2007). Moreover, the *Nicotiana benthamiana* TNL Roq1 directly interacts with both XopQ and HopQ1 from *Xanthomonas* and *Pseudomonas* pathogenic bacteria respectively (Qi *et al.*, 2018).

An alternate, and arguably more elegant method of effector detection, is the "guard" model (Dangl and Jones, 2001). Instead of directly interacting with an effector, the NLR confers resistance by interacting with the target of the effector, the guardee, and detecting the action of the effector upon it. A major example is the RPS5-PBS1-AvrPphB system. AvrPphB is a *Pseudomonas* cysteine protease that targets and cleaves multiple receptor-like kinases involved in PTI, such as BIK1, PBL1, PBL2, and PBL27 (Zhang *et al.*, 2010). However, it also cleaves PBS1, which, unlike other members of its family, does not appear to have a direct involvement in disease resistance. Rather, PBS1 appears to be a decoy, guarded by RPS5, that is targeted unintentionally by AvrPphB due to sharing a cleavage site with the other targets. RPS5 doesn't directly interact with AvrPphB, as expression of both halves of PBS1 is sufficient to initiate defense responses in the absence of AvrPphB (DeYoung *et al.*, 2012). Interestingly, it was recently found that barley PBR1 (AvrPphB Response 1), which is unrelated to Arabidopsis RPS5, also appears to recognize the cleavage of PBS1 by AvrPphB (Carter *et al.*, 2019). Moreover, in

soybean, there is indication of another R protein that responds to the cleavage of PBS1 by AvrPphB (Helm *et al.*, 2019). This indicates that selection pressure has caused convergent evolution of multiple R proteins to detect cleavage of the same effector target.

The structure and function of the HRS Complex in Immunity

Many NLRs require the HRS core co-chaperone complex to function, which is formed from a symmetric conformation of two HSP90 (Heat shock protein 90), one RAR1 (Required for *Mla12* resistance 1), and two SGT1 (Suppressor of G-two allele of *Skp1*) (Shirasu, 2009, Siligardi *et al.*, 2018). This complex functions to control NLR protein abundance and facilitate signaling (Azevedo *et al.*, 2002, Mestre and Baulcombe, 2006, Kud *et al.*, 2013). In addition, this complex is involved in a multitude of essential cell processes, such as growth, development, and hormone signaling (Kitagawa *et al.*, 1999, Gray *et al.*, 2003, Hoser *et al.*, 2013).

HSP90 functions as a dimer and has three essential domains, the N-terminal (ND), middle (MD) and C-terminal (CD) domains. HSP90 is involved in the formation of many complexes in addition to the HRS complex, including several viral-derived protein complexes (Siligardi *et al.*, 2018). HSP90 cycles between a closed ATP-bound conformation and an open ADP-bound conformation (Ali *et al.*, 2006). This cycling allows HSP90 to interact with co-chaperones in the closed conformation and then eject co-chaperones by returning to its open conformation. SGT1, which interacts with HSP90 through its ND, is expected to be greatly affected by this cycling (Kadota *et al.*, 2008). The closed ATP-bound conformation dimerizes the HSP90 ND domains and forms an ATPase enzymatic structure in conjunction with the MD. The binding of co-chaperones to HSP90 appears to inhibit the ATPase activity, increasing the longevity of HSP90 complexes (Kadota and Shirasu, 2012). HSP90 is required for most NLRs to

function (Takahashi *et al.*, 2003, Bhattarai *et al.*, 2007). However, there appear to be some exceptions to the requirement of HSP90 to function, such as *Rpi-blb2*-mediated resistance to late blight when transiently expressed in *N. benthamiana* (Oh *et al.*, 2014).

RAR1 is comprised of two zinc-binding CHORD (Cysteine and histidine rich) domains bridged by the cysteine and histidine containing motif, CCCH (Siligardi *et al.*, 2018). Each CHORD domain is found to be able to interact with HSP90 and SGT1. Loss of RAR1 reduces the accumulation of NLR proteins, though the explicit requirement of RAR1 for function appears to vary (Tornero *et al.*, 2002, Takahashi *et al.*, 2003, Bieri *et al.*, 2004, Bhaskar *et al.*, 2008, Oh *et al.*, 2014). RAR1 does not interact directly with NLRs. However, RAR1 has been found to augment the interaction between HSP90 and SGT1, suggesting its mode of action is in complex structural support (Boter *et al.*, 2007). Moreover, the requirement for RAR1 by MLA alleles was found to be determined by a single position, MLA_{721}, in the LRR domain, the domain that directly interacts with the SGS domain of SGT1 (Halterman and Wise, 2004, Kadota *et al.*, 2010). This may suggest that RAR1 promotes a more optimal HSP90-SGT1-NLR conformation, and that a stronger interaction between the NLR LRR and SGT1 SGS domains alleviates the requirement for RAR1.

SGT1 is comprised of three distinct separate domains attached together by variable linker regions, the tetratricopeptide repeat (TPR), CHORD and SGT1 (CS), and SGT1-specific (SGS) domains (Zhang *et al.*, 2008). The separated domains have caused compartmentalization of the function of SGT1. The TPR domain does not appear to be directly involved in assisting disease resistance signals (Boter *et al.*, 2007, da Silva Correia *et al.*, 2007). However, its involvement with the SCF (Skp1, Cullin, F-box) complex suggests that it is involved in

ubiquitination-mediated degradation of NLRs to reduce autoactivation (Willhoft *et al.*, 2017). The CS domain interacts with both HSP90 and RAR1, likely only playing a role in formation of the complex (Boter *et al.*, 2007). The function of the SGS domain appears to be to interact with NLR LRR domains directly (Kadota *et al.*, 2010).

Sgt1 is present and relatively well conserved in all Eukaryotes, to the extent that human *Sgt1* can complement a yeast *Sgt1* null mutant (Kitagawa *et al.*, 1999). Diploid organisms tend to have only a single copy of *Sgt1*. However, Arabidopsis and soybean both have two copies which have functionally diverged from one another so that they are only 76% and 66% identical, respectively (Austin *et al.*, 2002, Fu *et al.*, 2009). *Sgt1* has been found to be vital for eukaryotic cell function (Azevedo *et al.*, 2006, Bansal *et al.*, 2009, Martins *et al.*, 2009). The only exception is yeast, which can survive with an *Sgt1* knock-out, though it is very detrimental (Kitagawa *et al.*, 1999). Moreover, when *Sgt1* is silenced in plants it causes severe stunting or even lethality (Peart *et al.*, 2002, Bhattarai *et al.*, 2007, Thao *et al.*, 2007, Wang *et al.*, 2015b).

Oligomerization of NLR proteins

Many NLRs form monomeric or multimeric complexes after activation by cognate ligands, and these are found to be critical for their function (Danot *et al.*, 2009). Some NLRs tend to form oligomeric structures termed “resistosomes” following ligand detection (Yang *et al.*, 2018, van Wersch *et al.*, 2020). It is the NB domains that appear to drive this oligomerization in this case. These complexes can also be made up of multiple different proteins, such as the NAIP-NLRC4 complex whereby ligand perception by a single NAIP2 (NLR family apoptosis inhibitory proteins 2) caused it to oligomerize with ten NLRC4 (NLR family caspase recruitment domain (CARD)–containing protein 4), forming a barrel structure (Zhang *et*

al., 2015a). Another NLR that oligomerizes to form a barrel-like structure is the CNL ZAR1. Recently, the crystal structure of full-length ZAR1 was identified. Upon uridylylation of its guardee PBL2, ZAR1 pentamerizes to form a ring-like structure (Wang *et al.*, 2019a). In addition, the CNL RPP7 also form a monomeric pentameric structure required for signaling (Li *et al.*, 2019). These barrel-like structures have been theorized to function as pores, perhaps allowing the movement of defense signals such as Ca^{2+} (van Wersch *et al.*, 2020, Zhou and Zhang, 2020).

Both CNLs and TNLs have been found to dimerize by way of their N-terminal domains, such as MLA (Maekawa *et al.*, 2011, Huber *et al.*, 2015, Casey *et al.*, 2016, Zhang *et al.*, 2017). In addition, NLRs have been found that function in heteromeric pairs, such as the pair RGA4/RGA5 in rice against *M. oryzae*, and RPS4/RRS1 in Arabidopsis against *Colletotrichum higginsianum* (Birker *et al.*, 2009, Cesari *et al.*, 2013). So far, this appears to represent a key difference between many NLRs, they either oligomerize into groups of four of more and don't require the HRS, or they function in homo-dimeric or hetero-dimeric pairs and do require the HRS. Therefore, as the HRS complex is predicted to be able to dock two NLRs simultaneously (Siligardi *et al.*, 2018), it is possible that the HRS confers the dimeric constraint on NLRs that it assists in signaling.

Cellular Localization is Important for Resistance Signaling Proteins

NLRs appear to be spread across many subcellular compartments, sometimes simultaneously. Moreover, while some translocate upon activation, such as Rx1 and R3a, others, such as RPM1, do not (Slootweg *et al.*, 2010, Gao *et al.*, 2011, Engelhardt *et al.*, 2012).

The presence of NLRs in the nucleus is observed and expected as some NLRs have nuclear localizing signals, such as I-2 and N (Hoser *et al.*, 2013, Ma *et al.*, 2013). However, others such as MLA, which maintains a small nuclear abundance, do not have clear nuclear localization signals. Not only is MLA10 able to translocate to the nucleus, its ability to confer resistance is dependent on the translocation, not merely on the presence of MLA10 within the nucleus (Shen *et al.*, 2007, Bai *et al.*, 2012). It could be extrapolated that the presence or absence of a nuclear localizing signal would indicate where the NLR is expected to encounter its cognate effector. However, I-2 requires nuclear localization of Avr2 to initiate defense response, but Avr2 does not require nuclear localization to repress host defense responses (Di *et al.*, 2017). Therefore, the associations between localization and function are not entirely clear.

Similarly, the HRS exists primarily in the cytoplasm with a small contingent in the nucleus (Hoser *et al.*, 2013, Niikura and Kitagawa, 2019). As these results are snapshots of the activity of the cell, it is possible that an equilibrium is managed whereby the HRS complex translocates back and forth between the cytoplasm and the nucleus, favoring nucleus export. The transport of both the HRS and NLRs appears to be dependent on the interaction between SGT1 and NLRs, suggesting that the HRS shuttles its interactors alongside it (Hoser *et al.*, 2014, Liu *et al.*, 2016). Interestingly, phosphorylation of a MAPK-targeted site in the SGS domain appears to be necessary for SGT1 translocation to the nucleus (Noël *et al.*, 2007, Hoser *et al.*, 2013). *Sgt1* has been shown to be significantly induced during infection or during other stresses, though actual protein levels do not change (Azevedo *et al.*, 2006, Noël *et al.*, 2007). This could suggest a feedback mechanism whereby an increase in *Sgt1* expression compensates for the loss of SGT1 that translocates to the nucleus. In contrast, RAR1 expression does not

increase past the very low native levels, perhaps reflecting the lack of involvement of RAR1 with processes not involved in disease resistance. That is, if the cell will not survive the hypersensitive reaction initiated when RAR1 is translocated, then there is no need to replace it.

Targeting of HRS by pathogens

The importance of the HRS complex is exemplified by the recent discoveries of multiple effectors that target it to disrupt disease resistance. The *U. maydis* effector See1 targets and specifically interacts with the SGT1 SGS domain to block phosphorylation and thus translocation, though this may be secondary to blocking other interactions (Redkar *et al.*, 2015). Moreover, *Xanthomonas campestris* AvrBsT interacts with the pepper (*Capsicum annuum)* SGT1 CS domain to prevent phosphorylation of two serines in the TPR and VR2 domains by PIK1, likely with similar results to See1 (Kim *et al.*, 2014). In contrast, the *Salmonella enterica* effector SspH2 interacts with the SGT1 CS and SGS domains to enhance NLR-mediated cell death, facilitating necrosis and the bacteria's growth (Bhavsar *et al.*, 2013). The broadly conserved bacterial HopBF1 effectors instead target and phosphorylate HSP90, disabling its ability to assist NLR-mediated defense (Lopez *et al.*, 2019). Other pathogens that appear to target SGT1, HSP90, or RAR1, specifically to promote virulence include *B. cinerea*, *F. culmorum*, and *P. syringae* (El Oirdi and Bouarab, 2007, Hann and Rathjen, 2007, Cuzick *et al.*, 2009). Additionally, other pathogens may also target the HRS to promote their pathogenicity, such as PVX, *Ralstonia solanacearum*, *Xanthomonas oryzae*, and *Magnaporthe oryzae* (Wang *et al.*, 2008, Ito *et al.*, 2015).

Concluding remarks

This dissertation has two main sections. In chapter 2, we aimed to identify new factors in *Mla*-based disease resistance in barley by screening a fast-neutron-derived mutagenesis population for induced susceptibility to *Bgh*. We identified a small deletion within *Sgt1*, $Sgt1_{\Delta KL308\text{-}309}$, which selectively disrupted disease resistance, without the lethality or stunting common to *Sgt1* mutations. In chapter 3, we aimed to elucidate how and why the $Sgt1_{\Delta KL308\text{-}309}$ mutation causes a susceptibility phenotype. Utilizing molecular and proteomic techniques, we discover that the $Sgt1_{\Delta KL308\text{-}309}$ mutation appears to weaken intermolecular interactions between SGT1 and MLA, causing a reduction in MLA abundance below a threshold required for effective resistance. This work paves the way for investigating the true requirement of SGT1 by NLRs by allowing the generation of defense-deficient non-lethal *Sgt1* mutant lines by mimicking the $Sgt1_{\Delta KL308\text{-}309}$ in other species.

References

Ali, M.M.U., Roe, S.M., Vaughan, C.K., Meyer, P., Panaretou, B., Piper, P.W., Prodromou, C. and Pearl, L.H. (2006) Crystal structure of an Hsp90–nucleotide–p23/Sba1 closed chaperone complex. *Nature*, 440, 1013-1017.

Austin, M.J., Muskett, P., Kahn, K., Feys, B.J., Jones, J.D.G. and Parker, J.E. (2002) Regulatory role of SGT1 in early R gene-mediated plant defenses. *Science*, 295, 2077-2080.

Azevedo, C., Betsuyaku, S., Peart, J., Takahashi, A., Noël, L., Sadanandom, A., Casais, C., Parker, J. and Shirasu, K. (2006) Role of SGT1 in resistance protein accumulation in plant immunity. *The EMBO Journal*, 25, 2007-2016.

Azevedo, C., Sadanandom, A., Kitagawa, K., Freialdenhoven, A., Shirasu, K. and Schulze-Lefert, P. (2002) The RAR1 interactor SGT1, an essential component of R gene-triggered disease resistance. *Science*, 295, 2073-2076.

Bacete, L., Mélida, H., Miedes, E. and Molina, A. (2018) Plant cell wall-mediated immunity: cell wall changes trigger disease resistance responses. *The Plant Journal*, 93, 614-636.

Bai, S., Liu, J., Chang, C., Zhang, L., Maekawa, T., Wang, Q., Xiao, W., Liu, Y., Chai, J., Takken, F.L., Schulze-Lefert, P. and Shen, Q.H. (2012) Structure-function analysis of barley NLR immune receptor MLA10 reveals its cell compartment specific activity in cell death and disease resistance. *PLoS Pathogens*, 8, e1002752.

Bansal, P.K., Mishra, A., High, A.A., Abdulle, R. and Kitagawa, K. (2009) Sgt1 dimerization is negatively regulated by protein kinase CK2-mediated phosphorylation at Ser^{361}. *Journal of Biological Chemistry*, 284, 18692-18698.

Bernoux, M., Burdett, H., Williams, S.J., Zhang, X., Chen, C., Newell, K., Lawrence, G.J., Kobe, B., Ellis, J.G., Anderson, P.A. and Dodds, P.N. (2016) Comparative analysis of the flax immune receptors L6 and L7 suggests an equilibrium-based switch activation model. *The Plant cell*, 28, 146-159.

Bhaskar, P.B., Raasch, J.A., Kramer, L.C., Neumann, P., Wielgus, S.M., Austin-Phillips, S. and Jiang, J. (2008) *Sgt1*, but not *Rar1*, is essential for the *RB*-mediated broad-spectrum resistance to potato late blight. *BMC Plant Biology*, 8, 8.

Bhattarai, K.K., Li, Q., Liu, Y., Dinesh-Kumar, S.P. and Kaloshian, I. (2007) *Mi-1*-mediated pest resistance requires *Hsp90* and *Sgt1*. *Plant Physiology*, 144, 312-323.

Bhavsar, A.P., Brown, N.F., Stoepel, J., Wiermer, M., Martin, D.D.O., Hsu, K.J., Imami, K., Ross, C.J., Hayden, M.R., Foster, L.J., Li, X., Hieter, P. and Finlay, B.B. (2013) The *Salmonella* type III effector SspH2 specifically exploits the NLR co-chaperone activity of SGT1 to subvert immunity. *PLOS Pathogens*, 9, e1003518.

Bieri, S., Mauch, S., Shen, Q.-H., Peart, J., Devoto, A., Casais, C., Ceron, F., Schulze, S., Steinbiss, H.-H., Shirasu, K. and Schulze-Lefert, P. (2004) RAR1 positively controls steady state levels of barley MLA resistance proteins and enables sufficient MLA6 accumulation for effective resistance. *The Plant Cell*, 16, 3480-3495.

Birker, D., Heidrich, K., Takahara, H., Narusaka, M., Deslandes, L., Narusaka, Y., Reymond, M., Parker, J.E. and O'Connell, R. (2009) A locus conferring resistance to *Colletotrichum higginsianum* is shared by four geographically distinct Arabidopsis accessions. *The Plant Journal*, 60, 602-613.

Bolton, M.D., Van Esse, H.P., Vossen, J.H., De Jonge, R., Stergiopoulos, I., Stulemeijer, I.J.E., Van Den Berg, G.C.M., Borrás-Hidalgo, O., Dekker, H.L., De Koster, C.G., De Wit, P.J.G.M., Joosten, M.H.A.J. and Thomma, B.P.H.J. (2008) The novel *Cladosporium fulvum* lysin motif effector Ecp6 is a virulence factor with orthologues in other fungal species. *Molecular Microbiology*, 69, 119-136.

Boter, M., Amigues, B., Peart, J., Breuer, C., Kadota, Y., Casais, C., Moore, G., Kleanthous, C., Ochsenbein, F., Shirasu, K. and Guerois, R. (2007) Structural and functional analysis of SGT1 reveals that its interaction with HSP90 is required for the accumulation of Rx, an R protein involved in plant immunity. *The Plant Cell*, 19, 3791-3804.

Brefort, T., Doehlemann, G., Mendoza-Mendoza, A., Reissmann, S., Djamei, A. and Kahmann, R. (2009) *Ustilago maydis* as a pathogen. *Annu Rev Phytopathol*, 47, 423-445.

Burch-Smith, T.M., Schiff, M., Caplan, J.L., Tsao, J., Czymmek, K. and Dinesh-Kumar, S.P. (2007) A novel role for the TIR domain in association with pathogen-derived elicitors. *PLoS Biol*, 5, e68.

Buscaill, P., Chandrasekar, B., Sanguankiattichai, N., Kourelis, J., Kaschani, F., Thomas, E.L., Morimoto, K., Kaiser, M., Preston, G.M., Ichinose, Y. and van der Hoorn, R.A.L. (2019) Glycosidase and glycan polymorphism control hydrolytic release of immunogenic flagellin peptides. *Science*, 364, eaav0748.

Carter, M.E., Helm, M., Chapman, A.V.E., Wan, E., Restrepo Sierra, A.M., Innes, R.W., Bogdanove, A.J. and Wise, R.P. (2019) Convergent evolution of effector protease recognition by Arabidopsis and barley. *Molecular Plant-Microbe Interactions*, 32, 550-565.

Casey, L.W., Lavrencic, P., Bentham, A.R., Cesari, S., Ericsson, D.J., Croll, T., Turk, D., Anderson, P.A., Mark, A.E., Dodds, P.N., Mobli, M., Kobe, B. and Williams, S.J. (2016) The CC domain structure from the wheat stem rust resistance protein Sr33 challenges paradigms for dimerization in plant NLR proteins. *Proceedings of the National Academy of Sciences*, 113, 12856-12861.

Cesari, S., Thilliez, G., Ribot, C., Chalvon, V., Michel, C., Jauneau, A., Rivas, S., Alaux, L., Kanzaki, H., Okuyama, Y., Morel, J.-B., Fournier, E., Tharreau, D., Terauchi, R. and Kroj, T. (2013) The rice resistance protein pair RGA4/RGA5 recognizes the *Magnaporthe oryzae* effectors AVR-Pia and AVR1-CO39 by direct binding. *The Plant Cell*, 25, 1463-1481.

Chakraborty, S., Pan, H., Tang, Q., Woolard, C. and Xu, G. (2018) The extracellular domain of Pollen Receptor Kinase 3 is structurally similar to the SERK family of co-receptors. *Scientific Reports*, 8, 2796.

Chen, J., Upadhyaya, N.M., Ortiz, D., Sperschneider, J., Li, F., Bouton, C., Breen, S., Dong, C., Xu, B., Zhang, X., Mago, R., Newell, K., Xia, X., Bernoux, M., Taylor, J.M., Steffenson, B., Jin, Y., Zhang, P., Kanyuka, K., Figueroa, M., Ellis, J.G., Park, R.F. and Dodds, P.N. (2017) Loss of *AvrSr50* by somatic exchange in stem rust leads to virulence for *Sr50* resistance in wheat. *Science*, 358, 1607-1610.

Choi, J., Tanaka, K., Cao, Y., Qi, Y., Qiu, J., Liang, Y., Lee, S.Y. and Stacey, G. (2014) Identification of a plant receptor for extracellular ATP. *Science*, 343, 290-294.

Choi, W.-G., Hilleary, R., Swanson, S.J., Kim, S.-H. and Gilroy, S. (2016) Rapid, long-distance electrical and calcium signaling in plants. *Annual Review of Plant Biology*, 67, 287-307.

Choquer, M., Fournier, E., Kunz, C., Levis, C., Pradier, J.M., Simon, A. and Viaud, M. (2007) *Botrytis cinerea* virulence factors: new insights into a necrotrophic and polyphageous pathogen. *FEMS Microbiol Lett*, 277, 1-10.

Collier, S.M., Hamel, L.P. and Moffett, P. (2011) Cell death mediated by the N-terminal domains of a unique and highly conserved class of NB-LRR protein. *Molecular Plant-Microbe Interactions*, 24, 918-931.

Cord-Landwehr, S., Melcher, R.L.J., Kolkenbrock, S. and Moerschbacher, B.M. (2016) A chitin deacetylase from the endophytic fungus *Pestalotiopsis* sp. efficiently inactivates the elicitor activity of chitin oligomers in rice cells. *Scientific Reports*, 6, 38018.

Couto, D. and Zipfel, C. (2016) Regulation of pattern recognition receptor signalling in plants. *Nature Reviews Immunology*, 16, 537-552.

Cuzick, A., Maguire, K. and Hammond-Kosack, K.E. (2009) Lack of the plant signalling component SGT1b enhances disease resistance to *Fusarium culmorum* in Arabidopsis buds and flowers. *New Phytologist*, 181, 901-912.

da Silva Correia, J., Miranda, Y., Leonard, N. and Ulevitch, R. (2007) SGT1 is essential for Nod1 activation. *PNAS*, 104, 6764-6769.

Dangl, J.L. and Jones, J.D.G. (2001) Plant pathogens and integrated defence responses to infection. *Nature*, 411, 826-833.

Danot, O., Marquenet, E., Vidal-Ingigliardi, D. and Richet, E. (2009) Wheel of life, wheel of death: a mechanistic insight into signaling by STAND proteins. *Structure*, 17, 172-182.

de Jonge, R., Peter van Esse, H., Kombrink, A., Shinya, T., Desaki, Y., Bours, R., van der Krol, S., Shibuya, N., Joosten, M.H.A.J. and Thomma, B.P.H.J. (2010) Conserved fungal LysM effector Ecp6 prevents chitin-triggered immunity in plants. *Science*, 329, 953-955.

DeYoung, B.J., Qi, D., Kim, S.-H., Burke, T.P. and Innes, R.W. (2012) Activation of a plant nucleotide binding-leucine rich repeat disease resistance protein by a modified self protein. *Cellular Microbiology*, 14, 1071-1084.

Di, X., Cao, L., Hughes, R.K., Tintor, N., Banfield, M.J. and Takken, F.L.W. (2017) Structure–function analysis of the *Fusarium oxysporum* Avr2 effector allows uncoupling of its immune-suppressing activity from recognition. *New Phytologist*, 216, 897-914.

Dodds, P.N. and Rathjen, J.P. (2010) Plant immunity: towards an integrated view of plant-pathogen interactions. *Nature Reviews Genetics*, 11, 539-548.

Doehlemann, G., Ökmen, B., Zhu, W. and Sharon, A. (2017) Plant pathogenic fungi. *Microbiology Spectrum*, 5.

Draz, I.S., Esmail, S.M., Abou-Zeid, M.A.E.-H. and Essa, T.A.E.-M. (2019) Powdery mildew susceptibility of spring wheat cultivars as a major constraint on grain yield. *Annals of Agricultural Sciences*, 64, 39-45.

Ebbole, D.J. (2007) *Magnaporthe* as a model for understanding host-pathogen interactions. *Annual Review of Phytopathology*, 45, 437-456.

El Oirdi, M. and Bouarab, K. (2007) Plant signalling components EDS1 and SGT1 enhance disease caused by the necrotrophic pathogen *Botrytis cinerea*. *New Phytologist*, 175, 131-139.

Engelhardt, S., Boevink, P.C., Armstrong, M.R., Ramos, M.B., Hein, I. and Birch, P.R.J. (2012) Relocalization of late blight resistance protein R3a to endosomal compartments is associated with effector recognition and required for the immune response. *The Plant Cell*, 24, 5142-5158.

Felix, G., Duran, J.D., Volko, S. and Boller, T. (1999) Plants have a sensitive perception system for the most conserved domain of bacterial flagellin. *The Plant Journal*, 18, 265-276.

Fischer, I., Diévart, A., Droc, G., Dufayard, J.-F. and Chantret, N. (2016) Evolutionary dynamics of the leucine-rich repeat receptor-like kinase (LRR-RLK) subfamily in Angiosperms. *Plant Physiology*, 170, 1595-1610.

Fliegmann, J., Mithofer, A., Wanner, G. and Ebel, J. (2004) An ancient enzyme domain hidden in the putative beta-glucan elicitor receptor of soybean may play an active part in the perception of pathogen-associated molecular patterns during broad host resistance. *J Biol Chem*, 279, 1132-1140.

Fu, D.-Q., Ghabrial, S. and Kachroo, A. (2009) GmRAR1 and GmSGT1 are required for basal, R gene-mediated and systemic acquired resistance in soybean. *MPMI*, 22, 86-95.

Gan, P., Ikeda, K., Irieda, H., Narusaka, M., O'Connell, R.J., Narusaka, Y., Takano, Y., Kubo, Y. and Shirasu, K. (2013) Comparative genomic and transcriptomic analyses reveal the hemibiotrophic stage shift of *Colletotrichum* fungi. *New Phytologist*, 197, 1236-1249.

Gao, F., Zhang, B.S., Zhao, J.H., Huang, J.F., Jia, P.S., Wang, S., Zhang, J., Zhou, J.M. and Guo, H.S. (2019) Deacetylation of chitin oligomers increases virulence in soil-borne fungal pathogens. *Nat Plants*, 5, 1167-1176.

Gao, Z., Chung, E.-H., Eitas, T.K. and Dangl, J.L. (2011) Plant intracellular innate immune receptor Resistance to *Pseudomonas syringae pv. maculicola 1* (RPM1) is activated at, and functions on, the plasma membrane. *Proceedings of the National Academy of Sciences*, 108, 7619-7624.

Genot, B., Lang, J., Berriri, S., Garmier, M., Gilard, F., Pateyron, S., Haustraete, K., Van Der Straeten, D., Hirt, H. and Colcombet, J. (2017) Constitutively active arabidopsis MAP Kinase 3 triggers defense responses involving salicylic acid and SUMM2 resistance protein. *Plant Physiology*, 174, 1238-1249.

Godfrey, D., Zhang, Z., Saalbach, G. and Thordal-Christensen, H. (2009) A proteomics study of barley powdery mildew haustoria. *Proteomics*, 9, 3222-3232.

Gray, W.M., Muskett, P.R., Chuang, H.-W. and Parker, J.E. (2003) Arabidopsis SGT1b is required for SCF-TIR-1-mediated auxin response. *The Plant Cell*, 15, 1310-1319.

Gómez-Gómez, L., Bauer, Z. and Boller, T. (2001) Both the extracellular leucine-rich repeat domain and the kinase activity of FSL2 are required for flagellin binding and signaling in Arabidopsis. *Plant Cell*, 13, 1155-1163.

Halterman, D.A. and Wise, R.P. (2004) A single-amino acid substitution in the sixth leucine-rich repeat of barley MLA6 and MLA13 alleviates dependence on RAR1 for disease resistance signaling. *The Plant Journal*, 38, 215-226.

Hann, D.R. and Rathjen, J.P. (2007) Early events in the pathogenicity of *Pseudomonas syringae* on *Nicotiana benthamiana*. *The Plant Journal*, 49, 607-618.

Hao, W., Collier, S.M., Moffett, P. and Chai, J. (2013) Structural basis for the interaction between the potato virus X resistance protein (Rx) and its cofactor Ran GTPase-activating protein 2 (RanGAP2). *The Journal of biological chemistry*, 288, 35868-35876.

Helm, M., Qi, M., Sarkar, S., Yu, H., Whitham, S.A. and Innes, R.W. (2019) Engineering a decoy substrate in soybean to enable recognition of the soybean mosaic virus NIa protease. *Molecular Plant-Microbe Interactions*, 32, 760-769.

Hoser, R., Lichocka, M., Żurczak, M., Hennig, J. and Krzymowska, M. (2014) Emerging role of SGT1 as a regulator of NB-LRR-receptor nucleocytoplasmic partitioning. *Plant Signaling & Behavior*, 9, e28724.

Hoser, R., Zurczak, M., Lichocka, M., Zuzga, S., Dadlez, M., Samuel, M.A., Ellis, B.E., Stuttmann, J., Parker, J.E., Hennig, J. and Krzymowska, M. (2013) Nucleocytoplasmic partitioning of tobacco N receptor is modulated by SGT1. *The New Phytologist*, 200, 158-171.

Hu, Z., Yan, C., Liu, P., Huang, Z., Ma, R., Zhang, C., Wang, R., Zhang, Y., Martinon, F., Miao, D., Deng, H., Wang, J., Chang, J. and Chai, J. (2013) Crystal structure of NLRC4 reveals its autoinhibition mechanism. *Science*, 341, 172-175.

Huber, R.G., Eibl, C. and Fuchs, J.E. (2015) Intrinsic flexibility of NLRP pyrin domains is a key factor in their conformational dynamics, fold stability, and dimerization. *Protein Science*, 24, 174-181.

Ito, M., Ohnishi, K., Hikichi, Y. and Kiba, A. (2015) Molecular chaperons and co-chaperons, Hsp90, RAR1, and SGT1 negatively regulate bacterial wilt disease caused by *Ralstonia solanacearum* in *Nicotiana benthamiana*. *Plant Signaling & Behavior*, 10, e970410.

Jaswal, R., Kiran, K., Rajarammohan, S., Dubey, H., Singh, P.K., Sharma, Y., Deshmukh, R., Sonah, H., Gupta, N. and Sharma, T.R. (2020) Effector biology of biotrophic plant fungal pathogens: Current advances and future prospects. *Microbiological Research*, 241, 126567.

Jones, J.D.G., Vance, R.E. and Dangl, J.L. (2016) Intracellular innate immune surveillance devices in plants and animals. *Science*, 354, aaf6395.

Kadota, Y., Amigues, B., Ducassou, L., Madaoui, H., Ochsenbein, F., Guerois, R. and Shirasu, K. (2008) Structural and functional analysis of SGT1–HSP90 core complex required for innate immunity in plants. *EMBO reports*, 9, 1209-1215.

Kadota, Y. and Shirasu, K. (2012) The HSP90 complex of plants. *Biochimica et Biophysica Acta*, 1823, 689-697.

Kadota, Y., Shirasu, K. and Guerois, R. (2010) NLR sensors meet at the SGT1–HSP90 crossroad. *Trends in Biochemical Sciences*, 35, 199-207.

Kessler, S.C., Zhang, X., McDonald, M.C., Gilchrist, C.L.M., Lin, Z., Rightmyer, A., Solomon, P.S., Turgeon, B.G. and Chooi, Y.-H. (2020) Victorin, the host-selective cyclic peptide toxin from the oat pathogen *Cochliobolus victoriae*, is ribosomally encoded. *Proceedings of the National Academy of Sciences*, 117, 24243-24250.

Kim, N.H., Kim, D.S., Chung, E.H. and Hwang, B.K. (2014) Pepper Suppressor of the G2 Allele of *skp1* interacts with the Receptor-Like Cytoplasmic Kinase1 and type III effector AvrBsT and Ppromotes the hypersensitive cell death response in a phosphorylation-dependent manner. *Plant Physiology*, 165, 76-91.

Kitagawa, K., Skowyra, D., Elledge, S.J., Harper, J.W. and Hieter, P. (1999) SGT1 Encodes an essential component of the yeast kinetochore assembly pathway and a novel subunit of the SCF ubiquitin ligase complex. *Molecular Cell*, 4, 21-33.

Klingenberg, H. and Meinicke, P. (2017) How to normalize metatranscriptomic count data for differential expression analysis. *PeerJ*, 5, e3859.

Kourelis, J. and van der Hoorn, R.A.L. (2018) Defended to the nines: 25 years of resistance gene cloning identifies nine mechanisms for R protein function. *The Plant Cell*, 30, 285-299.

Kud, J., Zhao, Z., Du, X., Liu, Y., Zhao, Y. and Xiao, F. (2013) SGT1 interacts with the Prf resistance protein and is required for Prf accumulation and *Prf*-mediated defense signaling. *Biochemical and Biophysical Research Communications*, 431, 501-505.

Kwaaitaal, M., Nielsen, M.E., Böhlenius, H. and Thordal-Christensen, H. (2017) The plant membrane surrounding powdery mildew haustoria shares properties with the endoplasmic reticulum membrane. *Journal of Experimental Botany*, 68, 5731-5743.

Li, L., Habring, A., Wang, K. and Weigel, D. (2019) Oligomerization of NLR immune receptor RPP7 triggered by atypical resistance protein RPW8/HR as ligand. *bioRxiv*, 682807.

Li, Z., Chakraborty, S. and Xu, G. (2017) Differential CLE peptide perception by plant receptors implicated from structural and functional analyses of TDIF-TDR interactions. *PLOS ONE*, 12, e0175317.

Lin, G., Zhang, L., Han, Z., Yang, X., Liu, W., Li, E., Chang, J., Qi, Y., Shpak, E.D. and Chai, J. (2017) A receptor-like protein acts as a specificity switch for the regulation of stomatal development. *Genes Dev*, 31, 927-938.

Liu, P.-L., Du, L., Huang, Y., Gao, S.-M. and Yu, M. (2017) Origin and diversification of leucine-rich repeat receptor-like protein kinase (LRR-RLK) genes in plants. *BMC Evolutionary Biology*, 17, 47.

Liu, Z.-q., Liu, Y.-y., Shi, L.-p., Yang, S., Shen, L., Yu, H.-x., Wang, R.-z., Wen, J.-y., Tang, Q., Hussain, A., Khan, M.I., Hu, J., Liu, C.-l., Zhang, Y.-w., Cheng, W. and He, S.-l. (2016) SGT1 is required in PcINF1/SRC2-1 induced pepper defense response by interacting with SRC2-1. *Scientific Reports*, 6, 21651.

Lopez, V.A., Park, B.C., Nowak, D., Sreelatha, A., Zembek, P., Fernandez, J., Servage, K.A., Gradowski, M., Hennig, J., Tomchick, D.R., Pawłowski, K., Krzymowska, M. and Tagliabracci, V.S. (2019) A bacterial effector mimics a host HSP90 client to undermine immunity. *Cell*, 179, 205-218.e221.

Ma, L., Cornelissen, B. and Takken, F. (2013) A nuclear localization for Avr2 from *Fusarium oxysporum* is required to activate the tomato resistance protein I-2. *Frontiers in Plant Science*, 4.

Maekawa, T., Cheng, W., Spiridon, L.N., Töller, A., Lukasik, E., Saijo, Y., Liu, P., Shen, Q.H., Micluta, M.A., Somssich, I.E., Takken, F.L.W., Petrescu, A.J., Chai, J. and Schulze-Lefert, P. (2011) Coiled-coil domain-dependent homodimerization of intracellular barley immune receptors defines a minimal functional module for triggering cell death. *Cell Host Microbe*, 9, 187-199.

Martins, T., Maia, A.F., Steffensen, S. and Sunkel, C.E. (2009) Sgt1, a co-chaperone of Hsp90 stabilizes Polo and is required for centrosome organization. *The EMBO Journal*, 28, 234-247.

Matsushima, N. and Miyashita, H. (2012) Leucine-rich repeat (LRR) domains containing intervening motifs in plants. *Biomolecules*, 2, 288-311.

Mestre, P. and Baulcombe, D.C. (2006) Elicitor-mediated oligomerization of the tobacco N disease resistance protein. *Plant Cell*, 18, 491-501.

Miya, A., Albert, P., Shinya, T., Desaki, Y., Ichimura, K., Shirasu, K., Narusaka, Y., Kawakami, N., Kaku, H. and Shibuya, N. (2007) CERK1, a LysM receptor kinase, is essential for chitin elicitor signaling in Arabidopsis. *Proceedings of the National Academy of Sciences of the United States of America*, 104, 19613-19618.

Niikura, Y. and Kitagawa, K. (2019) Functions of SGT1, a co-chaperone. In *Heat Shock Protein 90 in Human Diseases and Disorders* (Asea, A.A.A. and Kaur, P. eds): Springer, pp. 317-370.

Noël, L.D., Cagna, G., Stuttmann, J., Wirthmüller, L., Betsuyaku, S., Witte, C.-P., Bhat, R., Pochon, N., Colby, T. and Parker, J.E. (2007) Interaction between SGT1 and cytosolic/nuclear HSC70 chaperones regulates *Arabidopsis* immune responses. *The Plant Cell*, 19, 4061-4076.

Oh, S.-K., Kim, H. and Choi, D. (2014) *Rpi-blb2*-mediated late blight resistance in *Nicotiana benthamiana* requires SGT1 and salicylic acid-mediated signaling but not RAR1 or HSP90. *FEBS Letters*, 588, 1109-1115.

Padmanabhan, M., Cournoyer, P. and Dinesh-Kumar, S.P. (2009) The leucine-rich repeat domain in plant innate immunity: a wealth of possibilities. *Cellular Microbiology*, 11, 191-198.

Peart, J.R., Lu, R., Sadanandom, A., Malcuit, I., Moffett, P., Brice, D.C., Schauser, L., Jaggard, D.A.W., Xiao, S., Coleman, M.J., Dow, M., Jones, J.D.G., Shirasu, K. and Baulcombe, D.C. (2002) Ubiquitin ligase-associated protein SGT1 is required for host and nonhost disease resistance in plants. *PNAS*, 99, 10865-10869.

Pel, M.J.C., van Dijken, A.J.H., Bardoel, B.W., Seidl, M.F., van der Ent, S., van Strijp, J.A.G. and Pieterse, C.M.J. (2014) *Pseudomonas syringae* evades host immunity by degrading Flagellin monomers with alkaline protease AprA. *Molecular Plant-Microbe Interactions*, 27, 603-610.

Qi, T., Seong, K., Thomazella, D.P.T., Kim, J.R., Pham, J., Seo, E., Cho, M.J., Schultink, A. and Staskawicz, B.J. (2018) NRG1 functions downstream of EDS1 to regulate TIR-NLR-mediated plant immunity in Nicotiana benthamiana. *PNAS*, 115, E10979-e10987.

Rairdan, G.J. and Moffett, P. (2006) Distinct domains in the ARC region of the potato resistance protein Rx mediate LRR binding and inhibition of activation. *The Plant Cell*, 18, 2082-2093.

Redkar, A., Hoser, R., Schilling, L., Zechmann, B., Krzymowska, M., Walbot, V. and Doehlemann, G. (2015) A secreted effector protein of *Ustilago maydis* guides maize leaf cells to form tumors. *The Plant Cell*, 27, 1332-1351.

Ruggieri, V., Nunziata, A. and Barone, A. (2014) Positive selection in the leucine-rich repeat domain of *Gro1* genes in *Solanum* species. *Journal of Genetics*, 93, 755-765.

Salcedo, A., Rutter, W., Wang, S., Akhunova, A., Bolus, S., Chao, S., Anderson, N., De Soto, M.F., Rouse, M., Szabo, L., Bowden, R.L., Dubcovsky, J. and Akhunov, E. (2017) Variation in the *AvrSr35* gene determines *Sr35* resistance against wheat stem rust race Ug99. *Science*, 358, 1604-1606.

Santiago, J., Brandt, B., Wildhagen, M., Hohmann, U., Hothorn, L.A., Butenko, M.A. and Hothorn, M. (2016) Mechanistic insight into a peptide hormone signaling complex mediating floral organ abscission. *eLife*, 5, e15075.

Saur, I.M.L., Bauer, S., Kracher, B., Lu, X., Franzeskakis, L., Muller, M.C., Sabelleck, B., Kummel, F., Panstruga, R., Maekawa, T. and Schulze-Lefert, P. (2019) Multiple pairs of allelic MLA immune receptor-powdery mildew AVR_A effectors argue for a direct recognition mechanism. *eLife*, 8, e44471.

Savary, S., Willocquet, L., Pethybridge, S.J., Esker, P., McRoberts, N. and Nelson, A. (2019) The global burden of pathogens and pests on major food crops. *Nature Ecology & Evolution*, 3, 430-439.

She, J., Han, Z., Kim, T.-W., Wang, J., Cheng, W., Chang, J., Shi, S., Wang, J., Yang, M., Wang, Z.-Y. and Chai, J. (2011) Structural insight into brassinosteroid perception by BRI1. *Nature*, 474, 472-476.

Shen, Q.-H., Saijo, Y., Mauch, S., Biskup, C., Bieri, S., Keller, B., Seki, H., Ulker, B., Somssich, I.E. and Schulze-Lefert, P. (2007) Nuclear activity of MLA immune receptors links isolate-specific and basal disease-resistance responses. *Science*, 315, 1098-1103.

Shirasu, K. (2009) The HSP90-SGT1 chaperone complex for NLR immune sensors. *Annu. Rev. Plant Biol.*, 60, 139-164.

Siligardi, G., Zhang, M. and Prodromou, C. (2018) The stoichiometric interaction of the Hsp90-Sgt1-Rar1 complex by CD and SRCD spectroscopy. *Frontiers in Molecular Biosciences*, 4.

Slootweg, E., Roosien, J., Spiridon, L.N., Petrescu, A.-J., Tameling, W., Joosten, M., Pomp, R., van Schaik, C., Dees, R., Borst, J.W., Smant, G., Schots, A., Bakker, J. and Goverse, A. (2010) Nucleocytoplasmic distribution is required for activation of resistance by the potato NB-LRR receptor Rx1 and is balanced by its functional domains. *The Plant Cell*, 22, 4195-4215.

Slootweg, E.J., Spiridon, L.N., Roosien, J., Butterbach, P., Pomp, R., Westerhof, L., Wilbers, R., Bakker, E., Bakker, J., Petrescu, A., Smant, G. and Goverse, A. (2013) Structural determinants at the interface of the ARC2 and leucine-rich repeat domains control the activation of the plant immune receptors Rx1 and Gpa2. *Plant Physiology*, 162, 1510-1528.

Sukarta, O.C.A., Slootweg, E.J. and Goverse, A. (2016) Structure-informed insights for NLR functioning in plant immunity. *Seminars in Cell & Developmental Biology*, 56, 134-149.

Sun, Y., Zhu, Y.-X., Balint-Kurti, P.J. and Wang, G.-F. (2020) Fine-tuning immunity: Players and regulators for plant NLRs. *Trends in Plant Science*, 25, 695-713.

Takahashi, A., Casais, C., Ichimura, K. and Shirasu, K. (2003) HSP90 interacts with RAR1 and SGT1 and is essential for RPS2-mediated disease resistance in *Arabidopsis*. *Proceedings of the National Academy of Sciences*, 100, 11777-11782.

Tameling, W.I.L. and Baulcombe, D.C. (2007) Physical association of the NB-LRR resistance protein Rx with a Ran GTPase–activating protein is required for extreme resistance to *Potato virus X*. *The Plant Cell*, 19, 1682-1694.

Tameling, W.I.L., Elzinga, S.D.J., Darmin, P.S., Vossen, J.H., Takken, F.L.W., Haring, M.A. and Cornelissen, B.J.C. (2002) The tomato *R* gene products I-2 and Mi-1 are functional ATP binding proteins with ATPase activity. *The Plant Cell*, 14, 2929-2939.

Tameling, W.I.L., Vossen, J.H., Albrecht, M., Lengauer, T., Berden, J.A., Haring, M.A., Cornelissen, B.J.C. and Takken, F.L.W. (2006) Mutations in the NB-ARC domain of I-2 that impair ATP hydrolysis cause autoactivation. *Plant Physiology*, 140, 1233-1245.

Tang, W., Ezcurra, I., Muschietti, J. and McCormick, S. (2002) A cysteine-rich extracellular protein, LAT52, interacts with the extracellular domain of the pollen receptor kinase LePRK2. *The Plant Cell*, 14, 2277-2287.

Thao, N.P., Chen, L., Nakashima, A., Hara, S.-i., Umemura, K., Takahashi, A., Shirasu, K., Kawasaki, T. and Shimamoto, K. (2007) RAR1 and HSP90 form a complex with Rac/Rop GTPase and function in innate-immune responses in rice. *The Plant Cell*, 19, 4035-4045.

Thomma, B.P., HP, V.A.N.E., Crous, P.W. and PJ, D.E.W. (2005) *Cladosporium fulvum* (syn. *Passalora fulva*), a highly specialized plant pathogen as a model for functional studies on plant pathogenic *Mycosphaerellaceae*. *Mol Plant Pathol*, 6, 379-393.

Tornero, P., Merritt, P., Sadanandom, A., Shirasu, K., Innes, R.W. and Dangl, J.L. (2002) *RAR1* and *NDR1* contribute quantitatively to disease resistance in Arabidopsis, and their relative contributions are dependent on the *R* gene assayed. *The Plant Cell*, 14, 1005-1015.

Toyota, M., Spencer, D., Sawai-Toyota, S., Jiaqi, W., Zhang, T., Koo, A.J., Howe, G.A. and Gilroy, S. (2018) Glutamate triggers long-distance, calcium-based plant defense signaling. *Science*, 361, 1112-1115.

van den Burg, H.A., Harrison, S.J., Joosten, M.H.A.J., Vervoort, J. and de Wit, P.J.G.M. (2006) *Cladosporium fulvum* Avr4 protects fungal cell walls against hydrolysis by plant chitinases accumulating during infection. *Molecular Plant-Microbe Interactions*, 19, 1420-1430.

van Esse, H.P., Van't Klooster, J.W., Bolton, M.D., Yadeta, K.A., van Baarlen, P., Boeren, S., Vervoort, J., de Wit, P.J. and Thomma, B.P. (2008) The *Cladosporium fulvum* virulence protein Avr2 inhibits host proteases required for basal defense. *Plant Cell*, 20, 1948-1963.

van Ooijen, G., Mayr, G., Kasiem, M.M., Albrecht, M., Cornelissen, B.J. and Takken, F.L. (2008) Structure-function analysis of the NB-ARC domain of plant disease resistance proteins. *Journal of Experimental Botany*, 59, 1383-1397.

van Wersch, R., Li, X. and Zhang, Y. (2016) Mighty dwarfs: Arabidopsis autoimmune mutants and their usages in genetic dissection of Plant Immunity. *Frontiers in Plant Science*, 7.

van Wersch, S., Tian, L., Hoy, R. and Li, X. (2020) Plant NLRs: The whistleblowers of plant immunity. *Plant Communications*, 1, 100016.

Wang, C., Zhou, M., Zhang, X., Yao, J., Zhang, Y. and Mou, Z. (2017) A lectin receptor kinase as a potential sensor for extracellular nicotinamide adenine dinucleotide in Arabidopsis thaliana. *eLife*, 6, e25474.

Wang, G.F., Ji, J., El-Kasmi, F., Dangl, J.L., Johal, G. and Balint-Kurti, P.J. (2015) Molecular and functional analyses of a maize autoactive NB-LRR protein identify precise structural requirements for activity. *PLoS Pathogens*, 11, e1004674.

Wang, J., Hu, M., Wang, J., Qi, J., Han, Z., Wang, G., Qi, Y., Wang, H.-W., Zhou, J.-M. and Chai, J. (2019a) Reconstitution and structure of a plant NLR resistosome conferring immunity. *Science*, 364, eaav5870.

Wang, J., Wang, J., Hu, M., Wu, S., Qi, J., Wang, G., Han, Z., Qi, Y., Gao, N., Wang, H.-W., Zhou, J.-M. and Chai, J. (2019b) Ligand-triggered allosteric ADP release primes a plant NLR complex. *Science*, 364, eaav5868.

Wang, Y., Gao, M., Li, Q., Wang, L., Wang, J., Jeon, J.S., Qu, N., Zhang, Y. and He, Z. (2008) OsRAR1 and OsSGT1 physically interact and function in rice basal disease resistance. *Mol Plant Microbe Interact*, 21, 294-303.

Wawra, S., Fesel, P., Widmer, H., Timm, M., Seibel, J., Leson, L., Kesseler, L., Nostadt, R., Hilbert, M., Langen, G. and Zuccaro, A. (2016) The fungal-specific β-glucan-binding lectin FGB1 alters cell-wall composition and suppresses glucan-triggered immunity in plants. *Nature Communications*, 7, 13188.

Wendler, P., Ciniawsky, S., Kock, M. and Kube, S. (2012) Structure and function of the AAA+ nucleotide binding pocket. *Biochimica et Biophysica Acta*, 1823, 2-14.

Willhoft, O., Kerr, R., Patel, D., Zhang, W., Al-Jassar, C., Daviter, T., Millson, S.H., Thalassinos, K. and Vaughan, C.K. (2017) The crystal structure of the Sgt1-Skp1 complex: the link between Hsp90 and both SCF E3 ubiquitin ligases and kinetochores. *Scientific Reports*, 7, 41626.

Yamada, K., Yamaguchi, K., Shirakawa, T., Nakagami, H., Mine, A., Ishikawa, K., Fujiwara, M., Narusaka, M., Narusaka, Y., Ichimura, K., Kobayashi, Y., Matsui, H., Nomura, Y., Nomoto, M., Tada, Y., Fukao, Y., Fukamizo, T., Tsuda, K., Shirasu, K., Shibuya, N. and Kawasaki, T. (2016) The Arabidopsis CERK1-associated kinase PBL27 connects chitin perception to MAPK activation. *The EMBO Journal*, 35, 2468-2483.

Yamaoka, N., Matsumoto, I. and Nishiguchi, M. (2006) The role of primary germ tubes (PGT) in the life cycle of *Blumeria graminis*: The stopping of PGT elongation is necessary for the triggering of appressorial germ tube (AGT) emergence. *Physiological and Molecular Plant Pathology*, 69, 153-159.

Yang, X., Yang, F., Wang, W., Lin, G., Hu, Z., Han, Z., Qi, Y., Zhang, L., Wang, J., Sui, S.-F. and Chai, J. (2018) Structural basis for specific flagellin recognition by the NLR protein NAIP5. *Cell Research*, 28, 35-47.

Ye, W., Munemasa, S., Shinya, T., Wu, W., Ma, T., Lu, J., Kinoshita, T., Kaku, H., Shibuya, N. and Murata, Y. (2020) Stomatal immunity against fungal invasion comprises not only chitin-induced stomatal closure but also chitosan-induced guard cell death. *PNAS*, 117, 20932-20942.

Zhang, J., Li, W., Xiang, T., Liu, Z., Laluk, K., Ding, X., Zou, Y., Gao, M., Zhang, X., Chen, S., Mengiste, T., Zhang, Y. and Zhou, J.-M. (2010) Receptor-like cytoplasmic kinases integrate signaling from multiple plant immune receptors and are targeted by a *Pseudomonas syringae* effector. *Cell Host & Microbe*, 7, 290-301.

Zhang, L., Chen, S., Ruan, J., Wu, J., Tong, A.B., Yin, Q., Li, Y., David, L., Lu, A., Wang, W.L., Marks, C., Ouyang, Q., Zhang, X., Mao, Y. and Wu, H. (2015) Cryo-EM structure of the activated NAIP2-NLRC4 inflammasome reveals nucleated polymerization. *Science*, 350, 404-409.

Zhang, M., Botër, M., Li, K., Kadota, Y., Panaretou, B., Prodromou, C., Shirasu, K. and Pearl, L.H. (2008) Structural and functional coupling of Hsp90- and Sgt1-centred multi-protein complexes. *The EMBO Journal*, 27, 2789-2798.

Zhang, X., Bernoux, M., Bentham, A.R., Newman, T.E., Ve, T., Casey, L.W., Raaymakers, T.M., Hu, J., Croll, T.I., Schreiber, K.J., Staskawicz, B.J., Anderson, P.A., Sohn, K.H., Williams, S.J., Dodds, P.N. and Kobe, B. (2017) Multiple functional self-association interfaces in plant TIR domains. *Proceedings of the National Academy of Sciences*, 114, E2046-E2052.

Zhang, X.S., Choi, J.H., Heinz, J. and Chetty, C.S. (2006) Domain-specific positive selection contributes to the evolution of Arabidopsis leucine-rich repeat receptor-like kinase (LRR RLK) genes. *Journal of Molecular Evolution*, 63, 612-621.

Zhang, Y., Berghaus, M., Klein, S., Jenkins, K., Zhang, S., McCallum, S.A., Morgan, J.E., Winter, R., Barrick, D. and Royer, C.A. (2018) High-pressure NMR and SAXS reveals how capping modulates folding cooperativity of the pp32 leucine-rich repeat protein. *Journal of Molecular Biology*, 430, 1336-1349.

Zhou, F., Emonet, A., Dénervaud Tendon, V., Marhavy, P., Wu, D., Lahaye, T. and Geldner, N. (2020) Co-incidence of damage and microbial patterns controls localized immune responses in roots. *Cell*, 180, 440-453.e418.

Zhou, M., Li, Y., Hu, Q., Bai, X.C., Huang, W., Yan, C., Scheres, S.H. and Shi, Y. (2015) Atomic structure of the apoptosome: mechanism of cytochrome c- and dATP-mediated activation of Apaf-1. *Genes & Development*, 29, 2349-2361.

CHAPTER 2. DISRUPTION OF BARLEY IMMUNITY TO POWDERY MILDEW BY AN IN-FRAME LYS-LEU DELETION IN THE ESSENTIAL PROTEIN SGT1

Antony V. E. Chapman[*†], Matthew Hunt[*†], Priyanka Surana[†‡], Valeria Velásquez-Zapata[†‡], Weihui Xu[†], Greg Fuerst[†§], and Roger P. Wise[*†‡§]

[*]Interdepartmental Genetics & Genomics, Iowa State University, Ames, IA 50011

[†]Department of Plant Pathology & Microbiology, Iowa State University, Ames, IA 50011

[‡]Program in Bioinformatics & Computational Biology, Iowa State University, Ames, IA 50011

[§]Corn Insects and Crop Genetics Research, USDA-Agricultural Research Service, Ames, IA 50011

Modified from a manuscript published in *GENETICS*

Abstract

Barley (*Hordeum vulgare* L.) *Mla (Mildew resistance locus a*) and its nucleotide-binding, leucine-rich-repeat receptor (NLR) orthologs protect many cereal crops from diseases caused by fungal pathogens. However, large segments of the *Mla* pathway and its mechanisms remain unknown. To further characterize the molecular interactions required for NLR-based immunity, we used fast-neutron mutagenesis to screen for plants compromised in MLA-mediated

response to the powdery mildew fungus, *Blumeria graminis* f. sp. *hordei*. One variant, m11526, contained a novel mutation, designated *rar3* (*required for Mla6 resistance3*), that abolishes race-specific resistance conditioned by the *Mla6*, *Mla7* and *Mla12* alleles, but does not compromise immunity mediated by *Mla1*, *Mla9*, *Mla10* and *Mla13*. This is analogous to, but unique from, the differential requirement of *Mla* alleles for the co-chaperone *Rar1 (required for Mla12 resistance1).* We used bulked-segregant-exome capture and fine mapping to delineate the causal mutation to an *in-frame* Lys-Leu deletion within the SGS domain of SGT1 (Suppressor of G-two allele of *Skp1, Sgt1*$_{\Delta KL308\text{-}309}$), the structural region that interacts with MLA proteins. In nature, mutations to *Sgt1* usually cause lethal phenotypes, but here we pinpoint a unique modification that delineates its requirement for some disease resistances, while unaffecting others as well as normal cell processes. Moreover, the data indicate that the requirement of SGT1 for resistance signaling by NLRs can be delimited to single sites on the protein. Further study could distinguish the regions by which pathogen effectors and host proteins interact with SGT1, facilitating precise editing of effector-incompatible variants.

Introduction

Blumeria graminis f. sp. *hordei* (*Bgh*), the causal agent of barley (*Hordeum vulgare* L.) powdery mildew, is an economically important biotrophic fungus (Murray and Brennan, 2010). The association between *Bgh* and barley represents a principle model for interactions among Triticeae grain crops and biotrophic pathogens, which are constrained to colonize and gain their nutrients from living tissue (Draz *et al.*, 2019). During infection, *Bgh* releases avirulence (AVR) effector proteins into the host via haustorial feeding structures (Kwaaitaal *et al.*, 2017, Jaswal *et al.*, 2020). These effectors function to subvert the host's initial

immune response to the presence of the pathogen and facilitate the absorption of nutrients (Krattinger and Keller, 2016, Langin *et al.*, 2020). In response, plants have evolved sets of resistance proteins that detect these effectors, initiating defense (Lo Presti *et al.*, 2015). The most prevalent class of resistance proteins employed in agriculture are nucleotide-binding, leucine-rich-repeat receptors (NLRs) (Sun *et al.*, 2020, van Wersch *et al.*, 2020), with notable exceptions (Kourelis and van der Hoorn, 2018).

Barley *Mla* (*mildew resistance locus a*) is a classic example of a complex resistance locus that encodes an NLR immune receptor; it is highly polymorphic with over 30 allelic variants conditioning race-specific immunity in diverse cultivars (Wei *et al.*, 2002, Halterman and Wise, 2004, Ridout *et al.*, 2006, Seeholzer *et al.*, 2010, Lu *et al.*, 2016, Saur *et al.*, 2019). To confer resistance, MLA proteins often require the assistance of the co-chaperones Heat Shock Protein 90 (HSP90) and Suppressor of G-two allele of *Skp1* (SGT1) (Bieri *et al.*, 2004). A third co-chaperone is also involved, the Zn^{2+} binding protein Required for Mla12 Resistance 1 (RAR1), which is essential for many, but not all MLA proteins (Shirasu *et al.*, 1999, Shen *et al.*, 2003, Bieri *et al.*, 2004, Halterman and Wise, 2004). Together HSP90, RAR1, and SGT1 form the HRS complex that acts to stabilize levels of MLA (Bieri *et al.*, 2004, Shirasu, 2009). Once MLA recognizes the presence of the appropriate effector, the MLA-HRS complex translocates to the nucleus where it initiates a signaling cascade, leading to immunity (Shen *et al.*, 2007, Bai *et al.*, 2012, Chang *et al.*, 2013).

Conserved *Mla* or *Mla* locus orthologs display diversified recognition specificities to powdery mildew in transgenic Arabidopsis (Maekawa *et al.*, 2012), wheat powdery mildew (Jordan *et al.*, 2011), wheat and rye Ug99 stem rust (Periyannan *et al.*, 2013, Mago *et al.*, 2015,

Cesari *et al.*, 2016), wheat stripe rust (J. Bettgenhaeuser and M. Moscou, Pers Comm), as well as to the metabolite victorin, the cause of oat Victoria blight (Moscou *et al.*, 2018), and rice blast (H. Brabham and M. Moscou, Pers Comm).

Herein, we present the molecular identification and phenotypic characterization of a 6-base-pair (bp) in-frame deletion in the SGS domain of *Sgt1* that selectively compromises *Mla*-dependent disease resistance. *Sgt1* has been historically difficult to investigate because silencing causes severe growth defects in most organisms and deletion is usually lethal (Azevedo *et al.*, 2006, Bhattarai *et al.*, 2007, Thao *et al.*, 2007). Developmental and physiological assessments indicate that there are no significant phenotypic differences among plants with or without the $Sgt1_{\Delta KL308\text{-}309}$ mutation, other than compromised disease resistance. Considering the recent discoveries of pathogen effectors that target SGT1 (Redkar *et al.*, 2015, Yu *et al.*, 2020), and how *Mla* orthologues are critical sources of immunity for economically important crops, pursuit of this unique modification will likely yield breakthroughs for understanding a breadth of disease resistance interactions.

Materials and methods

Biological materials

The barley cereal introduction (CI) lines 16151 (*Mla6*), 16137 (*Mla1*), 16147 (*Mla7*), 16149 (*Mla10*), 16155 (*Mla13*), and 16153 (*Mla15*) were developed by introgression of *Mla* alleles into the universal susceptible cv Manchuria (Moseman, 1972). Sultan-5 and *rar1-m100* were gifts from J. Helms Jørgensen (Risø National Laboratory, Roskilde, Denmark; Torp & Jørgensen, 1986). The Pallas lines P03 (*Mla6*) and P04B (*Mla7*) were gifts from Lisa Munk (Kolster *et al.*, 1986). *Bgh* isolates 5874 (AVR_{a1}, AVR_{a6} and AVR_{a12}) and CC148 (AVR_{a1}, AVR_{a7},

AVR_{a9}, AVR_{a10}, AVR_{a13} and *AVR_{a15})* were maintained on susceptible *H. vulgare* cv. Morex in separate growth chambers at 18°C (16/8 hour light/darkness).

Mutagenesis

Mutagenesis was performed as described in (Meng *et al.*, 2009, Xi *et al.*, 2009). Briefly, seeds of CI 16151 (*Mla6*) were treated with fast neutrons at 4 Gy Nf at the International Atomic Energy Agency (Vienna, Austria) and the resulting 34,800 M_2 families were screened for mutant segregants 7 days after inoculation with *Bgh* isolate 5874 (*AVR_{a6}*) following the method of (Wise and Ellingboe, 1985). Chlorophyll mutations were used to evaluate the mutation rate of the population; 936 families segregated albino, 233 families segregated pale yellow, 63 families segregated pale green, and 6 families segregated green/white striped for a total of 3.56% observed chlorophyll mutations. Individuals that produced cell death symptoms or sporulating *Bgh* colonies were selected for rescue.

For this study, susceptible mutant m11506, containing *Mla6* and *Bln1* deletions, was backcrossed and selfed twice to CI 16151 to select homozygous mutants m18982 (*mla6*, *Bln1, Rar3*), m19089 (*Mla6*, *bln1, Rar3*), and m19028 (*mla6*, *bln1, Rar3*)(Xu *et al.*, 2014). Similarly, the *rar3* mutant, m11526 (*Mla6*, *Bln1, rar3*), was made homozygous following two backcrosses to CI 16151 with selection. F2 populations for exome capture and fine mapping were created by crossing m11526 to the P03 (Pallas background, *Mla6*) or Sultan-5 (*Mla12*) and selfing the F1.

Phenotypic characterization

All plants were grown in a temperature-controlled greenhouse (16-20 degrees C; 16 hours supplementary light). Physiological measurements were performed on seedlings that were grown for 14, 21 or 28 days. Stress tests were conducted by growing seedlings to 7 days

old and then either moving to complete darkness, watering only with 100mM NaCl, or removing watering completely. Height was then measured at 14, 21 and 28 days old if the plant survived. Analysis was performed as a pairwise t-test between each mutant and its wildtype progenitor for each trait. Significance was determined at $p > 0.05$.

To measure developmental characteristics, 10 seed from each genotype were planted in a randomized block design. Two individuals from each line were blocked and placed in 5 different locations within the same greenhouse room to account for microclimate variances. Plants were measured at regular intervals for plant height and number of tillers. Additional end-point data was collected on the total number of florets, seed fertility, and seed weight. Time series data was analyzed using a linear model with mixed effects with fixed factors as Genotype + time + Genotype*time + Position and the accession as the random effect. The end-point data was analyzed using a linear model with fixed effects using the design Trait ~ Genotype + Position. A one-way ANOVA was performed and pairwise contrasts using the Tukey test. Genotypes were grouped using 0.01 significance level. All the analyses were run using the R software version 3.6 (R Core Team, 2019) and the packages lsmeans (Lenth, 2016) and multcompView (Graves *et al.*, 2019).

For disease assessments, seedlings were grown in the greenhouse before being transferred to the relevant *Bgh* growth chamber for inoculation with fresh *Bgh* conidiospores. Phenotyping was performed at 7 days after inoculation (DAI). A Chi-squared test was used to calculate the likelihood of phenotypic data matching expected genetic ratios.

Infection kinetics

Seedlings were grown in groups of 6 (one of each time point) by genotype in a randomized split plot design with genotype as the whole plot and time point as the sub plot before being inoculated with *Bgh* 5874. At each time point [16, 20, 24, 28, 32 & 48 hours after inoculation (HAI)], five leaves of each group of six was collected and submerged in clearing solution (3:1, alcohol : acetic acid). Once all leaves were collected and had been submerged in clearing solution for at least 24 hours, they were transferred to 70% ethanol for 24 hours. Lastly, leaves were transferred to 20% ethanol and stored at 4°C prior to scoring. Cleared leaves were treated with Coomassie blue for 2 minutes prior to scoring to visualize *Bgh* spores and trimmed to 5cm in length from the tip. Each experiment was replicated three times.

Leaves were scored on both abaxial and adaxial sides to count the number of spores which were in each of five infection stages, attached spore, appressorium attachment, hyphal index 1, hyphal index 2, and hyphal index 3 (**Figure 2-S1**). After scoring, % Elongating Secondary Hyphae (ESH) was calculated by using the following calculation:

$$\%\mathrm{ESH} = 100 * \frac{\sum \text{Hyphal indices}}{\sum \text{Appressorium} + \text{Hyphal indices}}$$

The analysis was performed using a mixed model as the fit for pairwise comparison between treatments with the response as percentage ESH using SAS software (SAS Institute Inc., Cary, North Carolina, USA). The fixed factors were set as treatment, leaf side and treatment * leaf side. The random factors were leaf (treatment), replication and treatment * replication in a mixed model design. A false discovery rate of 0.05 was used.

Genetic crosses and F2 characterization

The *rar3* mutant m11526 (*Mla6*, *rar3*) was crossed to multiple near-isogenic or diverse lines, and the F1s were selfed to generate segregating F2. F2 seed were planted in two 98-cell cone flats alongside both parents and F1, totaling 193 F2 seed sown. Each population was challenged with the appropriate *Bgh* isolate, 5874 or CC148, depending on *Mla*/*AVR* combinations. Parents, F1 and F2 were phenotyped at 7 DAI and scored on a 0-4 scale for sporulation (successful growth of fungal spores), necrosis (plant cell death), and chlorosis (bleaching of leaf tissue). Subsequent to infection phenotyping, plants were grouped into four main categories. These were: resistant (**R**; no sporulation and no necrosis), resistant with necrosis (**Rn**; no sporulation but significant necrosis), susceptible with necrosis (**Sn;** significant sporulation and significant necrosis), and susceptible (**S;** significant sporulation but no necrosis).

The resistance or susceptible phenotype can be considered the major phenotype as it shows whether the plant is successfully defending against the pathogen, whereas the necrosis phenotype can be considered the minor phenotype as it may show whether defense is slow but successful (**Rn**) or too slow and failing (**Sn**). Additionally, it is possible that the necrosis phenotype is not associated with a *Mla*-based interaction at all, but rather due to other segregating loci (Yu *et al.*, 2001).

CI 16151 reference genome

The CI 16151 genome sequence was based on the Morex genome (Assembly 082214v1, INSDC Assembly GCA_000326085.1)(Mayer *et al.*, 2012), with high confidence variants (SNPs and short indels) introduced based on the input variant vcf files. Thirty seeds of CI 16151 were

geminated on sterile 3M paper in each of 4 canisters. Eight-day old etiolated seedlings (1st leaf stage) were harvested, and DNA was isolated using a standard 2X CTAB prep. Samples were treated with RNAse A + T1, and their quality assessed on a 0.4% Tris-Phosphate-EDTA agarose gel. Samples were mechanically fragmented (~500 bp) prior to library construction, and whole genome sequencing libraries were prepared using a Nextera DNA Sample Preparation Kit (Illumina, Inc., San Diego, CA). Each sample was sequenced to 11.74x coverage (single-end read, 100 cycles) on one lane of an Illumina HiSeq 2000.

Reads from the four replicates were aligned to the Morex genome sequence using BWA (commands mem –v 0 –M –t 2 –p) version 0.7.12 (Li and Durbin, 2009). The output sam files were processed using the Genome Analysis Toolkit (GATK) program using described best practices (https://software.broadinstitute.org/gatk/best-practices/) (McKenna *et al.*, 2010). Briefly the BWA output sam files were merged with their unmapped versions using MergeBamAlignment from Picard tools (http://broadinstitute.github.io/picard) and duplicates were marked with MarkDuplicates from Picard tools.

The raw SNPs and Indels were called by the HaplotypeCaller GATK program and the output g.vcf files were merged using the GenotypeGVCFs GATK program. The SelectVariants GATK program identified the raw SNPs and Indels from the merged vcf file and the high-quality SNPs and Indels were selected using the VariantFiltration GATK program (–filterExpression "QD < 2.0 || FS > 60.0 || MQ < 40.0 || MQRankSum < -12.5 || ReadPosRankSum < -8.0"). The resulting four vcf files were then used along with the Morex genome to create a Morex-based CI 16151 genome assembly using the FastaAlternateReferenceMaker GATK program

(https://software.broadinstitute.org/gatk/documentation/tooldocs/3.8-0/org_broadinstitute_gatk_tools_walkers_fasta_FastaAlternateReferenceMaker.php).

Exome capture

Two-hundred 7-day old F2 seedlings from both the m11526 x P03 and m11526 x Sultan-5 populations (400 F2 in total) were inoculated with *Bgh* 5874, infection phenotyped 7 DAI, and then treated with fungicide. Tissue was harvested from 3rd leaves at 21 days old, into groups of 10 F2 seedlings per standard 2X CTAB DNA extraction. The grouped gDNA was then further pooled for a total of four population pools; 150 resistant P03-derived, 50 susceptible P03-derived, 150 resistant Sultan-5-derived and 50 susceptible Sultan-5-derived. Samples were processed for exome capture according to the SeqCap EZ Library SR User Guide (Roche NimbleGen, Version 5.1, Barley Exome Custom Sequence Capture design, 06740278001) and using the KAPA HyperPrep Kit (KK8500) and sequenced on a single lane of an Illumina HiSeq 3000.

Exome capture reads from the four pools were aligned to a custom CI 16151 barley genome sequence (published herein) using BWA (commands mem –v 0 –M –t 2 –p) version 0.7.12 (Li and Durbin, 2009). The output sam files were processed using the Genome Analysis Toolkit (GATK) program using described best practices (https://software.broadinstitute.org/gatk/best-practices/) (McKenna *et al.*, 2010). Briefly the BWA output sam files were merged with their unmapped versions using MergeBamAlignment from Picard tools (http://broadinstitute.github.io/picard) and duplicates were marked with MarkDuplicates from Picard tools.

Raw SNPs were processed by HaplotypeCaller, SelectVariants, and VariantFiltration GATK programs and the output g.vcf files were merged using the GenotypeGVCFs GATK program as described above for the CI 16151 reference genome. The output filtered vcf files were then converted to table format using the VariantsToTable GATK program. High quality SNPs were identified using the GQ quality metric (GQ > 99) using a custom bash script. Average SNP frequencies were calculated and graphed using custom bash and R scripts.

Fine mapping

As not all SNPs were similar in both P03 and Sultan-5 compared to m11526, we used the P03 x m11526 population for fine mapping so that we removed any potential affect the *Mla12* allele may have. Four-thousand five hundred P03 x m11526 F2 individuals were phenotyped with *Bgh* 5874 and harvested for DNA extraction.

Molecular markers were generated from the exome capture data to delineate the causal mutation to Chr3HL 408.3Mb to 420.2Mb. Markers were generated by examining the genes found in this region according to Ensembl (Assembly 082214v1, INSDC Assembly GCA_000326085.1) and looking for concurrent SNPs in the exome capture data. SNPs were examined for changes in restriction sites that would indicate a suitable Cleaved Amplified Polymorphic Sequence (CAPS) marker. CAPS markers that showed suitability for high-throughput genotyping were used on the F2 population (**Table 2-S1**). Genotyping results were used to identify individuals with recombination events within the candidate region.

Identification of the *Sgt1* mutation

The *Sgt1* gene was amplified from m11526 gDNA and cDNA using the primers Sgt1_3'_F1 (GCTCCCCAAAGTCTTCGTCT) and Sgt1_5'_R2 (TGTAAGCTGTTTGCGTGGCAGG) with

Phusion High-Fidelity DNA polymerase (Thermo Scientific). A nested PCR was performed on the *Sgt1* cDNA product using Sgt1_Start (ATGGCCGCCGCCGCC) and Sgt1_5'_R2 to make an in-frame transcript which was cloned into the pCR8 backbone using the pCR™8/GW/TOPO® TA Cloning Kit (ThermoFisher, K250020). Sequences were determined by Sanger sequencing.

Hydrogen peroxide accumulation and hypersensitive reactions

The observation of hypersensitive reactions (HR) was performed as described by Xu and colleagues (2014). Seven-day-old barley first leaves (PO:0007094) were inoculated with *Bgh* 5874, harvested at 24 HAI, fixed and decolorized for 48 h in ethanol : acetic acid (3 : 1, v/v) with one change with 70% ethanol (v/v). Following fixation, leaves were cleared in lactophenol : glycerol : water solution (1 : 1 : 1, v/v). Hypersensitive responses were examined using a fluorescence microscope (Leitz Fluovert, Wetzlar, Germany) with a fluorescein filter set H3 (excitation filter BP420-490, suppression filter LP 520).

Hydrogen peroxide (H_2O_2), a reactive oxygen species (ROS), was assayed by diaminobenzidine tetrahydrochloride (DAB) staining. First leaves inoculated with *Bgh* 5874 were cut at 16 HAI and moved to DAB solution (1 mg/ml). After 8 hours (total 24 HAI), the stained tissues were fixed and cleared. ROS accumulation was examined under a Leitz Fluovert microscope.

Differential transcript accumulation

RNA-Seq data were extracted from a time course of barley CI 16151 and derived fast-neutron mutants covering key stages of *Bgh* infection. First leaves were inoculated with fresh *Bgh*-conidiospores (Caldo *et al.*, 2004) and sampled from a split-plot design at 0, 16, 20, 24, 32,

and 48 HAI (5 genotypes x 6 time points x 3 biological replications) [NCBI-GEO GSE101304; (Hunt *et al.*, 2019)].

Samples were grouped by time point and analyzed using R package DESeq2 in Bioconductor (Love *et al.*, 2014). A model was fit with read counts as response, and timepoint and genotype terms as explanatory variables. Taxon-specific normalization was performed as described by (Klingenberg and Meinicke, 2017): count matrices were separated for barley and *Bgh* and size factors for DESeq2 were calculated, then those were combined to calculate the final normalized counts matrix. Differential expression analysis was done after normalization, adjusting the p-values controlling for multiple testing, using methods described by (Benjamini and Hochberg, 1995). Genes that had a log2 fold change of at least one, and were differentially expressed at a q-value of > 0.001, were considered significant.

Data Availability

Strains and plasmids are available upon request. Supplemental files available at FigShare. **Figure 2-S1** contains categorization of *Bgh* spore growth stages. **Figure 2-S2** contains phenotypes of m9450 and m9455 at 3, 5, and 7 DPI. **Figure 2-S3** phenotypes of crosses between m11526 and CI 16147 or CI 16155. **Table 2-S1** contains molecular markers used for fine mapping of *Rar3*. **Table 2-S2** contains a summary of fast-neutron mutants, phenotypes, and genes identified by them. **Table 2-S3** contains morphology data of mutant and wildtype barley under normal growing conditions. **Table 2-S4** contains measurements and analysis of *mla6*, *bln1*, and *rar3* mutants from seed-to-seed during development. **Table 2-S5** contains morphology data of mutant and wildtype barley under stressed growing conditions. **Table 2-S6** contains F2 infection type results from crosses among m11526 and other lines. **Table 2-S7**

contains expected ratios of F2 from cross m11526 (*Mla6, rar3*) and CI 16147 (*Mla7, Rar3*). **Table 2-S8** contains acronyms used.

Illumina sequence data to construct the CI 16151 reference genome are available in NCBI's Gene Expression Omnibus (GEO) under the accession number PRJNA630064. Illumina sequence data supporting the Exome capture is available under GEO accession number PRJNA645935. *HvSgt1* (HORVU3Hr1G055920) from CI 16151 and *rar3-m11526* are available under GenBank Accessions AF439974 and MT787218 respectively. RNA-Seq datasets are available in NCBI-GEO under the accession number GSE101304 (https://www.ncbi.nlm.nih.gov/gds/?term=GSE101304).

Results

m11526 (*rar3*) is developmentally equivalent to its resistant progenitor, CI 16151 (*Mla6*), and *Bgh* infection kinetics are indistinguishable from the susceptible m18982 (*mla6*)

To identify new factors in the *Mla* signaling pathway, we performed fast-neutron mutagenesis on CI 16151, which carries the *Mla6* resistance allele (Moseman, 1972), and challenged the resultant 34,800 M2 families with the avirulent *Bgh* isolate 5874 (AVR_{a6}) (Moscou *et al.*, 2011, Xu *et al.*, 2014). As shown in **Figure 2-1A**, we identified both localized (e.g., m9463, m9467 and m11542) and systemic (e.g., m9450 and m9455) cell-death mutants (**Figure 2-S2).**

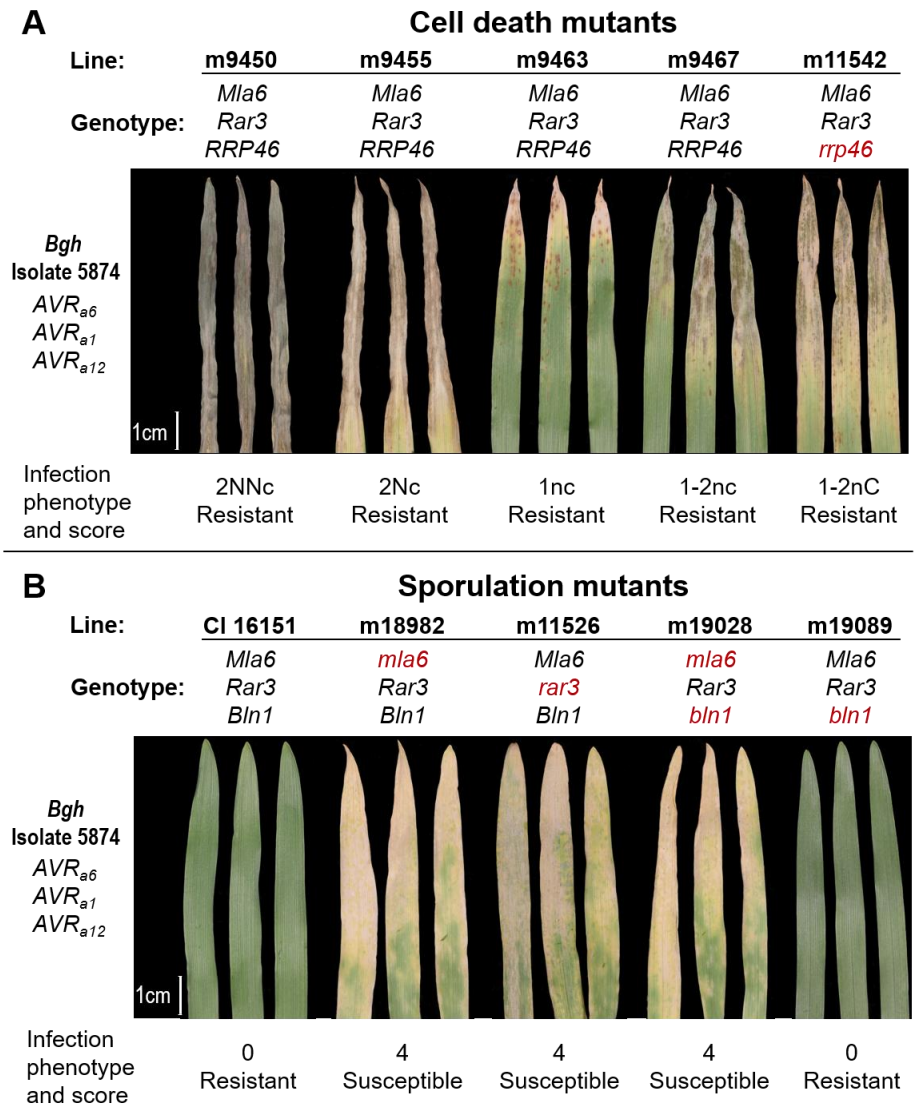

Figure 2-1. Barley line CI 16151 and its fast-neutron-derived mutants. **A**) Phenotypes of resistant mutants displaying cell death phenotypes, m9450, m9455, m9463, m9467, and m11542. The causal mutation for m11542 was previously cloned as *rrp46* (Xi *et al.*, 2009). **B**) Phenotypes of CI 16151 and the mutants displaying sporulation phenotypes, m18982, m19029, m11526, and m19089. The causal mutation present in m18982 and m19089 were previously characterized as *Mla6* (Halterman *et al.*, 2001) and *Bln1* (Meng *et al.*, 2009), respectively. Gene names indicate the presence of normal (black) or mutated (red) alleles of either *Mla6*, *Rar3*, *Bln1* or *RRP46*. Pictures show phenotypes at 7 days after inoculation with *Bgh* isolate 5874 (AVR_{a6}), with their designated macroscopic phenotype and score for sporulation. An infection type of 0 is resistant (no sporulation), 1–2 is considered resistant, but with minor *Bgh* colonization, and an infection type of 3–4 is susceptible (abundant sporulation). 1n, few small necrotic flecks (0.5 mm); 1–2n, significant small necrotic flecks (1 mm); 2N, abundant cell death (>2 mm); c, limited chlorosis; C, abundant chlorosis. Earlier timepoints for m9450 and m9455 are in **Figure 2-S2**.

Of particular interest to this report, however, were five M2 families that segregated 3 resistant (**R**; no *Bgh* colonization) to 1 susceptible (**S**; abundant *Bgh* colonization) (**Figure 2-1B**). We rescued the susceptible individuals, confirmed that they were homozygous, and established a diallel to determine complementation groups (**Table 2-S2)**. Sequencing of the *Mla6* allele in all identified mutants revealed that four of them, m9472, m9480, m11538, and m18982, possessed *Mla6* deletions (Xu *et al.*, 2014), but m11526 had no changes to *Mla6*. In addition, m11526-mediated susceptibility segregated independently from the four *mla6* mutations. Therefore, m11526 possesses a mutation in a gene other than *Mla6,* but is required for *Mla6*-specified resistance. This unknown gene was designated ***Rar3*** (*Required for Mla6 resistance 3*).

Comparisons were made between m11526 and the wild-type progenitor CI 16151 for multiple traits, as differences in these could suggest modes of action for *Rar3*. To examine developmental traits, plant height, root number and morphology, number of stem nodes, internodal distance, leaf size and leaf number were measured up to 4 weeks old (**Table 2-S3)**. In addition, plant height and number of tillers were also recorded every two weeks from seed-to-seed in the plant life cycle culminating in final number of seeds per spike, fertility, and seed weight (see Methods, **Table 2-S4).** Lastly, plants were grown under standard greenhouse conditions for 7 days and then put under dark (no light), salt (only watered with 100Mm $NaCl_2$) and drought (no watering) stress conditions (**Table 2-S5**). Height was measured for these individuals and overall phenotypes examined to see whether their macroscopic responses to stress differed. No significant differences were observed between CI 16151 and m11526 for any measured physiological characteristic, under normal or stress conditions.

To determine quantitative differences in development of *Bgh* on the different host lines, the infection kinetics of *Bgh* 5874 was scored microscopically on m11526 (*Mla6, Bln1, rar3*), m18982 (*mla6, Bln1, Rar3*) and CI 16151 leaves across a time course of primary infection. As shown in **Figure 2-2A,** we used elongating secondary hyphae (ESH) as an indicator of successful colonization, as it is a necessity to absorb nutrients from the host via functional haustoria during development (Ellingboe, 1972). Additionally, two other mutants from the same fast-neutron screen, m19089 (*Mla6*, *bln1, Rar3*) and m19028 (*mla6*, *bln1, Rar3*) were examined as resistant and susceptible controls, respectively (**Figure 2-1B**). For each genotype, 5 first leaves were harvested at 16, 20, 24, 28, 32 & 48 HAI. Leaves were cleared, stained to highlight spore development and examined under a light microscope at x5 to x20 magnification (**Figure 2-S1**). These data indicate a significant difference between the number of *Bgh* conidiospores able to successfully colonize epidermal cells when the resistant lines, CI 16151 or m19089, were compared to the susceptible lines m11526*,* m18982, or m19028. However, there was not a significant difference among the susceptible lines (**Figure 2-2B**).

Mla6-, *Mla7*- and *Mla12*-, but not *Mla1*-, *Mla9*-, *Mla10*-, and *Mla13*-mediated immunity are compromised by the *rar3* mutation

Most, but not all, *Mla*-encoded NLR variants require *Rar1* (HORVU2Hr1G097800) as part of the conserved HRS complex that influences resistance signaling (Torp and Jørgensen, 1986, Bieri *et al.*, 2004, Halterman and Wise, 2004). To determine which *Mla* alleles may be affected by the *rar3* mutation, m11526 was crossed to barley lines harboring a range of *Mla* alleles (Moseman, 1972), and the resultant F1 were self-pollinated to make large F2 populations. F2 segregants were analyzed 7 days after infection with the appropriate *Bgh* isolate (5874: AVR_{a1}, AVR_{a6} and AVR_{a12}, or CC148: AVR_{a1}, AVR_{a7}, AVR_{a9}, AVR_{a10} and AVR_{a13}) and chi-square tests were

used to ascertain whether the observed ratios differed significantly from the expected genetic interactions.

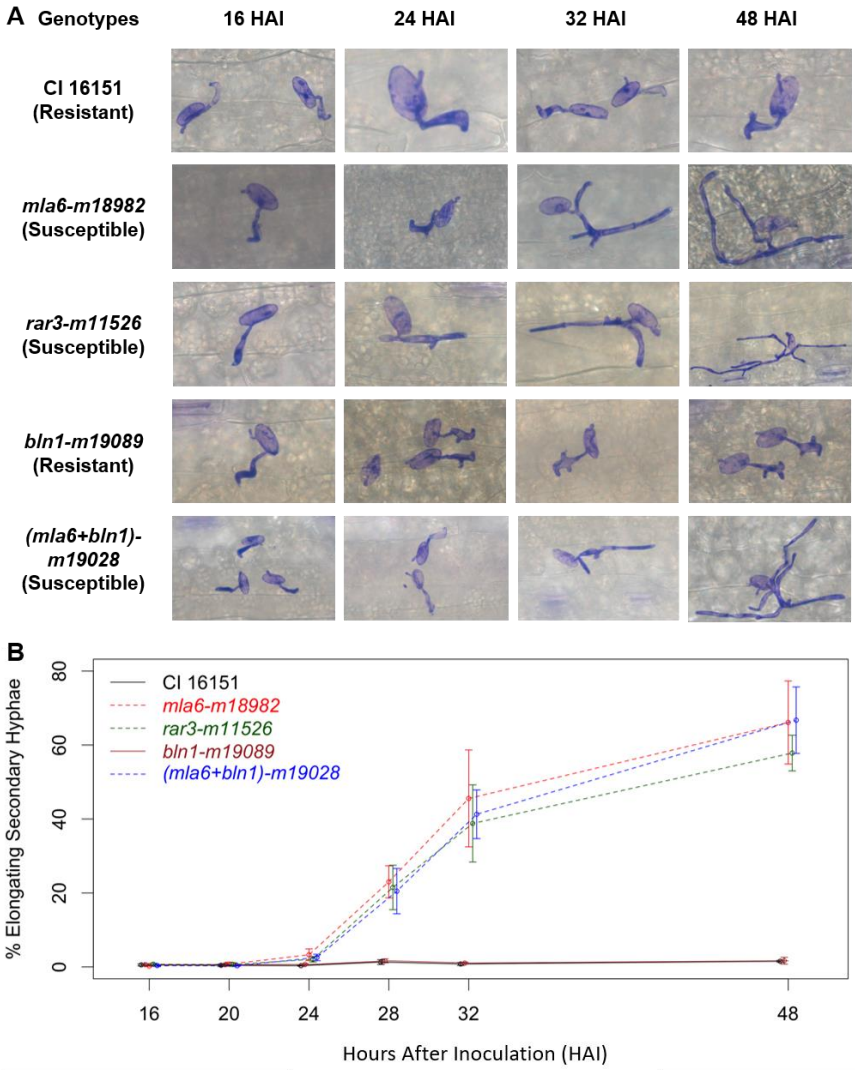

Figure 2-2. Percentage elongating secondary hyphae (ESH) from *Bgh* isolate 5874 measured at six time points on CI 16151 and its derived mutant genotypes. **A**) Microscopic images at 20x magnification of four time points (16, 24, 32 and 48 HAI) for each genotype. **B**) Time-course graphs representing infection kinetics of *Bgh* on resistant and susceptible genotypes. The x-axis represents the time points at which measurements were taken (Hours after inoculation, HAI) and the y-axis represents the percentage elongating secondary hyphae (which indicate successful colonization events (Ellingboe, 1972)). The percentage elongating secondary hyphae was calculated as 100 x (Sum of three hyphal indices / Total). Total is sum of spore, appressorium and the three hyphal indices. The dashed and solid lines represent the susceptible and resistant genotypes, respectively. Error bars indicate one standard deviation.

First, to verify that the m11526 phenotype is caused by a single locus, we examined the F2 progeny from crosses m11526 x CI 16151 (*Mla6*), m11526 x P03 (Pallas with introgressed *Mla6*), and m11526 x Sultan-5 (*Mla12*). F2 progeny from these three crosses all segregated 3R:1S (p=0.16, 0.68, and 0.77 respectively) as expected for a single gene (**Figure 2-3**). Second, to test whether *Rar3* segregates independently of *Mla6* and *Rar1*, we examined F2 progeny from crosses among the susceptible lines, m11526 x m9472 (*mla6*, *Rar1*, *Rar3*) and m11526 x *rar1*-m100 (*Mla12*, *rar1, Rar3*). The 9R:7S phenotypic ratios resulting from the cross to m9472 (p=0.68) did not differ significantly from what was expected for independent segregation. Though the m100 cross did not produce the expected 9R:7S ratio for independently segregating genes (p=0.015), it also did not fit the 1R:1S ratio expected for linked genes (p=0.000), suggesting that *Rar1* and *Rar3* are unlinked. In fact, the ratio of 11R:5S which generated more resistant F2 than predicted, suggests some genetic combination that confers greater resistance overall. This may involve some contribution from the Sultan-5 background interacting with the *rar1* or *rar3* loci.

Segregation ratios produced from crosses of m11526 to lines carrying *Mla1* (CI 16137 and Q21861, 15R:1S), *Mla9* (Hor11358, 3R:1S), and *Mla13* (CI 16155, 3R:1S) suggest that these alleles do not require *Rar3* to function as they segregate as dominant genes (**Figure 2-3; Table 2-S6**). Though the CI 16149 (*Mla10*) F2 ratio did not significantly fit any of the models, the closest applicable ratios were a 3R:1S at p=0.004 and 1R:2Sn:1S at p=0.015, which would suggest a *Rar3*-independent, semi-dominant model. Additionally, while *Mla9*, *Mla10* and *Mla13* do not appear to require *Rar3* to function (**Figure 2-3**), they do require *Rar1* (Halterman and Wise, 2004).

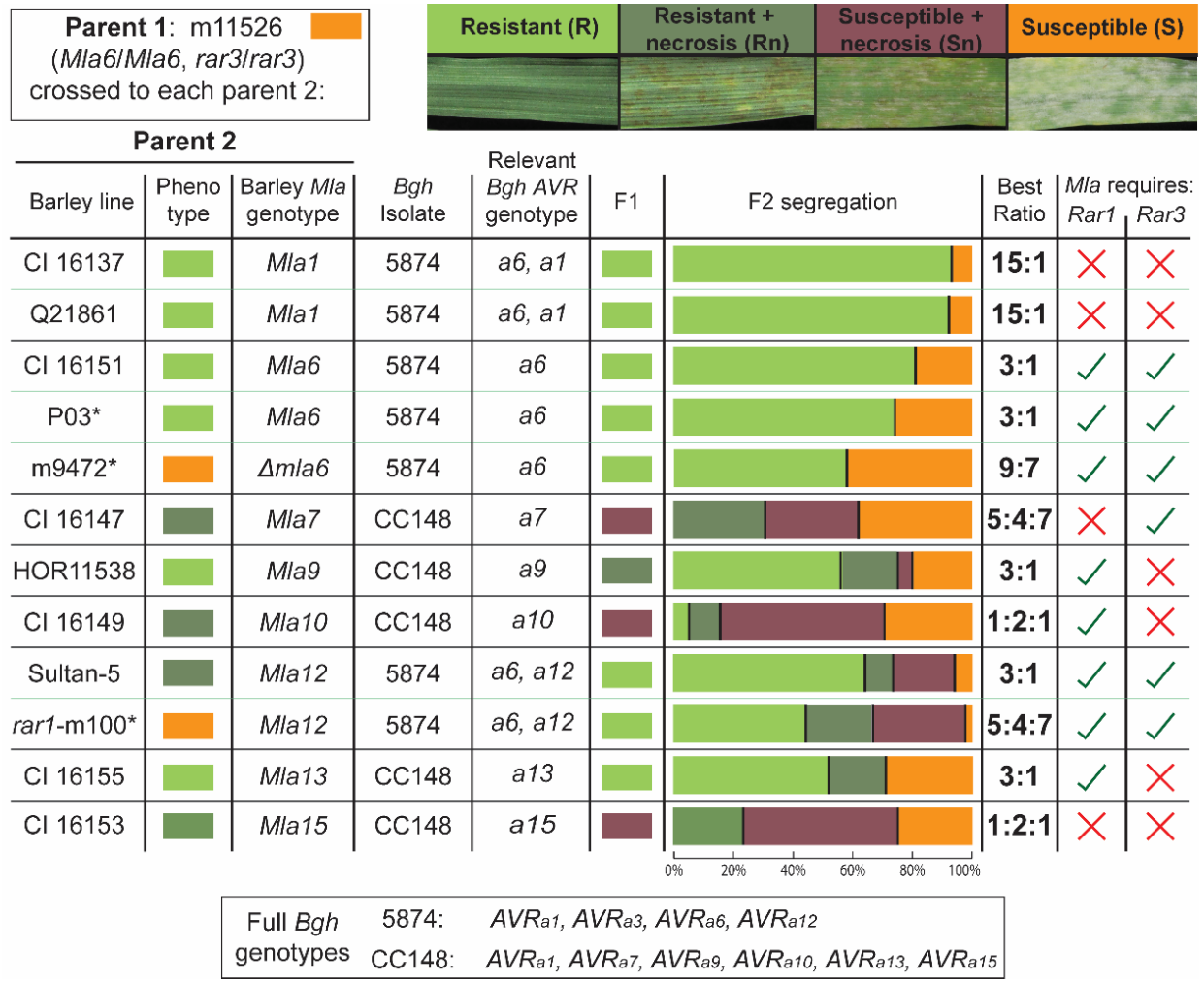

Figure 2-3. F2 segregation results from crosses between m11526 (*Mla6*, *rar3*) and multiple near-isogenic or diverse *Mla*-carrying lines. As *Bgh* isolates with different *AVR* genes were used, the *Bgh AVR* genes relevant to a cross are indicated under "Relevant *Bgh AVR* genotype" and the AVR_a genotypes of each strain are displayed in the box below. Representative images for each plant infection phenotype are shown above the table. Raw percentages of F2 populations are displayed, and a chi-squared test was used to determine which of the potential segregation ratios was most suitable according to the lowest P value. Ticks and X's are used to show whether an *Mla* variant appears to, or not to, require the indicated gene, respectively. * P03 (Pallas background, *Mla6* (Kolster *et al.*, 1986)), m9472 (CI 16151-derived fast-neutron mutant, *mla6*), m100 (Sultan-5 background, *Mla12*, *rar1* (Torp and Jørgensen, 1986)). Raw data is documented in **Table 2-S6.**

Curiously, the m11526 x CI 16147 (*Mla7*), HOR11358 (*Mla9*), and CI 16153 (*Mla15*) crosses generated F1 hybrids with a different phenotype to either of the parents. The m11526 x HOR11358 (*Mla9*) F1 displays a resistant with necrosis (Rn) phenotype, and there is a small

number of F2 that display susceptible with necrosis (Sn) phenotypes. Together these observations suggest that the *rar3* mutation may lessen the strength of the *Mla9* resistance, but not to an extent to overtly change the phenotype, i.e., *rar3* converts resistant (R) phenotype to Rn, instead of susceptible (S). Crosses to CI 16149 (*Mla10*) also generated F1 with the intermediate susceptible with necrosis phenotype but this is due to *Mla10* being semi-dominant, which does not seem to be dependent on *Rar3*. The F2 phenotypic ratios resulting from m11526 x CI 16147 (*Mla7*) suggest that *Mla7* does require *Rar3* to fully function (5R:11S P=0.83, 5Rn:4Sn:7S p=0.09). Together with the observation of intermediate function in the F1 (**Figure 2-S3**), these F2 phenotypic ratios suggest a dosage dependence model whereby *Mla7* partially requires *Rar3* to function. This model would indicate that when both loci have only a single functioning allele, the resistance does not reach a threshold necessary to prevent colonization (see **Table 2-S7** for table showing hypothetical models).

The cross between m11526 and CI 16153 (*Mla15*) may shed light on the interaction between *Mla7* and *Rar3*. *Mla7* and *Mla15* share the same sequence but appear to act slightly differently, as evidenced by *Bgh* infection kinetics (Wise and Ellingboe, 1983), and also by interpretation of the different segregation ratios. Whereas the *Mla7* cross generated a ratio of 5R:11S, or if we take necrosis into account 5Rn:4Sn:7S, the *Mla15* cross generated the ratio 1R:3S, or 1Rn:2Sn:1S, indicating a single semi-dominant gene.

Bulk segregant analysis with exome capture positions *rar3* on chromosome 3HL

At 5 Gb, the large and repetitive barley genome can be a challenge for isolating unknown genes (Mascher *et al.*, 2017). To overcome these challenges and position *rar3* in

m11526, we used a capture approach with ~2 million exome probes to reduce the sequenced portion of the genome to about 61.6 Mb (Mascher *et al.*, 2013).

Then, in order to generate a large set of diverse SNPs for exome capture, we generated F2 populations from the m11526 x P03 (*Mla6*) and m11526 x Sultan-5 (*Mla12*) F1 hybrids. These populations were selected because **1**) both *Mla6* and *Mla12* require *Rar3* for resistance function and **2**) P03 and Sultan-5 are two-row European lines that have genetic backgrounds distinct from the 6-row Manchuria background in CI 16151 and its m11526 derivative. Two-hundred segregating F2 progeny from each population were challenged with *Bgh* 5874 (AVR_{a6}, AVR_{a12}) and scored for resistance or susceptibility, creating four distinct groups based on genetic cross and infection phenotype. Both populations segregated 3R:1S as shown in **Figure 2-3**. DNA extractions were performed on tissue pooled from leaves within each group, amplified using the standard exome capture method and sent for Illumina sequencing.

Nearly 450,000 SNPs were generated from the exome capture and aligned to the barley reference genome (IBSC_V2, (Mascher et al., 2017)), as well as our reference genome for CI 16151 (PRJNA630064). For each SNP, the number of reads with SNP's matching the reference genome (reference SNPs) were measured for each group as a proportion of the total number of reads for each SNP location. SNPs that did not match the reference genome (alternative SNPs) must either be from the alternative parent (either P03 or Sultan-5), novel mutations in m11526, or sequencing errors which were filtered from the data set. The SNP frequencies in each pool were averaged over 5Mb intervals to reduce noise, and then plotted across the seven chromosomes. The results for most chromosomes did not display any major differences between the frequencies of resistant and susceptible pools in either cross. However,

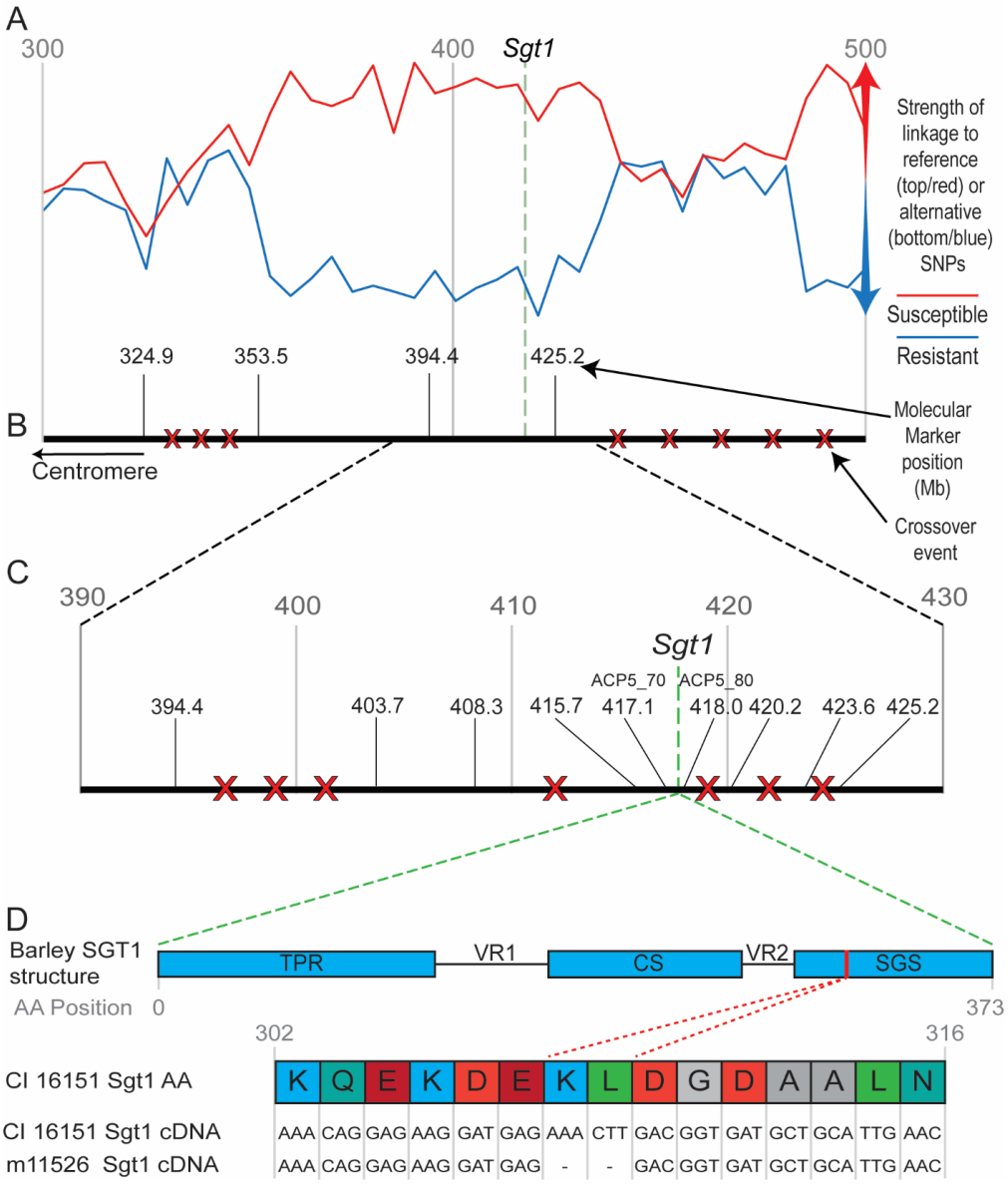

Figure 2-4. Mapping of the *Rar3* cosegregating region to chromosome 3H. **A**) Results of the exome capture allele frequencies. Allele frequencies were determined relative to proportion of reads that had SNPs which mapped to the reference genome, out of the total number of reads. Allele frequencies were averaged over 5Mb for the resistant and susceptible pools prior to plotting. Red and blue lines indicate allele frequencies for susceptible and resistant pools respectively. **B**) Physical map of chromosome 3H, Mb locations of genetic markers is indicated by black vertical lines with numbers. The orientation of the centromere is indicated by an arrow. The number of X's represent the number of observed crossover events between the flanking markers. The position of *Sgt1* is shown with a green dashed line at position 417.32Mb. **C**) Zoomed in location of closest flanking markers to *Sgt1*. **D**) Alignment of wildtype and m11526 *Sgt1* cDNA sequences covering the region containing the *rar3-m11526* mutation. Protein alignment and structure included for reference, red dashed line indicates location of mutation.

chromosome 3H revealed multiple regions where the resistant and susceptible frequencies diverged considerably, suggesting regions that may cosegregate with the observed phenotypes (Figure 2-4A).

High-resolution recombination mapping delineates *Rar3* to 12Mb on Chr 3H flanking *Sgt1*

To fine-map the *Rar3* locus, Cleaved Amplified Polymorphic Sequence (CAPS) markers were designed spanning chromosome 3H and tested on a small m11526 x P03 F2 population of 94 individuals. Markers with the closest linkage to *Rar3* were between ~325Mb and ~450Mb, which coincided with the largest co-segregating region from the exome capture. Fine mapping, using CAPS markers on 3470 m11526 x P03 F2 individuals, identified 15 recombination events that reduced the co-segregating region to between 408.3Mb (HORVU3Hr1G054770) and 420.2Mb (HORVU3Hr1G056080) on chromosome 3H (**Figure 2-4C**). This region contains 67 predicted genes, according to Ensembl, Assembly IBSC_V2, (annotations by the International Barley Sequencing Consortium, IBSC). Reads generated by the capture protocol aligned to each of the genes within the entire 12Mb co-segregating region, and the only difference between CI 16151 and m11526 was a small deletion in HORVU3Hr1G055920, corresponding to *Sgt1* (GenBank: AF439974.1). Subsequent re-isolation of full-length *Sgt1* from both m11526 and CI 16151 cDNA confirmed the 6bp in-frame deletion to be at position 922-927bp (**Figure 2-4D**). This comprises exactly two amino acids, lysine (K) 308 and leucine (L) 309 in the SGS-domain, the domain that directly interacts with NLRs (Zhang *et al.*, 2008). These data indicate that the $Sgt1_{\Delta KL308\text{-}309}$ mutation in m11526, as delineated by recombination, is the only candidate for causing susceptibility.

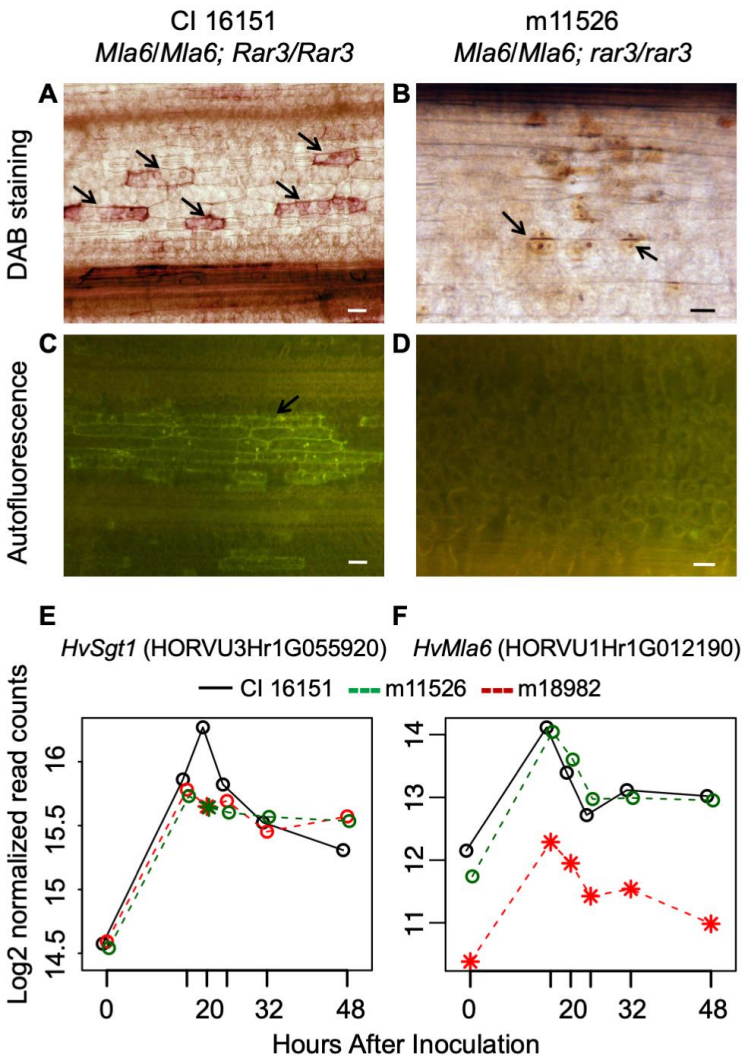

Figure 2-5. *Rar3* is required for *Mla*-mediated H_2O_2 accumulation and the hypersensitive reaction (HR). **A**) H_2O_2 accumulation evidenced by intense brown coloration produced by 3,3'-diaminobenzidine (DAB) staining in epidermal cells from CI 16151 (*Mla6*) at 24 HAI with *Bgh* isolate 5874 (AVR_{a6}). Bar, 25 µm. **B**) Decreased accumulation of H_2O_2, as indicated by fewer, and less intense, DAB-stained (brown) cells, was observed in the m11526 loss-of-function mutant. **C**) Consistent with ROS accumulation, whole-cell autofluorescence is observed in epidermal cells from wild-type CI 16151 at 24 HAI with *Bgh* isolate 5874 (AVR_{a6}). Bar, 25 µm. **D**) Autofluorescence was absent in the m11526 loss-of-function mutant. **E**) Transcript accumulation of *Sgt1* (HORVU3Hr1G055920) in wild-type CI 16151 (black solid lines) vs. m11526 (dashed green lines) and m18982 (dashed red lines). * indicates significant difference from CI 16151 at $P < 0.001$. **F**) Transcript accumulation of *Mla6* (HORVU1Hr1G012190) in wild-type CI 16151 vs. m11526.

The Lys-Leu deletion is associated with disruption of H_2O_2 accumulation and hypersensitive cell death

Rapid localized cell death, termed the hypersensitive reaction or HR, is often elicited by host recognition of invading pathogens. One of the major components of HR is the generation of reactive oxygen species (ROS), such as hydrogen peroxide (H_2O_2), which act as late stage signaling molecules (Lehmann *et al.*, 2015). Moreover, flavonoids, which function as antimicrobials, are often released as part of plant defense responses and will autofluoresce when examined under green fluorescence protein microscope filters (Cushnie and Lamb, 2011). We investigated whether the *rar3* mutation disrupted accumulation of H_2O_2 by DAB (3,3'-diaminobenzidine) staining. We observed obvious accumulation of H_2O_2 in *Bgh* challenged epidermal cells for CI 16151 (**Figure 2-5A**), but not in the m11526 loss-of-function mutant (**Figure 2-5B**). Moreover, while we see rampant autofluorescence in and around cells challenged by *Bgh* in CI 16151 (**Figure 2-5C**), we did not observe any autofluorescence in m11526 (**Figure 2-5D**).

Expression of *Sgt1* in CI 16151 and the *rar3* mutant m11526

Coincident with the absence of H_2O_2 accumulation and HR, we considered that accumulation of *Sgt1* transcripts may differ in the m11526 mutant as compared to its CI 16151 progenitor. As shown in **Figure 2-5E**, RNA transcript profiling revealed that *Sgt1* was significantly differentially expressed at 20 HAI just after *Bgh* penetration, but prior to development of haustoria, with marked up-regulation in CI 16151 plants as compared to the m11526 loss-of-function mutant (p-value cutoff = 0.001). However, when we compared the expression of *Sgt1* in m11526 at 20 HAI to the susceptible mutant m18982 (*mla6*), there was no significant difference. This suggests that the change in expression of *Sgt1* at 20 HAI may not be

directly attributed to the *rar3* mutation, but is indirectly associated with susceptibility, per se. Subsequently, transcript levels decreased post penetration at 24 – 48 HAI in wild-type plants but stabilize for the m11526 mutant. As expected, transcript accumulation was equivalent for the *Mla6* NLR in CI 16151 and m11526 (**Figure 2-5F**). Though there appeared to be some residual expression attributed to *Mla6* in the m18982 deletion mutant, this may be due to confounding by reads from *Mla6* paralogs present in the progenitor CI 16151 mapping to this gene.

Discussion

Sgt1$_{\Delta KL308\text{-}309}$ joins a list of invaluable mutants for elucidating molecular functions.

Phenotypes observed by mutagenesis often result from deletions of sections of DNA that result in loss of whole genes, frame shifts, truncations, and/or loss of functionality. However, substitutions of two, or even a single amino acid, can have a profound effect on protein function. For example, targeted in-frame deletions have been critical to unraveling complex dystrophin phenotypes of Duchenne/Becker muscular dystrophy (Aartsma-Rus *et al.*, 2006, Bello *et al.*, 2016). A single amino acid change in the envelope protein gene, E1-A226V, is responsible for Chikungunya virus adaptation to *Aedes albopictus* mosquitoes, resulting in increased host range and associated with a 2006 epidemic on Reunion island (Tsetsarkin *et al.*, 2007). Likewise, a two-amino acid difference in the coat protein of *Satellite panicum mosaic virus* is responsible for differential synergistic interactions with *Panicum mosaic virus* (Chowda-Reddy *et al.*, 2019). Moreover, a single G to D substitution in sedoheptulose 1,7-bisphosphatase reduces growth and yield in rice, (Li *et al.*, 2020) and a double L92A/I94A mutation in the gravitropism gene LAZY1 changed direction of auxin accumulation relative to gravity in

Arabidopsis (Yoshihara and Spalding, 2020). In barley, a single G to D substitution in MLA6 or MLA13 at position 721 alters the requirement for the co-chaperone RAR1 for resistance to powdery mildew (Halterman and Wise, 2004).

To further characterize NLR-based disease defense, a fast-neutron screen was used to identify *rar3-m11526*, a mutant that compromises *Mla6*-, *Mla7*- and *Mla12*-mediated immunity, but does not disrupt resistance specified by *Mla1*, *Mla9*, *Mla10* or *Mla13*. This is reminiscent of the differential requirement of *Mla* alleles for *Rar1,* but the allele set that requires *Rar3* is divergent from that of *Rar1* (Shirasu *et al.*, 1999, Shen *et al.*, 2003, Bieri *et al.*, 2004, Halterman and Wise, 2004)*,* and *Rar3* segregates independently of both *Mla6* and *Rar1*. Furthermore, though some of the alleles, such as *Mla9*, may not fully require *Rar3* to function, the *rar3* mutation does appear to lessen the strength of their resistance, evidenced by the appearance of the new resistant with necrosis phenotype of the F1 heterozygote. We delineated the causal mutation to a 6bp (Lys-Leu) in-frame deletion within the SGS domain of *Sgt1* (*Sgt1*$_{\Delta KL308\text{-}309}$), the structural region that interacts with NLR proteins (Zhang *et al.*, 2008). SGT1 is a highly conserved protein that is essential for life processes including growth, development, kinetochore formation, auxin and jasmonate recognition, in addition to disease defense (Kitagawa *et al.*, 1999, Gray *et al.*, 2003, Hoser *et al.*, 2013, Zhang *et al.*, 2015b). Most diploids like barley have a single copy of *Sgt1*, though *Arabidopsis* and soybean have two copies that have diverged enough to not be entirely redundant (Austin *et al.*, 2002, Fu *et al.*, 2009).

Potential molecular effects of the ΔKL308-309 mutation on *Sgt1*

Stable silencing of *Sgt1* in *N. benthamiana* and hexaploid wheat results in severely stunted growth (Peart *et al.*, 2002, Wang *et al.*, 2015a) and is lethal in rice and tomato

(Bhattarai *et al.*, 2007, Thao *et al.*, 2007). Furthermore, lethality is common for *Sgt1* mutants, including Arabidopsis double mutants, (Azevedo *et al.*, 2006) and transposon insertions in Drosophila (Martins *et al.*, 2009). Even a single change in the phosphomimic SGT1-S361D is enough for lethality in yeast and human cells (Bansal *et al.*, 2009). Transient virus-induced-gene silencing of *Sgt1* in barley by barley stripe mosaic virus (BSMV) does not lead to any obvious growth defects, however, it is suggested that this could be because the virus' used in other systems are able to infect meristematic tissue and thus cause silencing at an earlier stage of shoot development (Hein *et al.*, 2005).

Protein structure prediction with iTasser (Yang *et al.*, 2015) found little difference in the structure of the SGS domain between wildtype SGT1 and $SGT1_{\Delta KL308\text{-}309}$. Furthermore, X-ray crystallography showed that the SGS region of SGT1 is highly disordered as it lacks a fixed tertiary structure (Dunker *et al.*, 2008, Taube *et al.*, 2014). This decreases the likelihood that a two-amino-acid mutation could disorder the tertiary structure any further. These suggest that the difference in phenotype is not due to misfolding, but rather the loss of function that is tied directly to one or both of the deleted amino acids.

SGT1 consists of three highly conserved functional domains, the tetratricopeptide repeat (TPR), CHORD and *Sgt1* (CS) and *Sgt*-specific (SGS) domains, separated by two unconserved variable (Vr) domains (Zhang *et al.*, 2008). The SGS domain is responsible for interacting with the LRR domain of MLA proteins and is necessary for SGT1-mediated accumulation of resistance proteins (Boter *et al.*, 2007, Shirasu, 2009). As lysines are known to be involved in protein-protein interactions by creating salt bridges, the K308 could be an important residue specifically for the interaction between MLA and SGT1. Moreover, the SGS

region is not involved in kinetochore function or implicated in growth, which would explain why the plant appears to grow normally.

Genetic analysis of m11526 crossed to lines with various *Mla* alleles uncovered that, even though the susceptibility phenotype was similar to that of plants that contained *rar1*, those *Mla* alleles which required *Rar3* were different (**Figure 2-3**). Having now discovered that the *rar3-m11526* mutation is in the SGS domain of SGT1, we can look at the results of these crosses in a different light. If we consider that the requirement for RAR1 may be a need for a molecular "crutch" to assist the interaction with SGT1, we can rate MLA variants for how strongly they interact with SGT1 by their need for RAR1 and "RAR3". MLA1 would be the strongest interactor by not requiring either, whereas MLA7, MLA10 and MLA13 would be intermediate for only requiring one or the other and MLA6 and MLA12 would be the weakest by requiring both. MLA7 and MLA10 could be considered lesser interactors due to their necrotic phenotype, which is indicative of a late defense response, also known as trailing necrosis (Morel and Dangl, 1999). However, MLA7 and MLA10 have amino acid differences in the highly conserved CC domain (108LE insertion and E41D respectively), the region that associates with transcription factors to transmit the defense response, which are not present in other variants tested here. Therefore, the necrotic phenotypes may be caused by the signal not being transduced effectively after being initiated due to reduced binding with transcription factors.

By mining an RNA transcript profiling dataset, we observed a difference in *Sgt1* expression that does not appear to be caused directly by the *rar3* deletion. Indeed, the expression profile of *Sgt1* was not significantly different when m11526 was compared to the susceptible *mla6* mutant m18982 (**Figure 2-5F**), suggesting the difference in expression is

associated with susceptibility. Thus, our current hypothesis is that the SGT1$_{\Delta KL308\text{-}309}$ mutation appears to affect the function of SGT1 protein, and other proteins that interact with its SGS domain, such as COI1, HSC70 (Noël *et al.*, 2007), or perhaps an unknown interactor, rather than transcript accumulation of *Sgt1* (or *Mla6*). However, there may be a feedback or feed forward mechanism that indirectly affects the accumulation of transcripts.

Conclusion

To date, research on *Sgt1* has been hindered by the fact that all organisms are unable to survive when it has been deleted. Notable exceptions to this requirement are yeast and organisms that have evolved duplicates, such as Arabidopsis, though these organisms would not be able to survive without all duplicates so it's questionable whether they are in fact exceptions. The data presented here indicates that the *rar3* mutation, *Sgt1$_{\Delta KL308\text{-}309}$*, affects only interactions involved in disease resistance, while leaving other *Sgt1*-mediated processes intact.

The observation that the necessity of SGT1 by NLRs can be localized to a single protein domain provides a framework for other genes that interact with the SGS domain. For example, targeting *Sgt1$_{\Delta KL308\text{-}309}$* by directed CRISPR-Cas editing could uncover how SGT1 interacts with proteins for Sr33-mediated Ug99 stem rust- (Periyannan *et al.*, 2013) or Lr21-specified leaf rust resistance in wheat (Scofield *et al.*, 2005, Huang *et al.*, 2009). Recently, pathogen effectors have been identified that specifically target the HRS machinery, such as RipAC in *Ralstonia solanacearum* that interacts with the SGS domain to block interactions with MAP kinases (Yu *et al.*, 2020). By understanding how plant and fungal proteins specifically interact with SGT1, it could be possible to engineer crops with SGT1 variants without fungal effector interaction sites, whilst maintaining interactions with resistance proteins.

References

Aartsma-Rus, A., Van Deutekom, J.C.T., Fokkema, I.F., Van Ommen, G.-J.B. and Den Dunnen, J.T. (2006) Entries in the Leiden Duchenne muscular dystrophy mutation database: An overview of mutation types and paradoxical cases that confirm the reading-frame rule. *Muscle & Nerve*, 34, 135-144.

Austin, M.J., Muskett, P., Kahn, K., Feys, B.J., Jones, J.D.G. and Parker, J.E. (2002) Regulatory role of SGT1 in early R gene-mediated plant defenses. *Science*, 295, 2077-2080.

Azevedo, C., Betsuyaku, S., Peart, J., Takahashi, A., Noël, L., Sadanandom, A., Casais, C., Parker, J. and Shirasu, K. (2006) Role of SGT1 in resistance protein accumulation in plant immunity. *The EMBO Journal*, 25, 2007-2016.

Bai, S., Liu, J., Chang, C., Zhang, L., Maekawa, T., Wang, Q., Xiao, W., Liu, Y., Chai, J., Takken, F.L., Schulze-Lefert, P. and Shen, Q.H. (2012) Structure-function analysis of barley NLR immune receptor MLA10 reveals its cell compartment specific activity in cell death and disease resistance. *PLoS Pathogens*, 8, e1002752.

Bansal, P.K., Mishra, A., High, A.A., Abdulle, R. and Kitagawa, K. (2009) Sgt1 dimerization is negatively regulated by protein kinase CK2-mediated phosphorylation at Ser^{361}. *Journal of Biological Chemistry*, 284, 18692-18698.

Bello, L., Campadello, P., Barp, A., Fanin, M., Semplicini, C., Sorarù, G., Caumo, L., Calore, C., Angelini, C. and Pegoraro, E. (2016) Functional changes in Becker muscular dystrophy: implications for clinical trials in dystrophinopathies. *Scientific Reports*, 6, 32439.

Benjamini, Y. and Hochberg, Y. (1995) Controlling the false discovery rate: a practical and powerful approach to multiple testing. *Journal of the Royal Statistical Society: Series B (Methodological)*, 57, 289-300.

Bhattarai, K.K., Li, Q., Liu, Y., Dinesh-Kumar, S.P. and Kaloshian, I. (2007) *Mi-1*-mediated pest resistance requires *Hsp90* and *Sgt1*. *Plant Physiology*, 144, 312-323.

Bieri, S., Mauch, S., Shen, Q.-H., Peart, J., Devoto, A., Casais, C., Ceron, F., Schulze, S., Steinbiss, H.-H., Shirasu, K. and Schulze-Lefert, P. (2004) RAR1 positively controls steady state levels of barley MLA resistance proteins and enables sufficient MLA6 accumulation for effective resistance. *The Plant Cell*, 16, 3480-3495.

Boter, M., Amigues, B., Peart, J., Breuer, C., Kadota, Y., Casais, C., Moore, G., Kleanthous, C., Ochsenbein, F., Shirasu, K. and Guerois, R. (2007) Structural and functional analysis of SGT1 reveals that its interaction with HSP90 is required for the accumulation of Rx, an R protein involved in plant immunity. *The Plant Cell*, 19, 3791-3804.

Caldo, R.A., Nettleton, D. and Wise, R.P. (2004) Interaction-dependent gene expression in *Mla*-specified response to barley powdery mildew. *The Plant Cell*, 16, 2514-2528.

Cesari, S., Moore, J., Chen, C., Webb, D., Periyannan, S., Mago, R., Bernoux, M., Lagudah, E.S. and Dodds, P.N. (2016) Cytosolic activation of cell death and stem rust resistance by cereal MLA-family CC–NLR proteins. *PNAS*, 113, 10204-10209.

Chang, C., Yu, D., Jiao, J., Jing, S., Schulze-Lefert, P. and Shen, Q.-H. (2013) Barley MLA immune receptors directly interfere with antagonistically acting transcription factors to initiate disease resistance signaling. *The Plant Cell*, 25, 1158-1173.

Chowda-Reddy, R.V., Palmer, N., Edme, S., Sarath, G., Kovacs, F., Yuen, G., Mitchell, R. and Tatineni, S. (2019) A Two-Amino Acid Difference in the Coat Protein of Satellite panicum mosaic virus Isolates Is Responsible for Differential Synergistic Interactions with Panicum mosaic virus. *MPMI*, 32, 479-490.

Cushnie, T.P.T. and Lamb, A.J. (2011) Recent advances in understanding the antibacterial properties of flavonoids. *International Journal of Antimicrobial Agents*, 38, 99-107.

Draz, I.S., Esmail, S.M., Abou-Zeid, M.A.E.-H. and Essa, T.A.E.-M. (2019) Powdery mildew susceptibility of spring wheat cultivars as a major constraint on grain yield. *Annals of Agricultural Sciences*, 64, 39-45.

Dunker, A.K., Silman, I., Uversky, V.N. and Sussman, J.L. (2008) Function and structure of inherently disordered proteins. *Current Opinion in Structural Biology*, 18, 756-764.

Ellingboe, A.H. (1972) Genetics and physiology of primary infection by *Erysiphe graminis*. *Phytopathology*, 62, 401-406.

Fu, D.-Q., Ghabrial, S. and Kachroo, A. (2009) GmRAR1 and GmSGT1 are required for basal, R gene-mediated and systemic acquired resistance in soybean. *MPMI*, 22, 86-95.

Gietz, R.D. (2014) Yeast transformation by the LiAc/SS carrier DNA/PEG method. *Methods Mol Biol*, 1205, 1-12.

Graves, S., Piepho, H.-P., Selzer, L. and Dorai-Raj, S. (2019) multcompView: Visualizations of paired comparisons: R package version 0.1-8.

Gray, W.M., Muskett, P.R., Chuang, H.-W. and Parker, J.E. (2003) Arabidopsis SGT1b is required for SCF-TIR-1-mediated auxin response. *The Plant Cell*, 15, 1310-1319.

Halterman, D., Zhou, F., Wei, F., Wise, R.P. and Schulze-Lefert, P. (2001) The MLA6 coiled-coil, NBS-LRR protein confers *AvrMla6*-dependent resistance specificity to *Blumeria graminis* f. sp. *hordei* in barley and wheat. *The Plant Journal*, 25, 335-348.

Halterman, D.A. and Wise, R.P. (2004) A single-amino acid substitution in the sixth leucine-rich repeat of barley MLA6 and MLA13 alleviates dependence on RAR1 for disease resistance signaling. *The Plant Journal*, 38, 215-226.

Hein, I., Barciszewska-Pacak, M., Hrubikova, K., Williamson, S., Dinesen, M., Soenderby, I.E., Sundar, S., Jarmolowski, A., Shirasu, K. and Lacomme, C. (2005) Virus-induced gene silencing-based functional characterization of genes associated with powdery mildew resistance in barley. *Plant Physiology*, 138, 2155-2164.

Hoser, R., Zurczak, M., Lichocka, M., Zuzga, S., Dadlez, M., Samuel, M.A., Ellis, B.E., Stuttmann, J., Parker, J.E., Hennig, J. and Krzymowska, M. (2013) Nucleocytoplasmic partitioning of tobacco N receptor is modulated by SGT1. *The New Phytologist*, 200, 158-171.

Huang, L., Brooks, S., Li, W., Fellers, J., Nelson, J.C. and Gill, B. (2009) Evolution of new disease specificity at a simple resistance locus in a crop-weed complex: reconstitution of the *Lr21* gene in wheat. *Genetics*, 182, 595-602.

Hunt, M., Banerjee, S., Surana, P., Liu, M., Fuerst, G., Mathioni, S., Meyers, B.C., Nettleton, D. and Wise, R.P. (2019) Small RNA discovery in the interaction between barley and the powdery mildew pathogen. *BMC Genomics*, 20, 610.

Jaswal, R., Kiran, K., Rajarammohan, S., Dubey, H., Singh, P.K., Sharma, Y., Deshmukh, R., Sonah, H., Gupta, N. and Sharma, T.R. (2020) Effector biology of biotrophic plant fungal pathogens: Current advances and future prospects. *Microbiological Research*, 241, 126567.

Jordan, T., Seeholzer, S., Schwizer, S., Töller, A., Somssich, I.E. and Keller, B. (2011) The wheat *Mla* homologue *TmMla1* exhibits an evolutionarily conserved function against powdery mildew in both wheat and barley. *The Plant Journal*, 65, 610-621.

Kitagawa, K., Skowyra, D., Elledge, S.J., Harper, J.W. and Hieter, P. (1999) SGT1 Encodes an essential component of the yeast kinetochore assembly pathway and a novel subunit of the SCF ubiquitin ligase complex. *Molecular Cell*, 4, 21-33.

Klingenberg, H. and Meinicke, P. (2017) How to normalize metatranscriptomic count data for differential expression analysis. *PeerJ*, 5, e3859.

Kolster, P., Munk, L., Stolen, O. and Lohde, J. (1986) Near-isogenic barley lines with genes for resistance to powdery mildew. *Crop Breeding, Genetics & Cytology*, 903-907.

Kourelis, J. and van der Hoorn, R.A.L. (2018) Defended to the nines: 25 years of resistance gene cloning identifies nine mechanisms for R protein function. *The Plant Cell*, 30, 285-299.

Krattinger, S.G. and Keller, B. (2016) Molecular genetics and evolution of disease resistance in cereals. *New Phytologist*, 212, 320-332.

Kwaaitaal, M., Nielsen, M.E., Böhlenius, H. and Thordal-Christensen, H. (2017) The plant membrane surrounding powdery mildew haustoria shares properties with the endoplasmic reticulum membrane. *Journal of Experimental Botany*, 68, 5731-5743.

Langin, G., Gouguet, P. and Üstün, S. (2020) Microbial effector proteins – A journey through the proteolytic landscape. *Trends in Microbiology*, 28, 523-535.

Lehmann, S., Serrano, M., L'Haridon, F., Tjamos, S.E. and Metraux, J.-P. (2015) Reactive oxygen species and plant resistance to fungal pathogens. *Phytochemistry*, 112, 54-62.

Lenth, R.V. (2016) Least-Squares Means: The R Package lsmeans. *Journal of Statistical Software*, 69, 33.

Li, C., Li, N., Huang, R., Chen, C., Guo, J., Yang, X., Zhang, X., Sun, C., Deng, X. and Wang, P. (2020) A single nucleotide substitution at the 3'-end of SBPase gene involved in Calvin cycle severely affects plant growth and grain yield in rice. *BMC Plant Biology*, 20.

Li, H. and Durbin, R. (2009) Fast and accurate short read alignment with Burrows–Wheeler transform. *Bioinformatics*, 25, 1754-1760.

Lo Presti, L., Lanver, D., Schweizer, G., Tanaka, S., Liang, L., Tollot, M., Zuccaro, A., Reissmann, S. and Kahmann, R. (2015) Fungal effectors and plant susceptibility. *Annu. Rev. Plant Biol.*, 66, 513-545.

Love, M.I., Huber, W. and Anders, S. (2014) Moderated estimation of fold change and dispersion for RNA-seq data with DESeq2. *Genome Biology*, 15, 550.

Lu, X., Kracher, B., Saur, I.M.L., Bauer, S., Ellwood, S.R., Wise, R., Yaeno, T., Maekawa, T. and Schulze-Lefert, P. (2016) Allelic barley MLA immune receptors recognize sequence-unrelated avirulence effectors of the powdery mildew pathogen. *Proceedings of the National Academy of Sciences*, 113, E6486-E6495.

Maekawa, T., Kracher, B., Vernaldi, S., Ver Loren van Themaat, E. and Schulze-Lefert, P. (2012) Conservation of NLR-triggered immunity across plant lineages. *PNAS*, 109, 20119-20123.

Mago, R., Zhang, P., Vautrin, S., Šimková, H., Bansal, U., Luo, M.-C., Rouse, M., Karaoglu, H., Periyannan, S., Kolmer, J., Jin, Y., Ayliffe, M.A., Bariana, H., Park, R.F., McIntosh, R., Doležel, J., Bergès, H., Spielmeyer, W., Lagudah, E.S., Ellis, J.G. and Dodds, P.N. (2015) The wheat *Sr50* gene reveals rich diversity at a cereal disease resistance locus. *Nature Plants*, 1, 15186.

Martins, T., Maia, A.F., Steffensen, S. and Sunkel, C.E. (2009) Sgt1, a co-chaperone of Hsp90 stabilizes Polo and is required for centrosome organization. *The EMBO Journal*, 28, 234-247.

Mascher, M., Gundlach, H., Himmelbach, A., Beier, S., Twardziok, S.O., Wicker, T., Radchuk, V., Dockter, C., Hedley, P.E., Russell, J., Bayer, M., Ramsay, L., Liu, H., Haberer, G., Zhang, X.-Q., Zhang, Q., Barrero, R.A., Li, L., Taudien, S., Groth, M., Felder, M., Hastie, A., Šimková, H., Staňková, H., Vrána, J., Chan, S., Muñoz-Amatriaín, M., Ounit, R., Wanamaker, S., Bolser, D., Colmsee, C., Schmutzer, T., Aliyeva-Schnorr, L., Grasso, S., Tanskanen, J., Chailyan, A., Sampath, D., Heavens, D., Clissold, L., Cao, S., Chapman, B., Dai, F., Han, Y., Li, H., Li, X., Lin, C., McCooke, J.K., Tan, C., Wang, P., Wang, S., Yin, S., Zhou, G., Poland, J.A., Bellgard, M.I., Borisjuk, L., Houben, A., Doležel, J., Ayling, S., Lonardi, S., Kersey, P., Langridge, P., Muehlbauer, G.J., Clark, M.D., Caccamo, M., Schulman, A.H., Mayer, K.F.X., Platzer, M., Close, T.J., Scholz, U., Hansson, M., Zhang, G., Braumann, I., Spannagl, M., Li, C., Waugh, R. and Stein, N. (2017) A chromosome conformation capture ordered sequence of the barley genome. *Nature*, 544, 427-433.

Mascher, M., Richmond, T.A., Gerhardt, D.J., Himmelbach, A., Clissold, L., Sampath, D., Ayling, S., Steuernagel, B., Pfeifer, M., D'Ascenzo, M., Akhunov, E.D., Hedley, P.E., Gonzales, A.M., Morrell, P.L., Kilian, B., Blattner, F.R., Scholz, U., Mayer, K.F.X., Flavell, A.J., Muehlbauer, G.J., Waugh, R., Jeddeloh, J.A. and Stein, N. (2013) Barley whole exome capture: a tool for genomic research in the genus Hordeum and beyond. *The Plant Journal*, 76, 494-505.

Mayer, K.F., Waugh, R., Brown, J.W., Schulman, A., Langridge, P., Platzer, M., Fincher, G.B., Muehlbauer, G.J., Sato, K., Close, T.J., Wise, R.P. and Stein, N. (2012) A physical, genetic and functional sequence assembly of the barley genome. *Nature*, 491, 711-716.

McKenna, A., Hanna, M., Banks, E., Sivachenko, A., Cibulskis, K., Kernytsky, A., Garimella, K., Altshuler, D., Gabriel, S. and Daly, M. (2010) The Genome Analysis Toolkit: a MapReduce framework for analyzing next-generation DNA sequencing data. *Genome Research*, 20, 1297-1303.

Meng, Y., Moscou, M. and Wise, R. (2009) *Blufensin1* negatively impacts basal defense in response to barley powdery mildew. *Plant Physiology*, 149, 271-285.

Morel, J.B. and Dangl, J.L. (1999) Suppressors of the Arabidopsis *lsd5* cell death mutation identify genes involved in regulating disease resistance responses. *Genetics*, 151, 305-319.

Moscou, M.J., Lauter, N., Caldo, R.A., Nettleton, D. and Wise, R.P. (2011) Quantitative and temporal definition of the *Mla* transcriptional regulon during barley–powdery mildew interactions. *MPMI*, 24, 694-705.

Moscou, M.J., Lorang, J., Immaculada, H.-P., Tinker, N., Leonard, J.M. and Wolpert, T.J. (2018) Map-based cloning of *Pc2/Vb:* A doubled-edge sword of immunity. In *Plant and Animal Genome XXVI*. San Diego, CA, pp. https://pag.confex.com/pag/xxvi/meetingapp.cgi/Paper/28867.

Moseman, J.G. (1972) Isogenic barley lines for reaction to *Erysiphe graminis* F. sp. *hordei*. *Crop Science*, 12, 681-682.

Murray, G. and Brennan, J. (2010) Estimating disease losses to the Australian barley industry. *Australasian Plant Pathology*, 39, 85-96.

Noël, L.D., Cagna, G., Stuttmann, J., Wirthmüller, L., Betsuyaku, S., Witte, C.-P., Bhat, R., Pochon, N., Colby, T. and Parker, J.E. (2007) Interaction between SGT1 and cytosolic/nuclear HSC70 chaperones regulates *Arabidopsis* immune responses. *The Plant Cell*, 19, 4061-4076.

Peart, J.R., Lu, R., Sadanandom, A., Malcuit, I., Moffett, P., Brice, D.C., Schauser, L., Jaggard, D.A.W., Xiao, S., Coleman, M.J., Dow, M., Jones, J.D.G., Shirasu, K. and Baulcombe, D.C. (2002) Ubiquitin ligase-associated protein SGT1 is required for host and nonhost disease resistance in plants. *PNAS*, 99, 10865-10869.

Periyannan, S., Moore, J., Ayliffe, M., Bansal, U., Wang, X., Huang, L., Deal, K., Luo, M., Kong, X., Bariana, H., Mago, R., McIntosh, R., Dodds, P., Dvorak, J. and Lagudah, E. (2013) The gene *Sr33*, an ortholog of barley *Mla* genes, encodes resistance to wheat stem rust race Ug99. *Science*, 341, 786-788.

R Core Team (2019) R: A Language and Environment for Statistical Computing. Vienna, Austria: R Foundation for Statistical Computing.

Redkar, A., Hoser, R., Schilling, L., Zechmann, B., Krzymowska, M., Walbot, V. and Doehlemann, G. (2015) A secreted effector protein of *Ustilago maydis* guides maize leaf cells to form tumors. *The Plant Cell*, 27, 1332-1351.

Ridout, C.J., Skamnioti, P., Porritt, O., Sacristan, S., Jones, J.D.G. and Brown, J.K.M. (2006) Multiple avirulence paralogues in cereal powdery mildew fungi may contribute to parasite fitness and defeat of plant resistance. *The Plant Cell*, 18, 2402-2414.

Saur, I.M.L., Bauer, S., Kracher, B., Lu, X., Franzeskakis, L., Muller, M.C., Sabelleck, B., Kummel, F., Panstruga, R., Maekawa, T. and Schulze-Lefert, P. (2019) Multiple pairs of allelic MLA immune receptor-powdery mildew AVR_A effectors argue for a direct recognition mechanism. *eLife*, 8, e44471.

Scofield, S.R., Huang, L., Brandt, A.S. and Gill, B.S. (2005) Development of a virus-induced gene-silencing system for hexaploid wheat and its use in functional analysis of the *Lr21*-mediated leaf rust resistance pathway. *Plant Physiology*, 138, 2165-2173.

Seeholzer, S., Tsuchimatsu, T., Jordan, T., Bieri, S., Pajonk, S., Yang, W., Jahoor, A., Shimizu, K.K., Keller, B. and Schulze-Lefert, P. (2010) Diversity at the *Mla* powdery mildew resistance locus from cultivated barley reveals sites of positive selection. *MPMI*, 23, 497-509.

Shen, Q.-H., Saijo, Y., Mauch, S., Biskup, C., Bieri, S., Keller, B., Seki, H., Ulker, B., Somssich, I.E. and Schulze-Lefert, P. (2007) Nuclear activity of MLA immune receptors links isolate-specific and basal disease-resistance responses. *Science*, 315, 1098-1103.

Shen, Q.-H., Zhou, F., Bieri, S., Haizel, T., Shirasu, K. and Schulze-Lefert, P. (2003) Recognition specificity and RAR1/SGT1 dependence in barley *Mla* disease resistance genes to the powdery mildew fungus. *The Plant Cell*, 15, 732-744.

Shirasu, K. (2009) The HSP90-SGT1 chaperone complex for NLR immune sensors. *Annu. Rev. Plant Biol.*, 60, 139-164.

Shirasu, K., Lahaye, T., Tan, M.-W., Zhou, F., Azevedo, C. and Schulze-Lefert, P. (1999) A novel class of eukaryotic zinc-binding proteins is required for disease resistance signaling in barley and development in *C. elegans*. *Cell*, 99, 355-366.

Sun, Y., Zhu, Y.-X., Balint-Kurti, P.J. and Wang, G.-F. (2020) Fine-tuning immunity: Players and regulators for plant NLRs. *Trends in Plant Science*, 25, 695-713.

Taube, M., Pieńkowska, J.R., Jarmołowski, A., Kozak, M. and Silman, I. (2014) Low-resolution structure of the full-length barley (*Hordeum vulgare*) SGT1 protein in solution, obtained using small-angle X-ray scattering. *PLOS ONE*, 9, e93313.

Thao, N.P., Chen, L., Nakashima, A., Hara, S.-i., Umemura, K., Takahashi, A., Shirasu, K., Kawasaki, T. and Shimamoto, K. (2007) RAR1 and HSP90 form a complex with Rac/Rop GTPase and function in innate-immune responses in rice. *The Plant Cell*, 19, 4035-4045.

Torp, J. and Jørgensen, J.H. (1986) Modification of barley powdery mildew resistance gene *Ml-a12* by induced mutation. *Canadian Journal of Genetics and Cytology*, 28, 725-731.

Tsetsarkin, K.A., Vanlandingham, D.L., McGee, C.E. and Higgs, S. (2007) A single mutation in Chikungunya virus affects vector specificity and epidemic potential. *PLOS Pathogens*, 3, e201.

van Wersch, S., Tian, L., Hoy, R. and Li, X. (2020) Plant NLRs: The whistleblowers of plant immunity. *Plant Communications*, 1, 100016.

Wang, G.-F., Fan, R., Wang, X., Wang, D. and Zhang, X. (2015) TaRAR1 and TaSGT1 associate with TaHSP90 to function in bread wheat (*Triticum aestivum* L.) seedling growth and stripe rust resistance. *Plant Molecular Biology*, 87, 577-589.

Wei, F., Wing, R.A. and Wise, R.P. (2002) Genome dynamics and evolution of the *Mla* (powdery mildew) resistance locus in barley. *Plant Cell*, 14, 1903-1917.

Wise, R. and Ellingboe, A. (1985) Fine structure and instability of the *Ml-a* locus in barley. *Genetics*, 111, 113-130.

Wise, R.P. and Ellingboe, A.H. (1983) Infection kinetics of *Erysiphe graminis* f. sp. *hordei* on barley with different alleles at the *Ml-a* locus. *Phytopathology*, 73, 1220-1222.

Xi, L., Moscou, M., Meng, Y., Xu, W., Caldo, R., Shaver, M., Nettleton, D. and Wise, R. (2009) Transcript-based cloning of *RRP46*, a regulator of rRNA processing and *R* gene-independent cell death in barley-powdery mildew interactions. *The Plant Cell*, 21, 3280-3295.

Xu, W., Meng, Y. and Wise, R.P. (2014) *Mla*- and *Rom1*-mediated control of microRNA398 and chloroplast copper/zinc superoxide dismutase regulates cell death in response to the barley powdery mildew fungus. *The New Phytologist*, 201, 1396-1412.

Yang, J., Yan, R., Roy, A., Xu, D., Poisson, J. and Zhang, Y. (2015) The I-TASSER Suite: protein structure and function prediction. *Nat Methods*, 12, 7-8.

Yoshihara, T. and Spalding, E.P. (2020) Switching the direction of stem gravitropism by altering two amino acids in AtLAZY1. *Plant Physiology*, 182, 1039-1051.

Yu, G., Xian, L., Xue, H., Yu, W., Rufian, J.S., Sang, Y., Morcillo, R.J.L., Wang, Y. and Macho, A.P. (2020) A bacterial effector protein prevents MAPK-mediated phosphorylation of SGT1 to suppress plant immunity. *bioRxiv*, 641241.

Yu, G.-X., Braun, E. and Wise, R.P. (2001) *Rds* and *Rih* mediate hypersensitive cell death independent of gene-for-gene resistance to the oat crown rust pathogen *Puccinia coronata* f. sp. *avenae*. *MPMI*, 14, 1376-1383.

Zhang, M., Botër, M., Li, K., Kadota, Y., Panaretou, B., Prodromou, C., Shirasu, K. and Pearl, L.H. (2008) Structural and functional coupling of Hsp90- and Sgt1-centred multi-protein complexes. *The EMBO Journal*, 27, 2789-2798.

Zhang, X.C., Millet, Y.A., Cheng, Z., Bush, J. and Ausubel, F.M. (2015) Jasmonate signalling in Arabidopsis involves SGT1b-HSP70-HSP90 chaperone complexes. *Nature Plants*, 1, 15049.

Appendix. Supplemental Tables and Figures

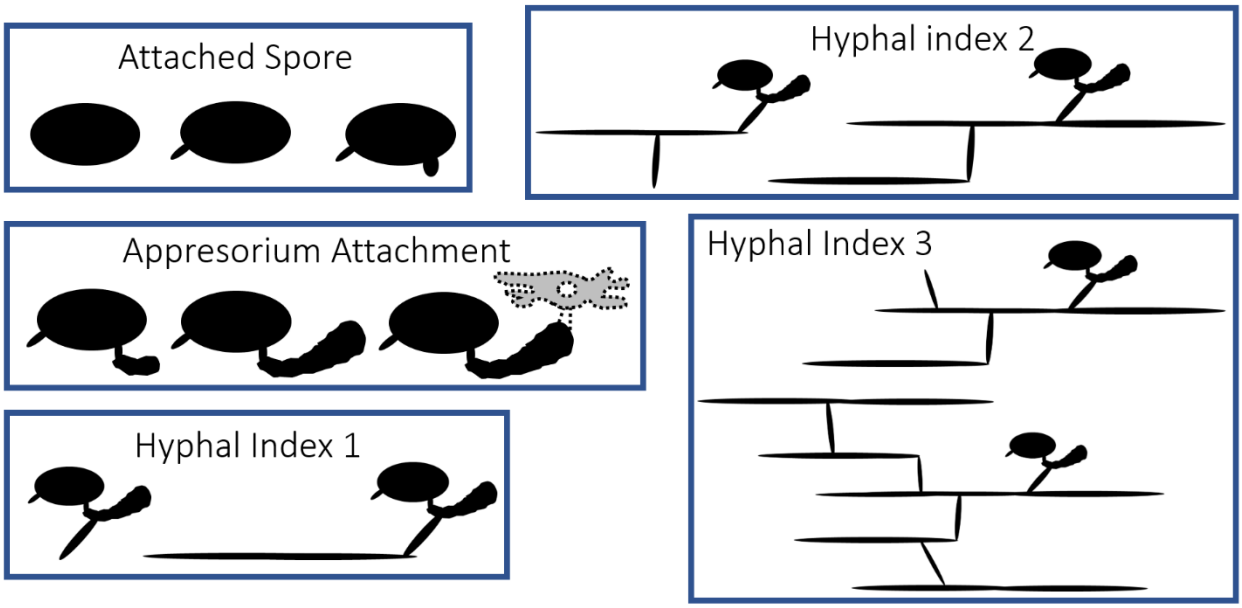

Figure 2-S1. Categorization of *Bgh* spore growth stages. *Bgh* phenotyped by light microscopy were categorized into one of five groups. Attached spore, a spore that did not display an attached appressorium and thus had likely aborted before encountering the plants ETI. Appressorium Attachment, the spore has successfully generated an appressorium and has likely penetrated the host cell to start interactions/feeding, not progressing past this stage is indicative of host defense responses preventing colonization. Hyphal index 1, Elongating secondary hyphae (ESH) is being produced from the appressorium, showing the acquisition of nutrients from the host cell and thus successful colonization. Hyphal index 2, the ESH is branching, showing continued growth. Hyphal Index 3, the ESH has branched numerous times, colonized other host cells and is on its way to sporulation.

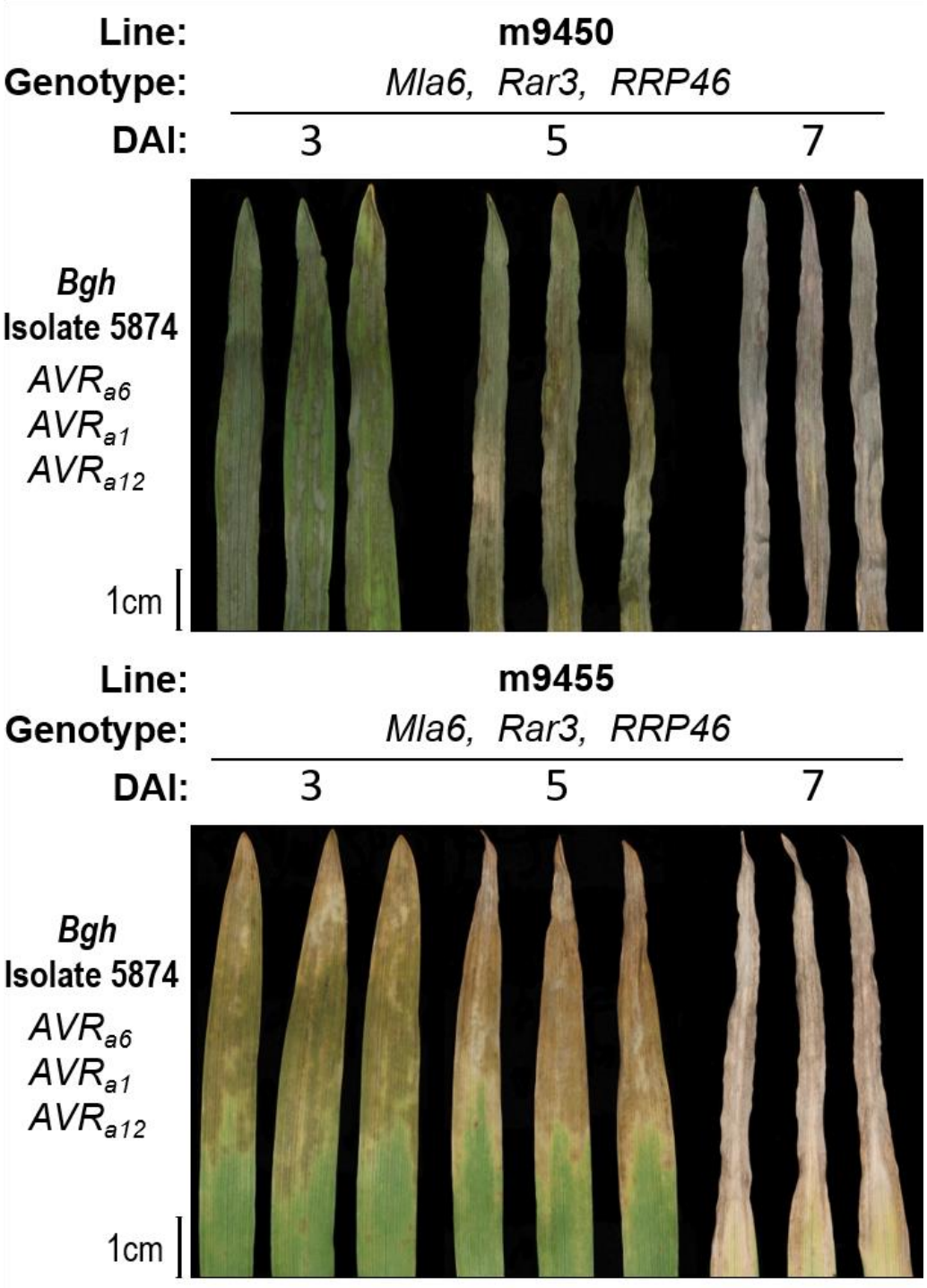

Figure 2-S2. Time-course phenotypes of m9450 and m9455. Phenotypes of the severe cell death mutants m9450 (*Mla6, Rar3, RRP46*) and m9455 (*Mla6, Rar3, RRP46*). Inoculated with *Bgh* 5874 (*AVRa6*) and photographed at 3, 5, and 7 days after inoculation.

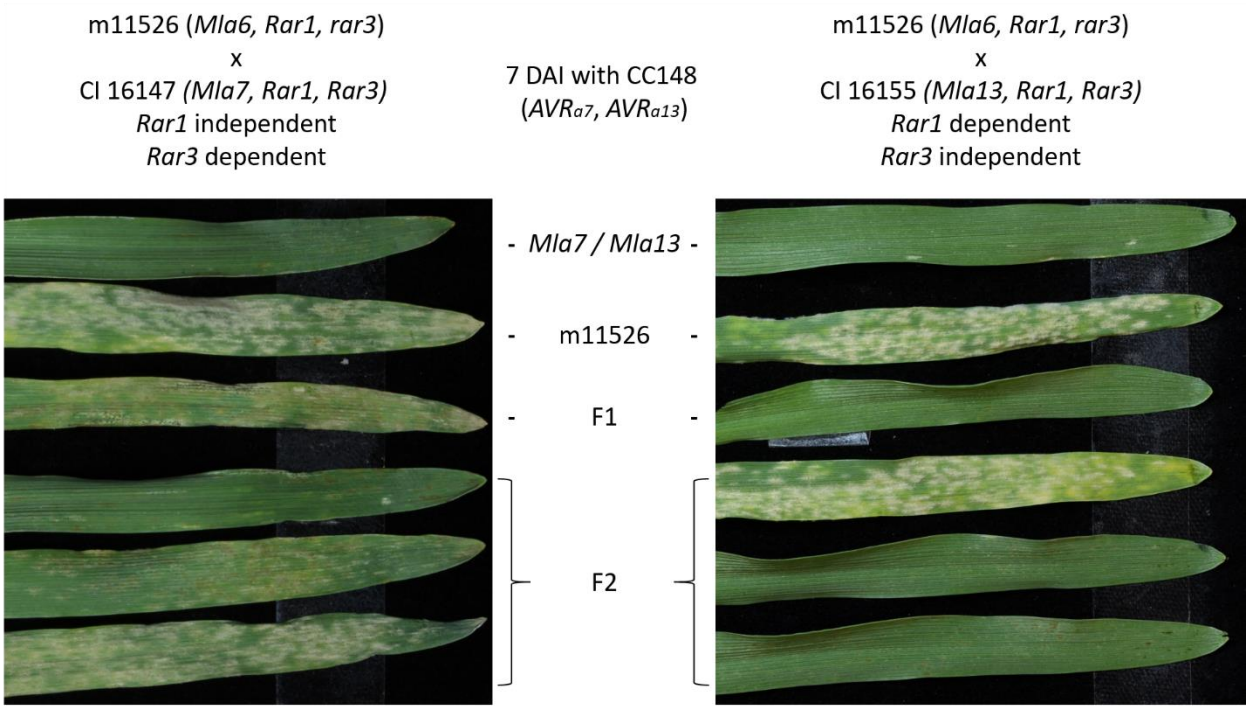

Figure 2-S3. Phenotypes of crosses between m11526 and CI 16147 and CI 16155. Images of parents, F1 and representative F2 from crosses between m11526 (*Mla6, Rar1, rar3*) and CI 16147 (*Mla7, Rar1, Rar3*), and CI 16155 (*Mla13, Rar1, Rar3*). Inoculated with CC148 (AVR_{a7}, AVR_{a13}) and photographed 7 days post inoculation.

Table 2-S1. **Molecular markers used for fine mapping of *Rar3***. Marker designation, location on chromosome 3H (Ensembl, Assembly 082214v1, INSDC Assembly GCA 000326085.1), type of marker (P/A = Presence or Absence, CAPS = Cleaved Amplified Polymorphic Sequence or Band Shift), which restriction enzyme was used for CAPS markers (NEB), Tm of primers for PCR, sequence of primers.

Marker	Location (Mb)	Type	Restriction Enzyme	Tm	F Sequence	R Sequence
ACP1_A2	34.2240	P/A	N/A	60	ATTTGGTGACCGATGATTCC	CGATGGATTGGTTTCTGCTT
ACP1_A11	136.3125	P/A	N/A	60	TCGTGAAAAGGGACTTGCTT	GGTACCCGCGTAATTCTCAA
ACP1_A12	200.6945	P/A	N/A	56	GTGCTGCTCTTGTTGCTCTG	ATTGTTGTGCGACAGTTCCA
ACP1_B3	239.9803	P/A	N/A	56	ATCGCGTACTAGGGGAAACC	CTCCCTCCCTCGCCATCT
ACP1_B6	291.1614	CAPS	*Acc*I	62	AGCAGCCTTTGGCTTTGAC	ACGTTGCAAACAATCACACC
ACP2_A5	324.8612	CAPS	*Mnl*I	60	TGGCTGTTCAAACTTCAAACC	TATGGTGAAGCTCACGTCCA
ACP2_A7	353.5489	CAPS	*Eag*I-HF	60	GATGCCTAGGGCACGAAATA	TTGGACCATCCGTTTGAGAT
ACP2_B3	394.3755	CAPS	*Hpy*166II	58	TGTTCACAGGGGTTGAACAG	GTCGCCAATTTGCATTCTTT
ACP4_A7	401.7989	CAPS	*Hinf*I	64	GTGGAAGCACAATACGGTCA	GAGGTATTCGGCAAGCATGT
ACP2_B5	403.6598	CAPS	*Nae*I	62	TGACCTTCCACCATATGCAA	GTGCTTGGTCCCATTAAGGA
ACP3_A12	408.2572	CAPS	*Nco*I	64	CCATTATGTCCTGGTGCTGA	CCCATTACCCTGGAACAAAA
ACP3_B3	411.4693	CAPS	*Bgl*I	62	AGGCACTGAGCTCTTTCTCG	GACGACGTTGTTGCTGAAGA
ACP5_70	417.0750	CAPS	*Mbo*II	64	TGGTGAAGTTGCAAAACAGC	TTCAAGAGCGACGGAAAGTT
SGT1_Del	417.3178	P/A	N/A	60	GGGCTGAATGTGAGCAAAAT	CAGCATCACCGTCAAGTTTC
ACP2_C4	417.3418	CAPS	*Dra*I	60	TGAGGGAACCCTTTGTTCAC	CTGGAAAGATGTCGGGAAAA
ACP5_75	417.5449	CAPS	*Drd*I	62	CCCCCTCAGTTACATGCTTGC	GTTTCGTGGCGCATTACTCT
ACP5_80	418.0084	CAPS	*Hpy*188III	64	GGCACCATAGGTGAGGCTAC	CCAACATAACGACGTGCAAA
ACP2_C7	420.2146	CAPS	*Dde*I	60	CAACTTGGGGTTTGTTACCG	TCCGAGGACTTGAAGCAAAT
ACP3_C9	423.6453	CAPS	*Hae*II	64	ACACATCACCCATGGAGCTT	AGAGGGATCGAGATGGGATT
ACP3_C12	425.2085	CAPS	*Mse*I	60	TTGCTGGTGTGTTGAGAAGG	GAGCACGCAGAAACTGTGAA
ACP3_D3	428.3593	CAPS	*Mse*I	60	GGGAAATGCGAGGCTTAAAT	CGTACGTCGGGATAGGAAGA
ACP1_C6	508.0488	P/A	N/A	60	GGGGAGCGTTGATTTTCAAT	GCAATGTGAGATGGCAACTG
ACP1_C8	534.8130	Band Shift	N/A	60	CACCGTCAACACCAGCACTA	GTCGGCCTTTTCTCGTGTAG
ACP1_C11	580.3021	P/A	N/A	60	CCAGCCAGATTACGATTGGT	ACGTCTCAAGACTGGCCAAC
ACP1_C12	598.1316	P/A	N/A	60	AACCACCCATACTGCACACA	CCCTCCGTCCCAAAATAAGT
ACP1_D2	627.4647	P/A	N/A	60	CCACACTATGACCAGCCTTATG	GATGCCCTTCATCTTCAACC
ACP1_D3	640.5317	P/A	N/A	60	GTGTGTCGCCTGAAGTCTGA	GGAGGTTCGGGAAGAAAGAT
ACP1_D4	656.4775	P/A	N/A	60	AAAGGACGGCTTCAAGATGA	AACAAGCAGGCACAAGTGAA
ACP1_D5	669.5853	P/A	N/A	60	CTGATCAATTCACCCCCAAT	GCCCGTCTTGACCCTTTG
ACP1_D6	696.0498	P/A	N/A	58	CTCTGCATTTTGCTCTGCTG	CAATGGTGGACCTTTGTTCC

Table 2-S2. **Summary of fast-neutron mutants, phenotypes, and genes identified by them.**

Mutant line	Sporulation phenotype	Other phenotype	Mutant designation (Gene)	Additional independent alleles	Reference
m11526	Susceptible		*rar3 (Sgt1)*		This paper
m11538	Susceptible		*mla6 (Mla6)*	3 (9472, 9480, 18982)	Xu et. al., 2014
m18982	Susceptible		*mla6 (Mla6)*	3 (9472, 9480, 11538)	Xu et. al., 2014
m19028	Susceptible		*mla6, bln1 (Mla6, Bln1)*		Xu et. al., 2014
m9472	Susceptible		*mla6 (Mla6)*	3 (9480, 11538, 18982)	Caldo et. al., 2006; Moscou et.al., 2011; Xu et. al., 2014
m9480	Susceptible		*mla6 (Mla6)*	3 (9472, 11538, 18982)	Xu et. al., 2014
m11542	Resistant	Cell death	*bcd1 (RRP46)*		Xi et. al., 2009
m9450	Resistant	Systemic cell death			This paper
m9455	Resistant	Systemic cell death			This paper
m9463	Resistant	Cell death		1 (9464)	This paper
m9467	Resistant	Cell death		1 (9469	This paper
m19089	Resistant		*bln1 (Bln1)*		Xu et. al., 2014; Meng et. al., 2009

Table 2-S3. Morphology data of mutant and wildtype barley under normal growing conditions.

Genotype	Bag Number		Height at # DAP (cm)			Leaves at # DAP (cm)			Nodes at # DAP (cm)		
			14	21	28	14	21	28	14	21	28
CI 16151	28850	Mean	25.2	27.7	29.8	2.7	3.0	4.2	1.1	2.0	3.1
		Std Dev	2.0	1.5	2.0	0.5	0.0	0.4	0.3	0.0	0.3
rar3-m11526	23720	Mean	23.7	26.9	29.2	2.6	3.2	4.7	1.0	2.0	3.2
		Std Dev	1.6	1.5	2.1	0.5	0.4	0.5	0.0	0.0	0.4
Sultan-5	31407	Mean	24.2	27.9	30.5	3.0	3.8	4.8	1.9	2.6	3.5
		Std Dev	1.4	2.2	2.9	0.0	0.4	0.4	0.3	0.5	0.7
rar1-m100	31063	Mean	24.0	27.5	30.7	3.0	3.9	5.0	1.9	2.9	3.9
		Std Dev	0.8	2.1	2.3	0.0	0.3	0.0	0.3	0.3	0.3

Genotype	Bag Number		Internodal distance (cm)				Leaf length at 28 DAP (cm)				
			0-1	1-2	2-3	3-4	1	2	3	4	5
CI 16151	28850	Mean	21.4	14.4	12.5	22.0	14.1	23.4	24.6	18.1	1.3
		Std Dev	3.5	4.0	5.3	0.0	0.8	1.7	1.9	1.8	0.5
rar3-m11526	23720	Mean	18.7	11.4	15.3	11.5	14.2	23.0	23.9	18.3	2.4
		Std Dev	4.6	2.9	3.5	2.5	0.8	1.1	1.9	4.2	1.2
Sultan-5	31407	Mean	16.9	18.4	20.1	0.3	11.2	20.2	22.4	24.3	8.6
		Std Dev	2.9	4.1	5.0	7.2	0.9	0.8	1.4	4.0	3.8
rar1-m100	31063	Mean	14.9	15.1	13.3	3.7	10.5	20.5	23.1	25.0	12.8
		Std Dev	3.7	4.6	6.2	4.1	0.7	0.6	1.7	2.4	3.7

Genotype	Bag Number		Root physiology at 14 DAP	
			Length	Number
CI 16151	28850	Mean	17.7	6.2
		Std Dev	0.8	0.4
rar3-m11526	23720	Mean	17.8	6.0
		Std Dev	1.6	0.6
Sultan-5	31407	Mean	18.4	7.2
		Std Dev	1.6	0.4
rar1-m100	31063	Mean	17.8	6.6
		Std Dev	0.6	0.8

Table 2-S4. **Measurements and analysis of *mla6*, *bln1*, and *rar3* mutants from seed-to-seed during development.** Fertile Florets is the data on how many florets were fertile per spike per plant. Filled Seed Heads Spikes is the data on how many heads filled with seed per plant. Filled Seed Weight is the data on the weight of 50 randomly selected seed per plant in grams. Number of Tillers is the data on the number of tillers per plant at each timepoint. Infertile Seed is the data on the proportion of infertile florets per spike per plant. Plant Height is the data on the plant height at each timepoint in centimeters. Spike Length is the data on the length of each spike per plant in centimeters. Genotype indicates which line was measured. Time (DAS) is the number of days after sowing that measurements were taken, only applicable for Number of Tillers and Plant Height. Mean is the mean of the data. SE is the standard error of the data. DF is the degrees of freedom for the data. Lower CL is the lower confidence limit of the data. Upper CL is the higher confidence limit of the data. Group indicates which statistical group each belongs to, matching letters indicate no significant difference between data at a confidence level of 0.01.

Fertile Florets						
Genotype	**Mean**	**SE**	**DF**	**Lower CL**	**Upper CL**	**Group**
mla6-m9472	42.06	1.13	328	38.97	45.15	a
mla6-m11538	45.73	1.33	328	42.07	49.39	ab
mla6-m9480	47.50	1.30	328	43.94	51.06	ab
mla6,bln1-19028	48.71	1.16	328	45.52	51.90	b
mla6-18982	50.53	1.37	328	46.77	54.30	bc
bln1-m19089	51.73	1.19	328	48.46	55.00	bc
CI 16151 (Mla6)	55.01	1.20	328	51.70	58.31	cd
rar3-m11526	59.03	1.18	328	55.80	62.26	d

Filled Seed Heads Spikes						
Genotype	**Mean**	**SE**	**DF**	**Lower CL**	**Upper CL**	**Group**
mla6-m11538	3.60	0.20	66	3.04	4.16	a
mla6-18982	3.78	0.21	66	3.18	4.37	ab
mla6-m9480	3.80	0.20	66	3.24	4.36	ab
CI 16151 (Mla6)	4.40	0.20	66	3.84	4.96	abc
rar3-m11526	4.60	0.20	66	4.04	5.16	abc
mla6,bln1-19028	4.70	0.20	66	4.14	5.26	bc
mla6-m9472	5.00	0.20	66	4.44	5.56	c
bln1-m19089	5.00	0.21	66	4.40	5.60	c

Filled Seed Weight						
Genotype	Mean (g)	SE	DF	Lower CL	Upper CL	Group
bln1-m19089	0.031	0.0011	65	0.028	0.034	a
mla6-m9472	0.037	0.0010	65	0.034	0.040	b
rar3-m11526	0.037	0.0010	65	0.035	0.040	b
mla6-18982	0.039	0.0011	65	0.036	0.042	bc
mla6-m11538	0.041	0.0010	65	0.038	0.044	bc
CI 16151 (Mla6)	0.041	0.0010	65	0.038	0.044	bc
mla6,bln1-19028	0.042	0.0010	65	0.039	0.045	bc
mla6-m9480	0.044	0.0010	65	0.041	0.046	c

Number of Tillers							
Genotype	Time (DAS)	Mean	SE	DF	Lower CL	Upper CL	Group
mla6,bln1-19028	16	2.30	0.31	66	1.44	3.16	a
bln1-m19089	16	2.31	0.32	66	1.40	3.22	a
rar3-m11526	16	2.40	0.31	66	1.54	3.26	a
mla6-m11538	16	2.40	0.31	66	1.54	3.26	a
mla6-18982	16	2.42	0.32	66	1.51	3.33	a
mla6-m9480	16	2.50	0.31	66	1.64	3.36	a
CI 16151 (Mla6)	16	2.60	0.31	66	1.74	3.46	a
mla6-m9472	16	2.80	0.31	66	1.94	3.66	a
mla6,bln1-19028	22	2.30	0.31	66	1.44	3.16	a
mla6-18982	22	2.42	0.32	66	1.51	3.33	a
mla6-m11538	22	2.80	0.31	66	1.94	3.66	a
bln1-m19089	22	2.87	0.32	66	1.96	3.78	a
CI 16151 (Mla6)	22	2.90	0.31	66	2.04	3.76	a
mla6-m9480	22	2.90	0.31	66	2.04	3.76	a
rar3-m11526	22	2.90	0.31	66	2.04	3.76	a
mla6-m9472	22	3.10	0.31	66	2.24	3.96	a
mla6,bln1-19028	28	3.50	0.31	66	2.64	4.36	a
mla6-18982	28	3.87	0.32	66	2.96	4.78	a
bln1-m19089	28	3.87	0.32	66	2.96	4.78	a
mla6-m11538	28	4.10	0.31	66	3.24	4.96	a
mla6-m9480	28	4.20	0.31	66	3.34	5.06	a
CI 16151 (Mla6)	28	4.30	0.31	66	3.44	5.16	a
rar3-m11526	28	4.30	0.31	66	3.44	5.16	a
mla6-m9472	28	5.00	0.31	66	4.14	5.86	a

Table 2-S4 Continued

Genotype	Time (DAS)	Mean	SE	DF	Lower CL	Upper CL	Group
mla6-18982	36	4.76	0.32	66	3.85	5.67	a
mla6,bln1-19028	36	5.00	0.31	66	4.14	5.86	a
mla6-m11538	36	5.20	0.31	66	4.34	6.06	a
mla6-m9480	36	5.20	0.31	66	4.34	6.06	a
CI 16151 (Mla6)	36	5.20	0.31	66	4.34	6.06	a
bln1-m19089	36	5.20	0.32	66	4.29	6.11	a
rar3-m11526	36	5.80	0.31	66	4.94	6.66	a
mla6-m9472	36	7.40	0.31	66	6.54	8.26	b
mla6-18982	43	6.20	0.32	66	5.29	7.11	a
CI 16151 (Mla6)	43	6.50	0.31	66	5.64	7.36	a
mla6-m11538	43	6.70	0.31	66	5.84	7.56	a
mla6,bln1-19028	43	6.70	0.31	66	5.84	7.56	a
mla6-m9480	43	6.90	0.31	66	6.04	7.76	a
bln1-m19089	43	6.98	0.32	66	6.07	7.89	a
rar3-m11526	43	7.40	0.31	66	6.54	8.26	ab
mla6-m9472	43	8.80	0.31	66	7.94	9.66	b
mla6-18982	56	7.09	0.32	66	6.18	8.00	a
mla6,bln1-19028	56	7.70	0.31	66	6.84	8.56	a
CI 16151 (Mla6)	56	7.70	0.31	66	6.84	8.56	a
rar3-m11526	56	7.90	0.31	66	7.04	8.76	a
mla6-m9480	56	8.10	0.31	66	7.24	8.96	a
mla6-m11538	56	8.40	0.31	66	7.54	9.26	ab
bln1-m19089	56	8.65	0.32	66	7.74	9.55	ab
mla6-m9472	56	9.90	0.31	66	9.04	10.76	b
mla6-18982	65	7.09	0.32	66	6.18	8.00	a
mla6,bln1-19028	65	7.70	0.31	66	6.84	8.56	ab
rar3-m11526	65	7.90	0.31	66	7.04	8.76	ab
CI 16151 (Mla6)	65	7.90	0.31	66	7.04	8.76	ab
mla6-m9480	65	8.20	0.31	66	7.34	9.06	ab
mla6-m11538	65	8.50	0.31	66	7.64	9.36	abc
bln1-m19089	65	8.87	0.32	66	7.96	9.78	bc
mla6-m9472	65	10.00	0.31	66	9.14	10.86	c
mla6-18982	73	7.31	0.32	66	6.40	8.22	a
mla6,bln1-19028	73	7.90	0.31	66	7.04	8.76	ab
rar3-m11526	73	8.20	0.31	66	7.34	9.06	ab
mla6-m11538	73	8.50	0.31	66	7.64	9.36	ab
CI 16151 (Mla6)	73	8.50	0.31	66	7.64	9.36	ab

Table 2-S4 Continued

Genotype	Time (DAS)	Mean	SE	DF	Lower CL	Upper CL	Group
mla6-m9480	73	9.20	0.31	66	8.34	10.06	bc
bln1-m19089	73	9.31	0.32	66	8.40	10.22	bc
mla6-m9472	73	10.10	0.31	66	9.24	10.96	c
mla6-18982	108	7.31	0.32	66	6.40	8.22	a
mla6,bln1-19028	108	7.90	0.31	66	7.04	8.76	ab
rar3-m11526	108	8.20	0.31	66	7.34	9.06	ab
mla6-m11538	108	8.50	0.31	66	7.64	9.36	ab
CI 16151 (Mla6)	108	8.50	0.31	66	7.64	9.36	ab
mla6-m9480	108	9.20	0.31	66	8.34	10.06	bc
bln1-m19089	108	9.31	0.32	66	8.40	10.22	bc
mla6-m9472	108	10.10	0.31	66	9.24	10.96	c

Infertile Seed						
Genotype	Mean	SE	DF	Lower CL	Upper CL	Group
rar3-m11526	0.088	0.011	328	0.058	0.118	a
mla6-18982	0.094	0.013	328	0.059	0.129	ab
bln1-m19089	0.095	0.011	328	0.065	0.126	ab
CI 16151 (Mla6)	0.102	0.011	328	0.071	0.133	ab
mla6-m9472	0.104	0.010	328	0.075	0.132	ab
mla6,bln1-19028	0.145	0.011	328	0.115	0.174	b
mla6-m11538	0.208	0.012	328	0.174	0.242	c
mla6-m9480	0.273	0.012	328	0.240	0.306	d

Plant Height							
Genotype	Time (DAS)	Mean (cm)	SE	DF	Lower CL	Upper CL	Group
rar3-m11526	16	13.75	2.35	66	7.14	20.36	a
mla6,bln1-19028	16	13.90	2.35	66	7.29	20.51	a
mla6-m9472	16	14.20	2.35	66	7.59	20.81	a
mla6-m11538	16	14.30	2.35	66	7.69	20.91	a
bln1-m19089	16	15.94	2.48	66	8.96	22.91	a
mla6-m9480	16	16.10	2.35	66	9.49	22.71	a
CI 16151 (Mla6)	16	16.10	2.35	66	9.49	22.71	a
mla6-18982	16	16.49	2.48	66	9.52	23.47	a

Table 2-S4 Continued

Genotype	Time (DAS)	Mean	SE	DF	Lower CL	Upper CL	Group
mla6-m9472	22	18.25	2.35	66	11.64	24.86	a
rar3-m11526	22	21.75	2.35	66	15.14	28.36	a
mla6,bln1-19028	22	22.95	2.35	66	16.34	29.56	a
CI 16151 (Mla6)	22	23.75	2.35	66	17.14	30.36	a
bln1-m19089	22	24.21	2.48	66	17.24	31.19	a
mla6-m9480	22	24.55	2.35	66	17.94	31.16	a
mla6-m11538	22	25.20	2.35	66	18.59	31.81	a
mla6-18982	22	25.60	2.48	66	18.63	32.58	a
mla6-m9472	28	27.10	2.35	66	20.49	33.71	a
rar3-m11526	28	31.25	2.35	66	24.64	37.86	a
bln1-m19089	28	32.77	2.48	66	25.79	39.75	a
CI 16151 (Mla6)	28	33.10	2.35	66	26.49	39.71	a
mla6-m9480	28	34.55	2.35	66	27.94	41.16	a
mla6,bln1-19028	28	35.20	2.35	66	28.59	41.81	a
mla6-18982	28	35.38	2.48	66	28.40	42.36	a
mla6-m11538	28	35.85	2.35	66	29.24	42.46	a
mla6-m9472	36	34.45	2.35	66	27.84	41.06	a
bln1-m19089	36	37.94	2.48	66	30.96	44.91	a
rar3-m11526	36	39.95	2.35	66	33.34	46.56	a
mla6-m11538	36	40.60	2.35	66	33.99	47.21	a
mla6-18982	36	40.82	2.48	66	33.85	47.80	a
CI 16151 (Mla6)	36	41.15	2.35	66	34.54	47.76	a
mla6-m9480	36	42.65	2.35	66	36.04	49.26	a
mla6,bln1-19028	36	45.95	2.35	66	39.34	52.56	a
mla6-m9472	43	41.40	2.35	66	34.79	48.01	a
mla6-m11538	43	44.85	2.35	66	38.24	51.46	ab
mla6-m9480	43	48.60	2.35	66	41.99	55.21	ab
rar3-m11526	43	54.00	2.35	66	47.39	60.61	bc
mla6-18982	43	55.21	2.48	66	48.24	62.19	bc
bln1-m19089	43	56.49	2.48	66	49.52	63.47	bc
CI 16151 (Mla6)	43	65.20	2.35	66	58.59	71.81	cd
mla6,bln1-19028	43	76.35	2.35	66	69.74	82.96	d
mla6-m9472	56	79.70	2.35	66	73.09	86.31	a
mla6-18982	56	82.71	2.48	66	75.74	89.69	ab
mla6-m11538	56	87.40	2.35	66	80.79	94.01	ab
bln1-m19089	56	93.94	2.48	66	86.96	100.91	bc
mla6-m9480	56	94.40	2.35	66	87.79	101.01	bc

Table 2-S4 Continued

Genotype	Time (DAS)	Mean	SE	DF	Lower CL	Upper CL	Group
mla6,bln1-19028	56	100.85	2.35	66	94.24	107.46	c
rar3-m11526	56	101.50	2.35	66	94.89	108.11	c
CI 16151 (Mla6)	56	102.10	2.35	66	95.49	108.71	c
mla6-m9472	65	80.80	2.35	66	74.19	87.41	a
mla6-18982	65	84.21	2.48	66	77.24	91.19	ab
mla6-m11538	65	88.95	2.35	66	82.34	95.56	abc
bln1-m19089	65	95.32	2.48	66	88.35	102.30	bcd
mla6-m9480	65	97.35	2.35	66	90.74	103.96	cd
mla6,bln1-19028	65	101.55	2.35	66	94.94	108.16	d
rar3-m11526	65	102.90	2.35	66	96.29	109.51	d
CI 16151 (Mla6)	65	103.45	2.35	66	96.84	110.06	d
mla6-m9472	73	82.25	2.35	66	75.64	88.86	a
mla6-18982	73	87.60	2.48	66	80.63	94.58	ab
bln1-m19089	73	96.44	2.48	66	89.46	103.41	bc
mla6-m11538	73	99.25	2.35	66	92.64	105.86	bc
mla6-m9480	73	102.15	2.35	66	95.54	108.76	c
mla6,bln1-19028	73	103.15	2.35	66	96.54	109.76	c
rar3-m11526	73	104.45	2.35	66	97.84	111.06	c
CI 16151 (Mla6)	73	105.60	2.35	66	98.99	112.21	c
mla6-m9472	108	82.25	2.35	66	75.64	88.86	a
mla6-18982	108	87.60	2.48	66	80.63	94.58	ab
bln1-m19089	108	96.44	2.48	66	89.46	103.41	bc
mla6-m11538	108	100.55	2.35	66	93.94	107.16	c
mla6,bln1-19028	108	103.15	2.35	66	96.54	109.76	c
mla6-m9480	108	103.65	2.35	66	97.04	110.26	c
rar3-m11526	108	104.90	2.35	66	98.29	111.51	c
CI 16151 (Mla6)	108	105.75	2.35	66	99.14	112.36	c

Spike Length						
Genotype	Mean (cm)	SE	DF	Lower CL	Upper CL	Group
bln1-m19089	6.49	0.14	328	6.11	6.87	a
mla6-m9472	6.97	0.13	328	6.61	7.33	ab
mla6,bln1-19028	7.09	0.13	328	6.72	7.46	ab
mla6-18982	7.36	0.16	328	6.93	7.80	bc
mla6-m11538	8.01	0.15	328	7.58	8.43	cd

Table 2-S4 Continued

Genotype	Mean (cm)	SE	DF	Lower CL	Upper CL	Group
CI 16151 (Mla6)	8.27	0.14	328	7.89	8.65	d
rar3-m11526	8.33	0.14	328	7.96	8.70	d
mla6-m9480	8.35	0.15	328	7.94	8.76	d

Table 2-S5. **Morphology data of mutant and wildtype barley under stressed growing conditions.** Plants were grown under standard conditions for 7 days and then transferred to stress conditions.

			Darkness	Salt			Drought	
Genotype	Bag Number		Height (cm) at # DAP					
			14	14	21	28	14	21
CI 16151	28850	Mean	16.4	25.7	29.2	29.2	21.0	24.1
		Std Dev	0.9	1.8	0.9	0.7	1.9	1.8
rar3-m11526	23720	Mean	16.8	24.2	28.1	28.5	20.5	19.9
		Std Dev	1.2	0.9	0.8	1.1	1.8	8.4
Sultan-5	31407	Mean	12.5	24.8	27.2	29.7	21.2	22.9
		Std Dev	0.9	1.0	0.2	0.4	1.2	0.5
rar1-m100	31063	Mean	12.1	23.9	27.5	29.7	22.6	22.7
		Std Dev	0.9	2.2	2.4	0.8	1.3	1.0

Table 2-S6. **F2 infection type results from crosses among m11526 and other lines**. Details of the F2 progeny of crosses between m11526 (*Mla6, rar3*, Manchuria background) and near-isogenic CI lines (*Mla, Rar3*, Manchuria background), mutants, or diverse lines (*Mla, Rar3*, other backgrounds). The genotypes of the two *Bgh* isolates used (*Bgh* 5874: AVR_{a1}, AVR_{a6}, AVR_{a12} and CC148: AVR_{a1}, AVR_{a7}, AVR_{a9}, AVR_{a10}, AVR_{a13}) are detailed as relevant if they correspond to an Mla allele present in the cross. Infection phenotype is characterized as either resistant (R), resistant with necrosis (Rn), susceptible with necrosis (Sn) or susceptible (S). Percentage of observed F2 displaying each infection phenotype are shown. The raw numbers of observed F2 displaying each phenotype were used for a chi-squared test against expected ratios for known genetic segregation ratios. With a cut-off of 0.05, ratios were either; significantly different from expected ratio, not significantly different from expected ratio, or not applicable due to a lack of phenotypes (E.g., a 1:2:1 ratio wasn't testable in a population that had only 2 phenotypes). Ratios that were not significantly different from expected ratios were examined against known genetic cross outcomes for 2 or 3 genes, with complete or incomplete linkage. Ratios that were not significantly different, and applicable in a genetic cross, were accepted. Multiple ratios could be accepted for a single cross depending on major and minor phenotypes, such as 3R:1S ratio would also be compatible with a 1R:2Rn:1S ratio.

m11526 crossed to each line:				Powdery Mildew		F1 Phenotype	% of progeny with Phenotype					Chi-squared test against expected ratios								
Line	*Mla* allele	Additonal Genotype	Infection Phenotype	Isolate	Relevent Genotype		Resistant (R)	Resistant with necrosis (Rn)	Susceptible with necrosis (Sn)	Susceptible (S)	# of F2	3:1	1:2:1	9:7	5:11	5:4:7	9:4:3	15:1	1:1	9:3:3:1
Morex	-	n/a	S	*Bgh* 5874	AVR_{a6}	R	55	0	0	45	165	0.00	n/a	0.66	0.00	n/a	n/a	0.00	0.00	n/a
Q21861	*Mla1*	n/a	R	*Bgh* 5874	AVR_{a1} AVR_{a6}	R	92	0	0	8	507	0.00	n/a	0.00	0.00	n/a	n/a	0.18	0.00	n/a
CI 16137	*Mla1*	n/a	R	*Bgh* 5874	AVR_{a1} AVR_{a6}	R	93	0	0	7	191	0.00	0.00	0.00	0.00	0.00	0.00	0.58	0.00	n/a
CI 16151	*Mla6*	n/a	R	*Bgh* 5874	AVR_{a6}	R	81	0	0	19	96	0.16	n/a	0.00	0.01	n/a	n/a	0.00	0.00	n/a
P03	*Mla6*	n/a	R	*Bgh* 5874	AVR_{a6}	R	74	0	0	26	190	0.74	n/a	0.00	0.12	n/a	n/a	0.00	0.00	n/a
mla6-m9472	*mla6*	n/a	S	*Bgh* 5874	AVR_{a6}	R	58	0	0	42	96	0.00	n/a	0.68	0.03	n/a	n/a	0.00	0.10	n/a
CI 16147	*Mla7*	n/a	Rn	CC148	AVR_{a7}	Sn	0	31	32	38	190	0.08	0.00	0.00	0.83	0.09	0.00	0.00	0.00	n/a
Hor11358	*Mla9*	n/a	R	CC148	AVR_{a9}	Rn	56	18	5	20	188	0.87	0.00	0.00	0.09	0.00	0.82	0.00	0.00	0.00
CI 16149	*Mla10*	n/a	Rn	CC148	AVR_{a10}	Sn	5	10	55	29	184	0.00	0.02	0.00	0.00	0.00	0.00	0.00	0.00	0.00
Sultan-5	*Mla12*	n/a	Rn	*Bgh* 5874	AVR_{a6} AVR_{a12}	R	64	9	21	6	185	0.50	0.00	0.00	0.22	0.00	0.00	0.00	0.00	0.01
rar1-m100	*Mla12*	*rar1*	Sn	*Bgh* 5874	AVR_{a6} AVR_{a12}	R	44	22	32	2	176	0.00	0.00	0.02	0.33	0.66	0.00	0.00	0.00	0.00
CI 16155	*Mla13*	n/a	R	CC148	AVR_{a13}	R	52	18	0	30	186	0.15	0.00	0.00	0.62	0.04	0.00	0.00	0.00	n/a
CI 16153	*Mla15*	n/a	Rn	CC148	AVR_{a7}	Sn	0	22	53	25	363	0.24	0.46	0.00	0.00	0.00	0.00	0.00	0.00	n/a

Full Genotype:	*Bgh* 5874	AVR_{a1}, AVR_{a6}, AVR_{a12}
	CC148	AVR_{a1}, AVR_{a7}, AVR_{a9}, AVR_{a10}, AVR_{a13}

0.05	Not Significantly different from expected
0.04	Significantly different from expected
n/a	Ratio not applicable due to lack of phenotype
	Accepted ratio

Table 2-S7. **Expected ratios of F2 from m11526 (*Mla6, rar3*) crosses. A**) Table detailing the two cross combinations and the possible phenotypic ratios when m11526 (*Mla6*, *rar3*) is crossed to a line with a non-functioning *mla* allele, with Morex (*mla*, *Rar3*) as the example. **B**) Table detailing the two cross combinations and the possible phenotypic ratios when m11526 crosses are inoculated with *Bgh* 5874, with CI 16137 (*Mla1*, *Rar3)* as the example. **C**) Table detailing the four cross combinations and the possible phenotypic ratios when m11526 crosses are inoculated with CC148, with HOR11358 (*Mla9*, *Rar3*) as the example. As CC148 does not harbor *AVR$_{a6}$*, the *Mla6* allele does not function in this interaction. **D)** Table detailing the cross results when m11526 is crossed to m100 (*Mla12, Rar1, Rar3*) if there is no linkage, or complete linkage.

A)

m11526 (*Mla6*, *rar3*) x morex (*mla*, *Rar3*)

All Genotype Possibilities			Ratio	Genetic interaction hypotheses	
				m11526 *Mla6* functional	m11526 *Mla6* nonfunctional
#	***Mla* locus**	***Rar3* Locus**		**Phenotype**	**Phenotype**
1	*mla/mla*	*Rar3/Rar3*	1/16	**S**	**S**
2	*mla/mla*	*Rar3/rar3*	2/16	**S**	**S**
3	*mla/mla*	*rar3/rar3*	1/16	**S**	**S**
4	*Mla6/mla*	*Rar3/Rar3*	2/16	**R**	**S**
5	*Mla6/mla*	*Rar3/rar3*	4/16	**R**	**S**
6	*Mla6/mla*	*rar3/rar3*	2/16	**S**	**S**
7	*Mla6/Mla6*	*Rar3/Rar3*	1/16	**R**	**S**
8	*Mla6/Mla6*	*Rar3/rar3*	2/16	**R**	**S**
9	*Mla6/Mla6*	*rar3/rar3*	1/16	**S**	**S**

R	9	0
S	7	1

Crosses matching ratio:
Morex (*mla*)
mla6-m9472 (*mla6*)

B)

m11526 (*Mla6*, *rar3*) x CI 16137 (*Mla1*, *Rar3*)

All Genotype Posibilities			Ratio	Genetic interaction hypotheses	
				Mla1 requires *Rar3*	*Mla1* doesn't require *Rar3*
#	*Mla* locus	*Rar3* Locus		Phenotype	Phenotype
1	*Mla1/Mla1*	*Rar3/Rar3*	1/16	R	R
2	*Mla1/Mla1*	*Rar3/rar3*	2/16	R	R
3	*Mla1/Mla1*	*rar3/rar3*	1/16	S	R
4	*Mla6/Mla1*	*Rar3/Rar3*	2/16	R	R
5	*Mla6/Mla1*	*Rar3/rar3*	4/16	R	R
6	*Mla6/Mla1*	*rar3/rar3*	2/16	S	R
7	*Mla6/Mla6*	*Rar3/Rar3*	1/16	R	R
8	*Mla6/Mla6*	*Rar3/rar3*	2/16	R	R
9	*Mla6/Mla6*	*rar3/rar3*	1/16	S	S

R	3	15
S	1	1

Crosses matching ratio:

CI 16151 (*Mla6*) Q21861 (*Mla1*)
P03 (*Mla6*) CI 16137 (*Mla1*)
Sultan-5 (*Mla12*)

C)

All Genotype Posibilities			Ratio	Genetic interaction hypotheses			
				Mla9 requires *Rar3*	*Mla9* doesn't require *Rar3*	*Mla9* Semi-dominant	Three functional alleles
#	*Mla* locus	*Rar3* Locus		Phenotype	Phenotype	Phenotype	Phenotype
1	*Mla9/Mla9*	*Rar3/Rar3*	1/16	R	R	R	R
2	*Mla9/Mla9*	*Rar3/rar3*	2/16	R	R	R	R
3	*Mla9/Mla9*	*rar3/rar3*	1/16	S	R	R	S
4	*Mla6/Mla9*	*Rar3/Rar3*	2/16	R	R	S	R
5	*Mla6/Mla9*	*Rar3/rar3*	4/16	R	R	S	S
6	*Mla6/Mla9*	*rar3/rar3*	2/16	S	R	S	S
7	*Mla6/Mla6*	*Rar3/Rar3*	1/16	S	S	S	S
8	*Mla6/Mla6*	*Rar3/rar3*	2/16	S	S	S	S
9	*Mla6/Mla6*	*rar3/rar3*	1/16	S	S	S	S

R	9	3	1	5
S	7	1	3	11

Crosses matching Ratio:

HOR11358 (*Mla9*) CI 16153 (*Mla15*) CI 16147 (*Mla7*)
CI 16155 (*Mla13*)

D)

m11526 (*Mla6*, *rar3, Rar1*) x m100 (*Mla12*, *Rar3, rar1*)

All Genotype Posibilities (Ignoring *Mla*)			Ratio	Genetic interaction hypotheses
				Rar3 / *Rar1* are unlinked
#	Rar1 Locus	*Rar3* Locus		Phenotype
1	*Rar1/Rar1*	*Rar3/Rar3*	1/16	R
2	*Rar1/rar1*	*Rar3/Rar3*	2/16	R
3	*rar1/rar1*	*Rar3/Rar3*	1/16	S
4	*Rar1/Rar1*	*Rar3/rar3*	2/16	R
5	*Rar1/rar1*	*Rar3/rar3*	4/16	R
6	*rar1/rar1*	*Rar3/rar3*	2/16	S
7	*Rar1/Rar1*	*rar3/rar3*	1/16	S
8	*Rar1/rar1*	*rar3/rar3*	2/16	S
9	*rar1/rar1*	*rar3/rar3*	1/16	S

R	9
S	7

Table 2-S8. **Acronyms used**.

Acronym	Definition
AVR	*Avirulence, r*eferring to a pathogen effector that is recognized by host resistance gene
Bgh	*Blumeria graminis* forma specialis *hordei*
CAPS	Cleaved Amplified Polymorphic Sequence
CR2	Variable region 2
CS	Chord and Sgt1
DAI	Days after inoculation
ESH	Elongating Secondary Hyphae
HAI	Hours after inoculation
HRS	HSP90, RAR1, SGT1
Hsp90	*Heatshock Protein 90*
Mla	*mildew resistance locus a*
NLR	Nucleotide-binding, Leucine-rich-repeat receptor
NOD	nucleotide-binding oligomerization domain
R	Resistant phenotype, no sporulation and no necrosis
Rar1	*Required for Mla12 Resistance 1*
Rar3	*Required for Mla6 Resistance 3*
Rn	Resistant with necrosis phenotype, no sporulation and significant necrosis
S	Susceptible phenotype, significant sporulation and no necrosis
SGS	*Sgt1*-specific
Sgt1	*Suppressor of G-two allele of Skp1*
$Sgt1_{\Delta KL308\text{-}309}$	*Sgt1* from m11526 which has 6bp deleted, corresponding to amino acid positions K308 and L309
Sn	Susceptible with necrosis phenotype, significant sporulation and significant necrosis
TPR	Tetratricopeptide repeat
VR	Variable region

CHAPTER 3. THE SGT1$_{\Delta KL308-309}$ NON-LETHAL MUTATION WEAKENS INTERACTIONS WITH MLA6, CAUSING A REDUCTION OF PROTEIN ACCUMULATION

Antony V. E. Chapman* †, J. Mitch Elmore†, Justin Walley* †, and Roger P. Wise* † ‡

*Interdepartmental Genetics & Genomics, Iowa State University, Ames, IA 50011

†Department of Plant Pathology & Microbiology, Iowa State University, Ames, IA 50011

‡Corn Insects and Crop Genetics Research, USDA-Agricultural Research Service, Ames, IA 50011

Modified from a manuscript to be submitted to *Molecular Plant-Microbe Interactions*

Abstract

It is vital to comprehend the molecular mechanisms underlying interactions among hosts and pathogens if we are to engineer resistance against diseases in the future. The *Mla* (*Mildew resistance locus a*) of barley (*Hordeum vulgare* L.) is a powerful model for cereal immunity against fungi. MLA, like many resistance proteins, requires the HRS complex to function, consisting of HSP90 (Heat shock protein 90), RAR1 (Required for Mla12 Resistance 1), and SGT1 (Suppressor of G-two allele of Skp1). *Sgt1* has been particularly difficult to study as full deletions are lethal. Previously, we identified the *Sgt1$_{\Delta KL308-309}$* mutation in a fast-neutron-derived barley population, that selectively disrupts resistance conferred by some *Mla* alleles against *Blumeria graminis* f. sp. *hordei* (*Bgh*), without lethality. Herein, using autoactive MLA6 and yeast strains with stably integrated *HvRar1* and *HvHsp90*, we discover that the mutation

weakens, but doesn't entirely disrupt, the interaction between SGT1 and MLA. This causes a concomitant reduction in MLA6 protein accumulation below the apparent threshold required for effective resistance. The deletion had a lesser effect on intramolecular interactions than alanine or arginine substitutions. MLA variants with inherently weaker interactions with SGT1 appear to be disproportionately affected by the $SGT1_{\Delta KL308\text{-}309}$ mutation. We hypothesize that those dimeric plant CC-NLRs that appear unaffected by *Sgt1* silencing are those with the strongest intermolecular interactions with it. Combining our data with recent work in CC-NLRs, we propose a cyclical model of the MLA-HRS resistosome interactions.

Introduction

Fungal pathogens represent a large and economically significant challenge to crops worldwide (Savary *et al.*, 2019). To lessen the impact of fungi on our food sources, we employ a variety of biological, chemical, and mechanical methods, to varying degrees of success. Recent focus has come upon the potential of utilizing molecular biology methods to quicken the development of genetically resistant crops, which would reduce the need of, and damage caused by, chemical fungicides (Knebel *et al.*, 2019, Carneiro *et al.*, 2020, van Wersch *et al.*, 2020). However, for these methods to be effective and durable, we must understand the molecular interactions between crops and pathogenic fungi as completely as possible (Zhang *et al.*, 2020). A key tool for expanding our understanding are model crop-pathogen systems where discoveries and innovation can be extrapolated to other crops.

The interaction between barley (*Hordeum vulgare* L.) and *Blumeria graminis* f. sp. *hordei* (*Bgh*), the cause of powdery mildew disease, is a model for investigating plant host-fungal pathogen interactions in large-genome cereals (Draz *et al.*, 2019). *Bgh* is an obligate biotrophic

fungus, meaning that it must parasitize living cells to feed (Yamaoka *et al.*, 2006). During infection, *Bgh* will penetrate the cell wall and release proteins directly into the host cell (Godfrey *et al.*, 2009). These proteins, called effectors, have specialized functions, such as subverting host defense responses and facilitating nutrient absorption (Krattinger and Keller, 2016). However, in parallel with the evolution of pathogen effectors, plants have evolved proteins that detect effectors directly, or indirectly (Jaswal *et al.*, 2020). Once detected, these resistance (R) proteins initiate severe defense responses that often culminate in the death of the infected cell, and consequently the death of the fungus (Lo Presti *et al.*, 2015).

The barley mildew resistance locus A (MLA) proteins provide defense against *Bgh* by recognizing specific cognate effectors (Jorgensen, 1994, Wei *et al.*, 2002, Halterman and Wise, 2004, Ridout *et al.*, 2006, Seeholzer *et al.*, 2010, Lu *et al.*, 2016, Saur *et al.*, 2019). MLA proteins are archetypical coiled-coil (CC), nucleotide-binding (**N**B), leucine-rich-repeat (**L**RR) **r**eceptor proteins, or NLRs (Shirasu, 2009, van Wersch *et al.*, 2020) (**Figure 3-1A**). To confer resistance, MLA proteins require association with the HRS complex, which is composed of the co-chaperones Heat Shock Protein 90 (HSP90), Required for MLA12 Resistance 1 (RAR1) and Suppressor of G-Two allele of *Skp1* (SGT1) (**Figure 3-1B**) (Bieri *et al.*, 2004). Once MLA recognizes the presence of the cognate effector, the complex translocates to the nucleus where it initiates a signaling cascade, including interactions with distinct transcription factors, that leads to the hypersensitive response and resistance (Shen *et al.*, 2007, Bai *et al.*, 2012, Chang *et al.*, 2013).

The complex interactions between NLRs and the HRS complex play a critical role in immune response to pathogens (Sun *et al.*, 2020). To identify unknown factors in this pathway,

we conducted fast-neutron mutagenesis of the resistant barley line, cereal introduction (CI) 16151 (Manchuria background, *Mla6*) and screened for loss of resistance to *Bgh* strain 5874 (AVR_{a6}). In the derived susceptible mutant m11526, we identified a 6 bp, in-frame Lys-Leu deletion within the SGS domain of *HvSgt1* (HORVU3H1G055920) as causing selective disruption of *Mla*-mediated, race-specific resistance to *Bgh* (Chapman *et al.*, 2020). The *required for mla6 resistance* (*rar3*) mutation, $Sgt1_{\Delta KL308\text{-}309}$, alters the function of *Mla6*, *Mla7*, and *Mla12* (named *Rar3*-dependent alleles) to defend against *Bgh*. However, it did not appear to affect the function of *Mla1*, *Mla9*, *Mla10*, *Mla13*, and *Mla15* (named *Rar3*-independent alleles).

Sgt1 is critical for a vast array of eukaryotic cell processes, as evidenced by the lethality of deletion mutants (Azevedo *et al.*, 2002, Martins *et al.*, 2009), or when it is silenced (Bhattarai *et al.*, 2007, Thao *et al.*, 2007). No lethality or stunting is displayed in the barley mutant line in which the $Sgt1_{\Delta KL308\text{-}309}$ mutation was discovered (Chapman *et al.*, 2020). This suggests that the $Sgt1_{\Delta KL308\text{-}309}$ mutation explicitly inhibits *Mla*-specified disease resistance but does not overtly affect other cell processes that *Sgt1* is involved with, such as hormone detection and kinetochore development (Meldau *et al.*, 2011). Thus, the $Sgt1_{\Delta KL308\text{-}309}$ mutation provides a unique opportunity to investigate the involvement of *Sgt1* in immunity.

To explore the intermolecular and structural relationship between SGT1 and NLRs, we took advantage of the $Sgt1_{\Delta KL308\text{-}309}$ mutation to investigate how it perturbs MLA-dependent disease resistance. First, we show that the previously unobserved interaction between MLA6 and SGT1 can be revealed in the Y2H system by utilizing full-length autoactive NLR mutants and reconstituting the HRS complex through yeast genome engineering. Using this system, we then

show that SGT1$_{\Delta KL308-309}$ destabilizes the interaction with both the *Rar3*-independent MLA1 and *Rar3*-dependent MLA6, compared to wildtype SGT1. Lastly, parallel reaction monitoring (PRM) mass spectrometry showed that MLA6 protein accumulates in the *Sgt1$_{\Delta KL308-309}$* mutant line to a lower, but still observable, level than in wildtype CI 16151. Combined with other recent evidence, these results suggest that SGT1 may be required by more NLRs than previously suspected. Moreover, the *Sgt1$_{\Delta KL308-309}$* mutation may be a new tool for investigating NLRs by isolating disease resistance signaling from other cellular processes.

Materials and Methods

Biological materials

Seven-day old barley seedlings of CI 16151 (*Mla6*, Manchuria background), its fast-neutron derived *rar3* mutant, m11526 (Chapman *et al.*, 2020), and P04B (*Mla7*, Pallas background) (Saur *et al.*, 2019) were infected with *Bgh* isolate 5874. Twenty-four hours after inoculation the first leaves of these seedlings were harvested, flash frozen in liquid nitrogen, and stored at -80°C before RNA was isolated as described (Caldo *et al.*, 2004). cDNA synthesis was performed with SuperScript III Reverse Transcriptase (Invitrogen, #18080093, Thermo, Waltham, MA). The P04B allele of *Mla7* was chosen over the allele present in the line CI 16147 (Manchuria background, *Mla7*) due to its stronger cell death phenotype (Saur *et al.*, 2019).

Nicotiana benthamiana seeds were germinated on the surface of soil for 7-10 days before being transplanted to 3-inch pots. *Agrobacterium tumefaciens* strain EHA105 was used for the transient expression of all constructs used in *N. benthamiana*, including pEG100 and pHG8.

Experimental Constructs

pEarleyGate100 (pEG100, Kan_{50}, ABRC stock CD3-724) was used to overexpress proteins of interest in *N. benthamiana* under control of the cauliflower mosaic virus 35S promoter. Genes were first amplified from barley cDNA and inserted into the gateway entry pCR8 TOPO TA backbone (Thermo, K250020, Waltham, MA), and then inserted into the appropriate vector via Gateway LR reactions, pEG100, p97-BD, or p86-AD.

Silencing constructs targeting *N. benthamiana Sgt1* (*NbSgt1*) were designed by aligning the available *NbSgt1* sequences (AY899199, AF494083, AF516180, and AF516181) and amplifying the most conserved regions at ~<600bp with PCR from cDNA (**Table 3-S1** for primers). Though the amino acid sequence is conserved between *N. benthamiana* and barley, the nucleotide sequences are unconserved with no consecutive matching bases longer than an outlier of 19bp, which is below the 20bp limit for hairpin formation. The amplicon of 78-586bp, 509bp long, was then inserted into the hairpin silencing construct pHELLSGATE8 (pHG8) (Helliwell and Waterhouse, 2003).

Mass-spectrometry sample preparation

For each genotype, CI 16151 (*Mla6, Rar3*), *mla6*-m18982 (*Δmla6, Sgt1*), *rar3*-m11526 (*Mla6*, $Sgt1_{\Delta KL308\text{-}309}$), Sultan-5 (*Mla12, Rar1*), and *rar1*-m100 (*Mla12, rar1-2*), three biological replicates of six seeds were planted in 3-inch pots, randomly placed in 16 cell flats. Of the six seed planted, five uniform leaves were collected at 7 days and frozen immediately in liquid nitrogen for storage prior to processing. Leaves were then ground to a fine powder in liquid

nitrogen using a mortar and pestle for 15 mins per sample. Maintaining a small pool of liquid nitrogen preserved sample quality during grinding.

Protein was extracted from barley tissue using a phenol extraction method, processed with Filter Aided Sample Preparation (FASP), which included digestion with Trypsin and Lys-C, and cleaned up using C18 cartridges, as described by (Song *et al.*, 2018). After processing, samples were resuspended in 0.1% formic acid (FA) and quantified using a Pierce BCA protein assay kit (Thermo, #23225 , Waltham, MA).

Media

E. coli were grown on Luria-Bertani (LB) agar with the appropriate antibiotics. Yeast was grown on YPD (Yeast Peptone Dextrose) or SC- (synthetic complete dropout) media (Burke *et al.*, 2000).

Yeast-two-hybrid (Y2H) system

The Y2H system, described by (Dreze *et al.*, 2010), utilizes yeast strains Y8800 *MATα* and Y8930 *MATα* (*trp1-901; leu2-3, 112; ura3-52; his3-200; gal4Δ; gal80Δ; GAL2-ADE2; LYS2::GAL1-HIS3; MET2::GAL7-lacZ; cyh2^{R}).* Transformation of yeast with plasmids were conducted using the LiAc/SS carrier DNA/PEG method (Gietz, 2014). The plasmids pDEST-DB (aka pPC97 or p97-BD, *Leu2p*) and pDEST-AD (aka pPC86 or p86-AD, *Trp1p*) are low copy ARS4/CEN6-based which encode for fusions to the GAL4 DNA-binding domain (DB) and GAL4 activating domain (AD) respectively. pDEST-DB and pDEST-AD allow for the growth of Y8800 or Y8930 on media lacking leucine (SC-L) or tryptophan (SC-W) respectively. Selection for Y8800-Y8930 diploids harboring both pDEST-AD and pDEST-DB are done by growing on SC- media lacking both leucine and

tryptophan (SC-LW). When the GAL4 activating and DNA-binding domains are in close proximity, caused by an interaction between their fused proteins, they induce expression of HIS3 by associating with the 125 bp GAL1 upstream activating sequence which has been inserted in the promoter region. The strength of the interaction between the proteins fused to the GAL4 AD and DB domains is estimated by the level of growth of the diploid on media lacking histidine (SC-LWH), a higher level of growth indicating a stronger interaction.

Stable yeast introgression

The yeast strain Y8800 was engineered to stably express HvRAR1 and HvHSP90 using the system developed by (Mikkelsen *et al.*, 2012). The yeast promoter *TEF1* from Y8800 was isolated using PCR from extracted genomic DNA (Lõoke *et al.*, 2011) with an added AsiSI restriction enzyme site on the 3' end of the reverse primer (See **Table 3-S2** for primer list). The *TEF1* promoter was inserted into plasmids pXI-5 and pXII-3, oriented to the ADH1 and CYC1 terminators respectively, creating the constructs pXI-5-*TEF1-ADH1* and pXII-3-*TEF1-CYC1*. *HvRar1* (HORVU2Hr1G097800) and *HvHsp90* (HORVU5Hr1G072420) were amplified from barley cDNA and inserted separately into both constructs.

Yeast strain Y8800 was transformed with each of the four constructs and then selected on SC-Uracil plates for successful transformation events indicated by presence of the *URA3* marker, and presence of the barley gene was confirmed by PCR amplification. The *URA3* marker is designed to excise out of the yeast genome by direct repeat recombination to allow for multiple uses in the same strain. Colonies of transformed Y8800 with the *URA3* gene excised were selected for by growth on SC media containing uracil and 5-fluoroorotic acid

(Thermo, #R0811, Waltham, MA), which is lethal to strains with a functional *URA3* gene. Loss of *URA3* marker gene was confirmed by a lack of growth on SC-Uracil media. Strains which were successfully engineered with a single gene, and which lost the URA3 marker, were transformed again with the complementary second gene and selected by the same method as described for the first transformation. For example, Y8800-XII-3-*Rar1-CYC1* was transformed with pXI-5-*TEF1-HSP90-ADH1*. This resulted in one strain (Y8800-XII-3-*Rar1-CYC1*-XI-5-*Hsp90-ADH1*, aka Y-RcHa, pronounced "Y archer") that had both *HvRar1* and *HvHSP90* integrated into the genome on chromosomes XII and XI, respectively, and with different terminators (CYC1 and ADH1, respectively). This strain was transformed with pDEST-AD plasmids to generate Y-RcHa strains for use in Y2H. A diagram of the process is outlined in **Figure 3-S3**.

Mutagenesis

We performed site-directed mutagenesis using the Quikchange Lightning site-directed Mutagenesis Kit (Agilent, #210519, Santa Clara, CA) as per the manufacturer's guidelines. Primers used for mutagenesis are listed in **Table 3-S2**.

Peptide design

Peptide design was conducted following guidelines set down by (Rauniyar, 2015). Peptides for MLA6 and SGT1 were designed using SkyLine software under a trypsin digest (Pino *et al.*, 2020). Candidate peptides were searched using BLASTp against the barley protein database on EnsemblPlants (IBSC v2) to look for uniqueness. PEPOtec grade 2 synthetic versions of these peptides with heavy leucines were ordered from Thermofisher (Waltham,

MA). Upon receipt, synthetic peptides were resuspended in 0.1% FA and working stocks were made at 1000fmol/ul.

PRM LC-MS Method

LC-MS was performed using an Ultimate 3000 RSLCnano HPLC coupled to a Q-Exactive Plus mass spectrometer with a nano-electrospary ion source (Thermo, Waltham, MA). 100 µM ID x 25 cm capillary columns were pulled to a ~10 µM tip with a laser puller (Sutter P-2000) and packed with ~1 cm 5 µM C18 particles (Agilent, Santa Clara, CA, Zorbax SB-C18) at the tip, and then filled up to the full length with 2.5 µM C18 particles (Waters, Milford, MA, XBridge BEH). 10 µL (1250ng) of peptide samples in buffer A (0.1% formic acid (v/v)) were injected using an autosampler with a 20 µL sample loop and pre-concentrated on a 300 µM by 5mm trap cartridge (Thermo, Waltham, MA, C18 PepMap100 5 µM) for 5 min at 10 µL/min using the loading pump. At 5 min the trap column was switched in-line with the nano-capillary pump set at 1% buffer B (0.1% formic acid (v/v), 80% acetonitrile (v/v)) at a flow rate of 250 nL/min. The 150 min LC program consisted of a gradient from 1% to 6.3% buffer B at 4-5min, followed by 6.3% to 31.3% for 5-110 min, then 31.3% to 56.3% for 110-135min, then 99% at 135.5-140.5 min, and reduced to 1% B at 141 min.

For PRM, the MS program consisted of a full MS scan followed by 4 DIA scans using an inclusion list (**Table 3-1**). The full MS scan was acquired at a resolution of 70,000, AGC target 1e6, maximum IT of 50ms, and scan range of 150 to 2000 m/z. The DIA scans used a resolution of 140,000, AGC target of 3e6, maximum IT of 500ms, loop count of 4, isolation window of 0.4 m/z, and NCE of 28. The optimal sample for detection of the peptides was 1.25ug of complex

samples were run with synthetic peptides added at an amount of 200 fm for SGT1 DANK and 10 fm for MLA6 WaVe.

Table 3-1. **Inclusion list used for PRM of synthetic heavy and endogenous light versions of SGT1 DANK and MLA6 WaVe**.

Mass [m/z]	Formula [M]	Species	CS [z]	Polarity	Start [min]	End [min]	NCE	Comment
669.830431			2	Positive			28	LGSYTEAVADANK (light)
673.339013			2	Positive			28	LGSYTEAVADANK (heavy)
502.295436			2	Positive			28	WVPPVHLR (light)
505.804018			2	Positive			28	WVPPVHLR (heavy)

Data analysis

Raw output files from Xcalibur for each run were imported into Skyline (Pino *et al.*, 2020) (version 20.1.0.155). Peptide settings were as shown in **Figure 3-S4**. The background proteome was the barley proteome downloaded from EnsemblPlants, ISBC v2. The reference library was generated from the .raw file PXD012684 downloaded from Proteome Exchange (http://proteomecentral.proteomexchange.org) (Lambertucci *et al.*, 2019).

Peptide detection

The synthesized peptides were first run on their own in order to evaluate the quality of the peptides and the suitability of the method at amounts ranging from 1 femtomole (fm) to 1000 fm. The resulting chromatograms were compared to results from a publicly available barley mass-spectrometry dataset (PXD012684, proteomexchange.org) (Lambertucci *et al.*,

2019), though differences in equipment and settings cause expected variability between studies. Besides the ATLAS control peptide, only two of the five synthesized peptides were consistently observed, MLA6.7.12_Pep3 “WaVe”, and HvSGT1_Pep2 “DANK” (**Figure 3-8**). These two peptides were then spiked into complex wildtype uninfected barley samples to look for the endogenous peptides and run using varying settings to optimize.

Statistical analyses

Data was analyzed with a linear model with the design Ratio ~ Genotype and a one-way ANOVA using the Tukey test was performed with pairwise contrasts. Contrasts were defined as significant at $p<0.05$. Raw total peak area data was exported from Skyline for analysis and all analyses were run using R (R Core Team, 2019) (Version 3.6), and the packages nlme (Pinheiro *et al.*, 2020), multcomp (Hothorn *et al.*, 2008), emmeans, multcompview (Graves *et al.*, 2019). Graphs were generated using the package ggplot2 (Wickham, 2016).

Results

Incorporating barley HSP90 and RAR1 into Y8800 yeast facilitates interactions between SGT1 and MLA

We previously demonstrated that the *rar3* mutation localized to an *in-frame* Lys-Leu deletion in the SGS domain of SGT1 (Chapman *et al.*, 2020). The LRR domain of NLRs interact directly with the SGS domain of SGT1 (**Figure 3-1**) (Bieri *et al.*, 2004), thus, the Lys-Leu deletion may be impairing the interaction between NLRs and SGT1, resulting in a non-functional immune response. SGT1 functions as part of the HRS complex with HSP90 and RAR1, and it has been shown that MLA6 requires both HSP90 and RAR1 to function (Bieri *et al.*, 2004). Further, it has been suggested that RAR1 may increase the affinity of SGT1 for NLRs (Kadota and Shirasu,

2012). Therefore, it is possible that the lack of barley HSP90 and RAR1 in the Y2H system prevents some NLRs, such as MLA6, from properly interacting with SGT1. We hypothesized that reconstituting the barley HRS complex in the Y2H system could be used to test interactions between SGT1 and NLRs.

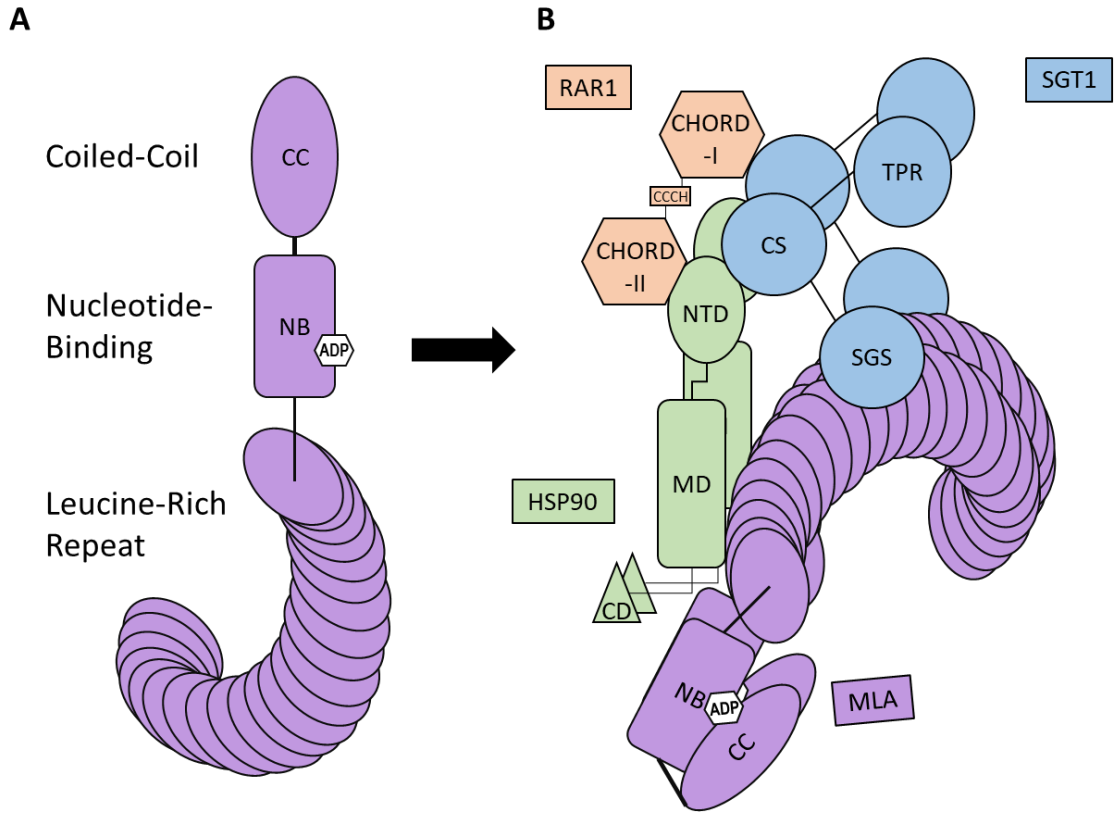

Figure 3-1. **Model for the structure of MLA and how it interacts with the HRS complex.** Adapted from (Boter *et al.*, 2007, Shirasu, 2009, Siligardi *et al.*, 2018). **A**) The MLA protein is comprised of the Coiled-Coil (CC) signaling, the Nucleotide-Binding (NB), and the Leucine-Rich Repeat (LRR) domains. The MLA NB domain binds adenosine di-phosphate (ADP) in its inactive state, which maintains intramolecular interactions with the CC domain to prevent signaling. **B**) MLA is required to interact with the HRS complex to function, this consists of 2 units of Heat Shock Protein 90 (HSP90), 1 unit of Required for MLA12 Resistance 1 (RAR1) and 2 units of Suppressor of G-Two allele of Skp1 (SGT1). RAR1 consists of the cysteine- and histidine-rich domains (CHORD-I and CHORD-II) and the cysteine- and histidine-containing motif (CCCH). HSP90 consists of the N-terminal (NTD), middle (MD), and C-terminal dimerization (CTD) domains. SGT1 consists of the TPR (tetratricopeptide repeat), CS (CHORD-SGT1), and SGS (SGT1-Specific) domains.

First, we compared the interaction between MLA and wildtype SGT1 or the $SGT1_{\Delta KL308-309}$ mutant using the GAL4 yeast-2-hybrid (Y2H) system (Dreze *et al.*, 2010). Heretofore, it had been required to use only the LRR domain of NLRs to test for these interactions as the whole NLR is autoinhibited (Bieri *et al.*, 2004). This could be due to the NLRs existing in a closed conformation naturally until they are activated by a cognate effector, or brought into the HRS scaffolding (Bernoux *et al.*, 2016). We tested multiple fragments of the MLA1 LRR, which had been shown previously to interact with SGT1 (Bieri *et al.*, 2004), against SGT1 WT and $SGT1_{\Delta KL308-309}$ (**Figure 3-2**). We found that the MLA LRR fragment 543-958 gave the strongest interaction (**Figure 3-2-B2**) with SGT1 WT (as determined by the rate and size of yeast colony growth), and that the interaction was slightly, but consistently, weaker with $SGT1_{\Delta KL308-309}$ (**Figure 3-2-B3**). However, consistent with previous reports, we did not observe an interaction between SGT1 and either full length MLA6 or the equivalent LRR fragment, indicated by the observed growth not being significantly higher than the negative controls (**Figure 3-2-E2** & **2-F2**).

Then, to test whether the inclusion of co-chaperones would facilitate the interaction between MLA6 and SGT1, we generated a yeast strain that harbored barley *Rar1* and *Hsp90*. *HvRar1* and *HvHsp90* were stably integrated into the genome of the yeast strain Y8800 to generate the "Y-archer" strain Y-RcHa (Y8800-*Rar1-cyc1-Hsp90-adh1*). When the interaction tests between SGT1 and MLA fragments were repeated using the Y-RcHa strain instead of Y8800, we saw increased evidence of interaction between MLA1 and SGT1 (**Figure 3-2-B4**). However, similar to the tests performed with the original Y8800 strain, the increased interaction using Y-RcHa was not observed in the interaction between MLA1 and $SGT1_{\Delta KL308-309}$

(**Figure 3-2-B5**), and, even in the Y-RcHa system, there was no observed interaction between MLA6 and SGT1 (**Figure 3-2-E4** & **2-F4**). As *Mla1* was found to be a *Rar3*-independent allele, this suggests that the $Sgt1_{\Delta KL308\text{-}309}$ mutation disrupts interactions with various MLA variants (Chapman *et al.*, 2020).

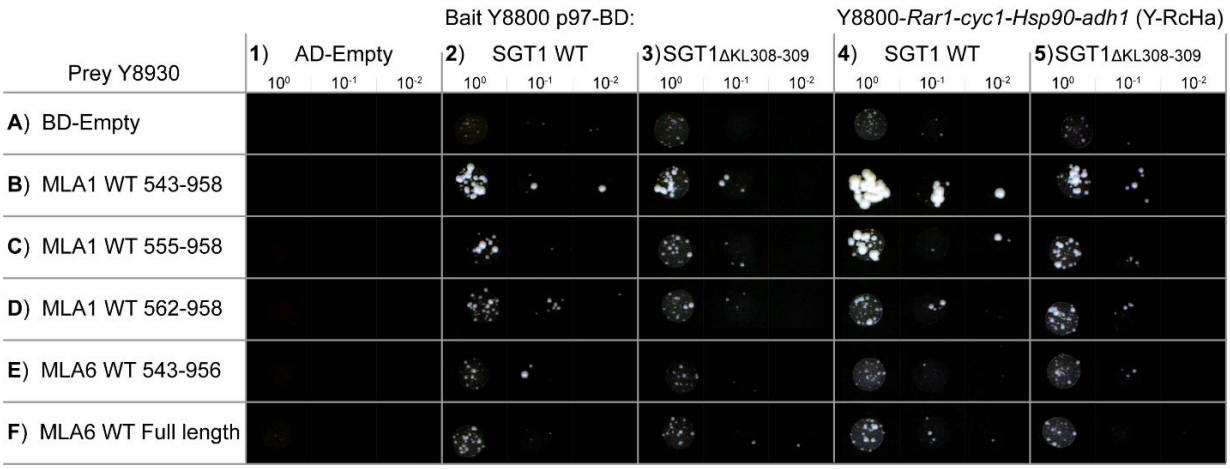

Figure 3-2. **Y2H interaction tests between MLA1 or MLA6 fragments and $SGT1_{\Delta KL308\text{-}309}$ with original Y8800 strain or modified Y-RcHa strain**. Rows and columns are labelled with letters and numbers respectively. E.g. AD-Empty/BD-Empty test is Figure 3-2-A1. Diploid Y8800 or Y-RcHa/Y8930 yeast expressing AD- and BD- grown on SC-LWH media. MLA1 WT 543-958 indicates that the fragment of MLA1 is from the wildtype sequence between amino acid position 543 to the stop codon at 958. MLA6 is two amino acids shorter than MLA1, therefore 956 corresponds to the MLA6 stop codon. Yeast was grown on SC-LWH, and images were taken 4 days after plating. Dilutions of diploids cells for plating are 10^0, 10^{-1}, and 10^{-2} of the original 0.5 OD culture.

Site-directed mutagenesis of *Sgt1* suggests KL308-309 are not direct interaction sites

To investigate further into why the $SGT1_{\Delta KL308\text{-}309}$ deletion affects interactions, we generated a series of *Sgt1* mutant constructs that would delineate the possible molecular mechanisms behind disruption. Using site-directed mutagenesis, we generated constructs with only one of the two candidate amino acids deleted to determine if a single position was causative ($Sgt1_{\Delta K308}$ and $Sgt1_{\Delta L309}$, **Figure 3-3-4 & 3-5**). In addition, we generated two single, and one double, alanine substitutions to determine whether the wildtype residue side-chains

were necessary for function or it was the loss of the position that caused the phenotype regardless of the side-chain (*Sgt1*$_{K308A}$, *Sgt1*$_{L309A}$, and *Sgt1*$_{KL308AA}$, **Figure 3-3-6, 3-7, & 3-8**). Lastly, as lysine is known to form intermolecular salt bridges with aspartates or glutamates (Kumar and Nussinov, 2002), and we are looking for the cause behind a weakened interaction, we generated *Sgt1*$_{K308R}$ (**Figure 3-3-9**). The arginine in this construct which would conserve the side chain nitrogen atoms required for the salt bridge to form, if that is the function of SGT1$_{K308}$.

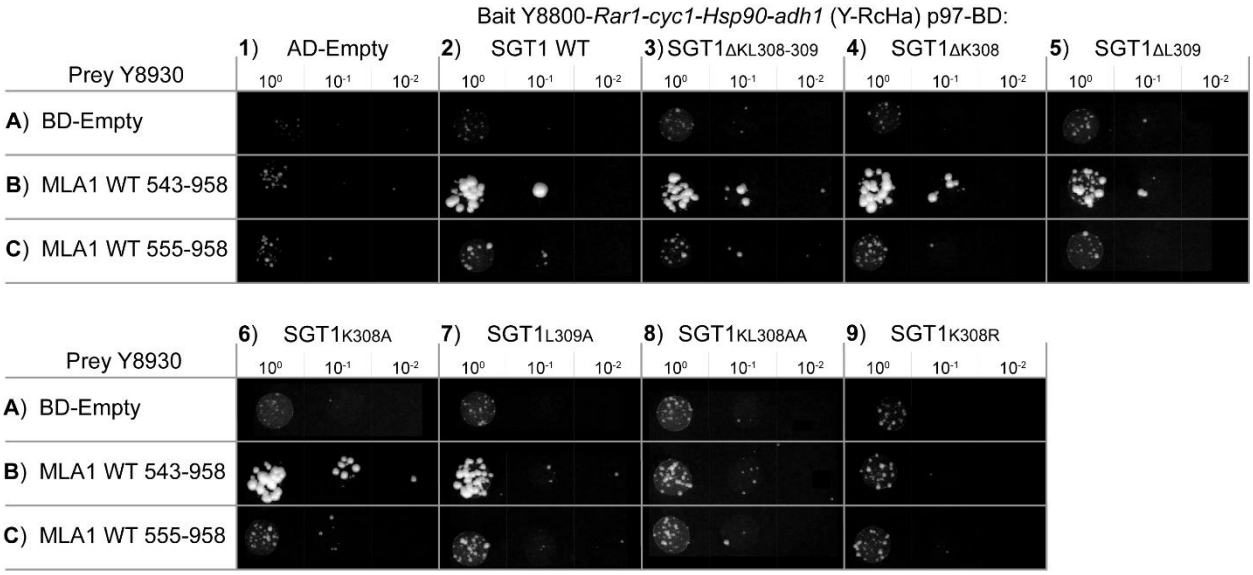

Figure 3-3. **Y2H interaction tests between MLA1 or MLA6 LRR fragments and SGT1 mutants**. Rows and columns are labelled with letters and numbers respectively. E.g. AD-Empty/BD-Empty negative control is Figure 3-3-A1. Diploid Y8800 or Y-RcHa/Y8930 yeast expressing AD- and BD- grown on SC-LWH media. MLA1 WT 543-958 indicates that the fragment of MLA1 is from the wildtype sequence between amino acid position 543 to the stop codon at 958. MLA6 is two amino acids shorter than MLA1, therefore 956 corresponds to the MLA6 stop codon. Yeast was grown on SC-LWH, and images were taken 4 days after plating. Dilutions of diploids cells for plating are 10^0, 10^{-1}, and 10^{-2} of the original 0.5 OD culture.

Interestingly, it was SGT1$_{\Delta L309}$ that appeared to mimic the lesser interaction of SGT1$_{\Delta KL308-309}$ with MLA, though the differences between the two interactions is small (**Figure 3-3-B5**). In contrast, neither of the single alanine substitutions appeared to have weakened interactions similar to the original *Sgt1*$_{\Delta KL308-309}$ (**Figure 3-3-B6 & 3-B7**). However, the double

alanine and the arginine substitutions both showed a complete loss of interaction (**Figure 3-3-B8 & 3-B9**).

As alanine is a relatively unreactive amino acid, it is surprising that the double alanine substitution had a greater effect on the strength of the interaction than the double deletion. The effect of the *Sgt1*$_{K308R}$ mutation may suggest that the function of SGT1$_{K308}$ is not in forming intermolecular salt-bridges. However, it has been shown before that mutating lysine to arginine can still disrupt established salt-bridges (Joseph *et al.*, 2018). In addition, the two amino acids after the deletion, which could be considered as taking the place of the deleted residues, are aspartate (D) and glycine (G). As aspartate forms the opposite side of a salt bridge to lysine, an aspartate replacing a lysine should destroy the proposed salt bridge. Alas, the deletion only causes a slight weakening of the interaction, especially when compared to alanine substitutions, this would suggest. In this regard, arginine has a guanidinium group that allows for more possibility of interactions because of the additional nitrogen atoms, and it has been shown to increase the intramolecular stability when compared to lysine (Sokalingam *et al.*, 2012). Therefore, as the SGS domain is considered extremely disordered due to its lack of a defined tertiary structure (Taube *et al.*, 2014), the *Sgt1*$_{K308R}$ mutation may cause an increase in stability of the SGS domain that somehow impairs its function.

MLA$_{797}$ and MLA$_{798}$ are essential for interactions with SGT1

Previously it had been found that the requirement for *Rar1* by *Mla6* and *Mla13* could be delineated to a single position in the LRR region, MLA$_{721}$ (Halterman and Wise, 2004). However, MLA6 and RAR1 do not directly interact (Bieri *et al.*, 2004). Rather, RAR1 interacts with both SGT1 and HSP90 and could function as structural support for the HRS complex to maintain it in

a conformation that promotes interaction with R proteins (Boter *et al.*, 2007). Therefore, we hypothesize that MLA_{721} confers requirement for *Rar1* by affecting the interaction between MLA and SGT1. It is interesting that *Rar1*-independent NLRs, such as MLA1, have an aspartate at this location as they are capable of forming intermolecular salt-bridges, whereas the glycine that *Rar1*-dependent NLRs, such as MLA6, have at this position are inactive. Therefore, $MLA1_{D721}$ may form an intermolecular salt bridge with SGT1. However, if this is the case, it can't be the only site of interaction between the two proteins as this change is not enough to confer MLA1-equivalent resistance response (Halterman and Wise, 2004). Therefore, we extrapolate that there may be a position within MLA that confers requirement for $Sgt1_{KL308\text{-}309}$.

To investigate key sites of interaction between MLA and SGT1, we scrutinized the differential "*Rar3*" requirement by MLA variants for amino acid consistencies between those defined as *Rar3*-dependent or -independent (Chapman *et al.*, 2020) (**Figure 3-4**). We identified three major sites which appear to show conservation or redundancy within each group. At MLA_{708}, *Rar3*-dependent variants have glutamate (E), whereas the *Rar3*-independent variants have either asparagine (N) and aspartate (D). These three amino acids are very similar and therefore, are generally interchangeable. They are polar, which means they prefer to be on the surface of proteins, exposed to an aqueous environment. Glutamate and aspartate are more similar in function than asparagine and aspartate. However, there are some key differences, while glutamate and aspartate can both form intermolecular salt-bridges, asparagine does not. Which would suggest that if the N/D at this position confers a stronger interaction with SGT1, it would not be due to the gaining of a salt-bridge. The main similarity between asparagine and

aspartate, which is not shared by glutamate, is the slightly shorter side chain. Which may suggest that its function may be structural if this is the key difference.

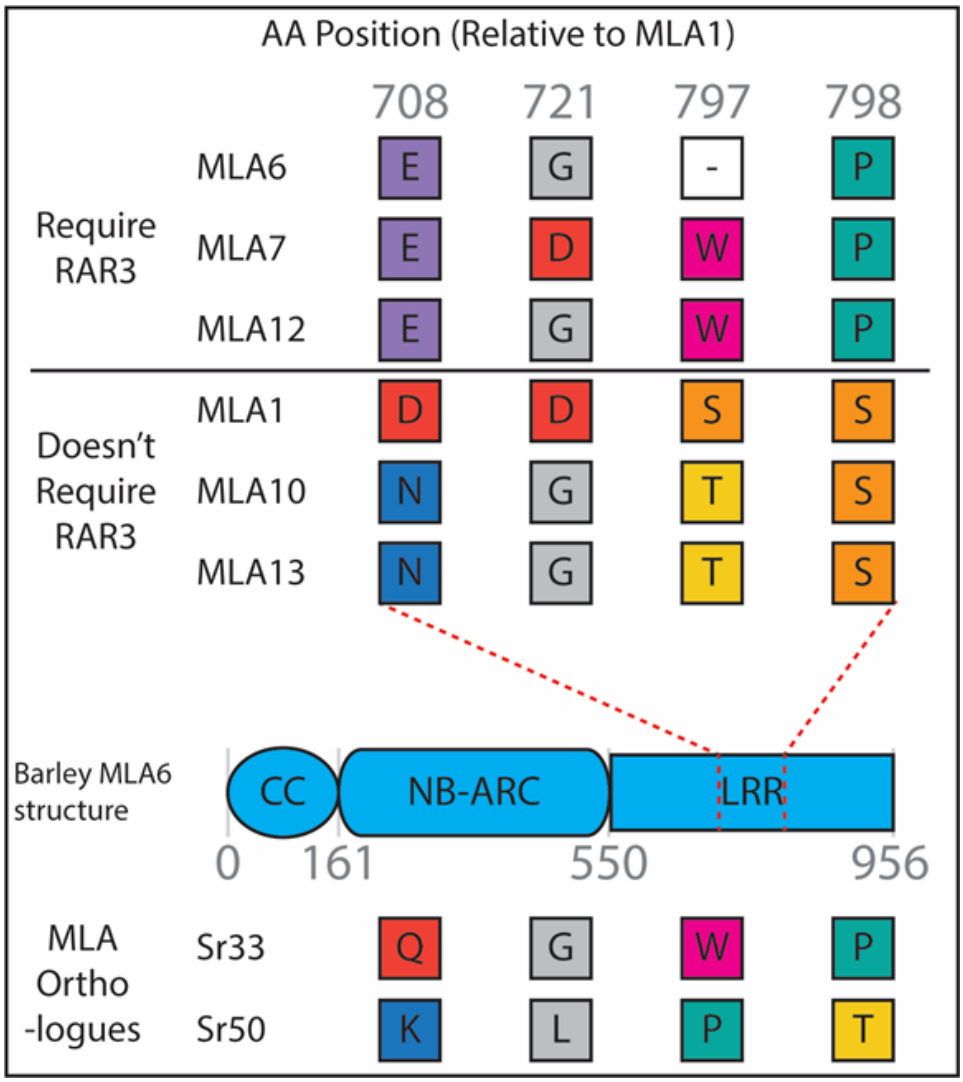

Figure 3-4. **Conservation of amino acids between *Rar3*-dependent or -independent MLA variants at multiple key sites**. Conservation is observed between *Rar3*-dependent alleles at 708, and between *Rar3*-independent alleles at 798. At position 797, *Rar3*-independent alleles contain either serine or threonine present, which can be functional redundant. Position 721, which confers genetic requirement for *Rar1* does not show conservation between the groups (Halterman and Wise, 2004). Below the structure are two MLA orthologues in wheat, Sr33 and Sr50 (Periyannan *et al.*, 2013, Chen *et al.*, 2017). Amino acid positions are labelled according to an amino acid alignment of all six alleles relative to MLA1. E = Glutamate, D = Aspartate, N = Asparagine, G = Glycine, W = Tryptophan, S = Serine, T = threonine, P = Proline, K = Lysine, L = Leucine, Q = Glutamine, "-" designates a gap in the alignment.

At MLA_{797}, MLA6 has uniquely deleted amino acid, whereas the other *Rar3*-dependent variants have tryptophan (W) and the *Rar3*-independent variants have either serine (S) or threonine (T). It is hard to attribute a function to a missing amino acid, however it may be that in this case tryptophan is not performing any particular function, or it is negatively associated with interactions and therefore a deletion could be functionally preferable. Conversely, serine and threonine are both small, polar, and can be phosphorylated. The phosphorylation of the LRR domains of proteins has not been observed in NLRs, but has been observed in many receptor kinases and receptor-like kinases (Park *et al.*, 2012).

Position MLA_{798} has the starkest contrast between the two groups. *Rar3*-dependent variants have a proline (P), whereas the *Rar3*-independent variants have serine (S). However, it is possible for the serine side-chain to form a hydrogen bond with the protein background whereby it acts as proline does structurally. Additionally, proline is fairly non-reactive. Therefore, it is possible that at this position, proline and serine act similarly structurally, while the serine in *Rar3*-independent variants performs an additional function that confers a stronger interaction with SGT1.

When we tested MLA1 and MLA6 site-directed mutants for interaction with SGT1, we observed that mutating $MLA1_{797}$ and $MLA1_{798}$ to the *Rar3*-dependent forms ($MLA1_{\Delta 797S}$ and $MLA1_{S798P}$) completely disrupted the interaction between MLA1 and SGT1 (**Figure 3-5-2E & 5-2F**). In contrast, the reciprocal mutations, $MLA6_{+797S}$ and $MLA6_{P797S}$, did not cause an equivalent gain of interaction (**Figure 3-5-2H & 5-2I**). However, we did observe an increase in interaction between $MLA6_{+797S}$ and SGT1 WT, whereas the interaction between $MLA6_{+797S}$ and $SGT1_{\Delta KL308-309}$

was weaker (**Figure 3-5-3I**). This is similar to the findings shown by (Halterman and Wise, 2004) whereby the MLA6$_{G721D}$ mutation alleviated the functional requirement for RAR1, but the reciprocal mutant, MLA1$_{D721G}$, did not gain a requirement for RAR1. Mutating MLA1$_{708}$ did not appear to affect interaction strength (**Figure 3-5-2D**). The proximity of the two positions that appear important for MLA1 to interact with SGT1, MLA1$_{797}$ and MLA1$_{798}$, may suggest an additive function whereby both are required to confer a strong interaction with SGT1 and, consequently, "*Rar3*-independence". Thus, it would be of interest to test a MLA6$_{+797S\ P798S}$ double mutant for interaction with SGT1. Additionally, as both serine and threonine can be phosphorylated, we could test phosphomimetic mutations at both positions.

One of the theorized dynamics between MLA and the HRS, is that the NLR naturally exists in an inactive, closed conformation (Ade *et al.*, 2007, Wang *et al.*, 2015b, Wang *et al.*, 2019b). If the R protein must be activated before it can interact with the HRS complex, that would explain why we don't see an interaction between full length MLA1 and SGT1, but instead must use only the LRR domain. To test the theory that full length MLA needs to be activated before it interacts with the HRS complex, we generated an auto-active version of full length MLA6, MLA6$_{D502V}$, which has a mutation in the MHD motif of the NB domain that mimics ATP binding (Tameling *et al.*, 2006). We found a small interaction when we tested MLA6$_{D502V}$ against SGT1 WT, but not with SGT1$_{\Delta KL308\text{-}309}$ (**Figure 3-5-2K & 5-3K**). This suggests that locking MLA6 in an active conformation, and reconstituting the HRS complex, facilitates the interaction between MLA6 and SGT1 to a level that can be detected using the Y2H "Y-archer" assay.

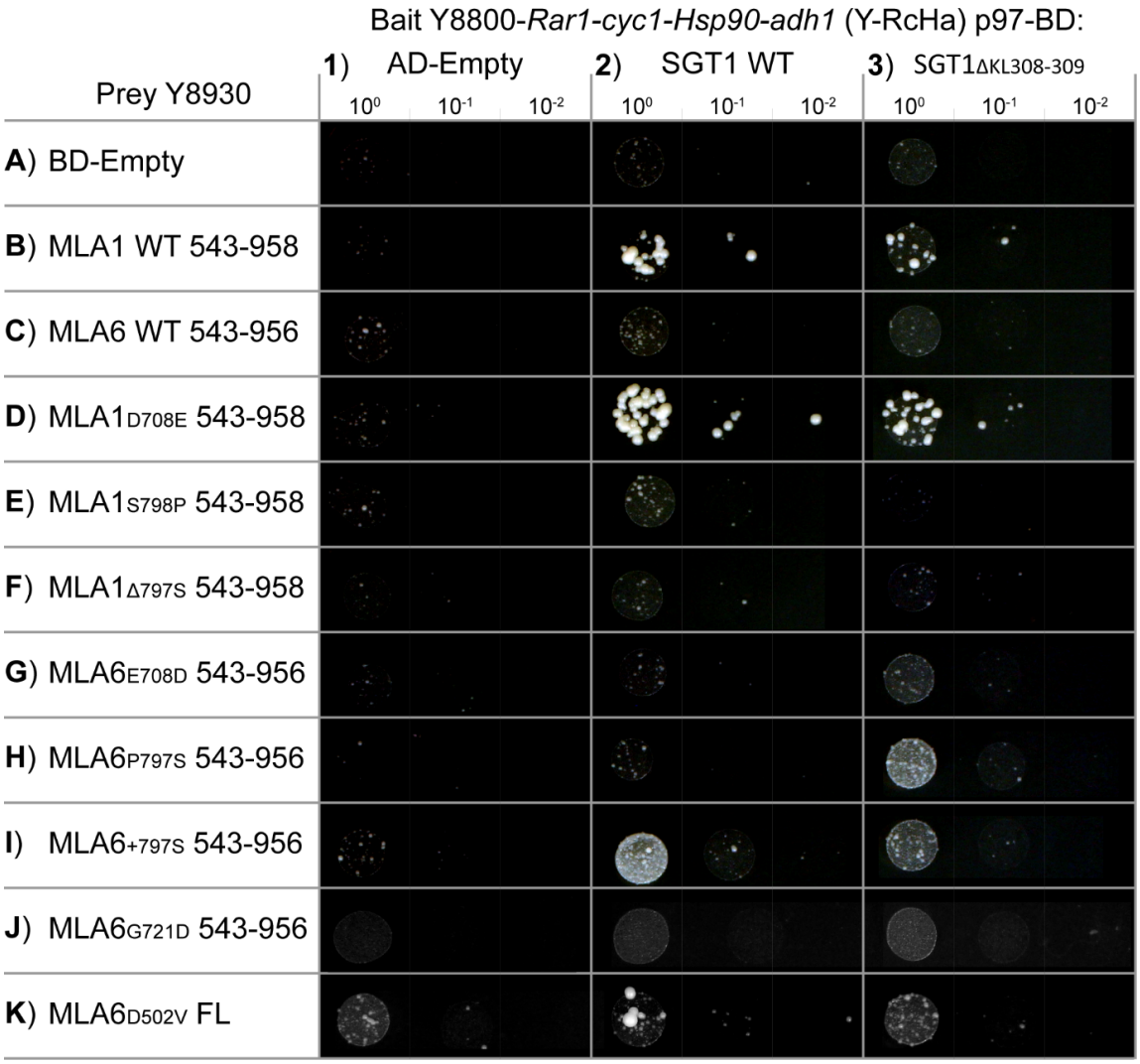

Figure 3-5. **Y2H interaction tests between MLA1 or MLA6 mutant LRR fragments and SGT1**. Rows and columns are labelled with letters and numbers respectively. E.g. AD-Empty/BD-Empty test is Figure 3-5-A1. Diploid Y8800 or Y-RcHa/Y8930 yeast expressing AD- and BD- grown on SC-LWH media. MLA1 WT 543-958 indicates that the fragment of MLA1 is from the wildtype sequence between amino acid position 543 to the stop codon at 958. MLA6 is two amino acids shorter than MLA1, therefore 956 corresponds to the MLA6 stop codon. Yeast was grown on SC-LWH, and images were taken 4 days after plating. Dilutions of diploids cells for plating are 10^0, 10^{-1}, and 10^{-2} of the original 0.5 OD culture.

Silencing of *NbSgt1* prevented cell-death caused by auto-active *Mla6*$_{D502V}$ and *Mla7*$_{D502V}$

To investigate how the SGT1$_{\Delta KL308-309}$ mutation and MLA interact in planta, we utilized the heterologous *Nicotiana benthamiana* system. An issue with studying *Sgt1* is that it is very well conserved in most eukaryotes (Kitagawa *et al.*, 1999). Consequently, for us to examine

HvSgt1 in *Nicotiana benthamiana*, we are required to silence the endogenous *NbSgt1*, made possible by the low similarity at the nucleotide level. Arabidopsis *Sgt1* has been shown to complement *NbSgt1* silencing (Boter *et al.*, 2007). However, it was found recently that silencing *Sgt1* in *N. benthamiana* inhibits subsequent transient expression of genes by *Agrobacterium*, suggesting that it co-opts host *Sgt1* for expression of transgenes (Yu *et al.*, 2019). To overcome this, we attempted to express *HvSgt1* prior to silencing *NbSgt1*, hypothesizing that *HvSgt1* would be able to complement *NbSgt1* and allow subsequent expression of transgenes.

It can take some time for the silencing of a gene to reduce the abundance of protein to low enough to affect its function, therefore we silenced *NbSgt1* prior to infiltration with the cell death constructs. Additionally, as the *Mla6* cognate effector, AVR_{a6}, is unknown at present, we made use of the autoactive mutants $Mla6_{D502V}$ and $Mla7_{D502V}$, whereby a D>V mutations in the MHD motif in the NB domain prevents hydrolysis of ATP and causes the MLA protein to be permanently stuck in the "On" conformation (Tameling *et al.*, 2006).

We infiltrated the 35s: *HvSgt1* or 35s: $HvSgt1_{\Delta KL308\text{-}309}$ (**Figure 3-9**, red bordered central region) at two to four days before infiltration (DBI) with the RNAi: *NbSgt1* construct in the same region. Then, at 2 days later the cell death construct was infiltrated overlapping the previously infiltrated region (**Figure 3-9**, black bordered overlapping region). We observed that silencing *NbSgt1* consistently prevented cell death from both $Mla6_{D502V}$ and $Mla7_{D502V}$. However, complementation of *NbSgt1* silencing was not observed when either 35s: *HvSgt1* or 35s: $HvSgt1_{\Delta KL308\text{-}309}$ was infiltrated. Isolation and sequencing of the *HvSgt1* constructs from the *Agrobacterium* strains that were used confirmed that the constructs do not have any errors

that may prevent expression or function. The 35S overexpression construct pEG100 was used for both *HvSgt1* and *Mla*, therefore it is unlikely that the construct itself is the issue as the *Mla* cell death construct appear to express well, indicated by the intense cell death phenotypes.

MLA6 protein abundance is reduced by the *Sgt1*$_{\Delta KL308\text{-}309}$ mutation

RAR1 and SGT1 are implicated in maintaining R-protein abundance and we have shown that the *Sgt1*$_{\Delta KL308\text{-}309}$ mutation appears to destabilize the interaction between SGT1 and MLA6. Therefore, we could expect the abundance of MLA6 to be significantly lower in the *Sgt1*$_{\Delta KL308\text{-}309}$ mutant line m11526 as compared to the wildtype progenitor, CI 16151. Previously, it was observed that, despite similar levels of expression of HA-tagged transgenes, MLA1 accumulates to almost 4 times the levels of MLA6 (Bieri *et al.*, 2004). However, both proteins exhibit a reduction of accumulation in *rar1* lines, despite a visible phenotype only appearing in lines also harboring *Mla6*. Interaction with SGT1 is necessary for the accumulation of many R proteins (Azevedo *et al.*, 2006, Mestre and Baulcombe, 2006, Boter *et al.*, 2007), therefore, the reason MLA1 functions in *rar1* backgrounds could be due to its inherently stronger interaction with SGT1, and thus a higher stability, which maintains MLA1 above a certain threshold required for HR activation. Thus, the differing effect of *Sgt1*$_{\Delta KL308\text{-}309}$ on MLA variants may be due to a similar action as lacking RAR1.

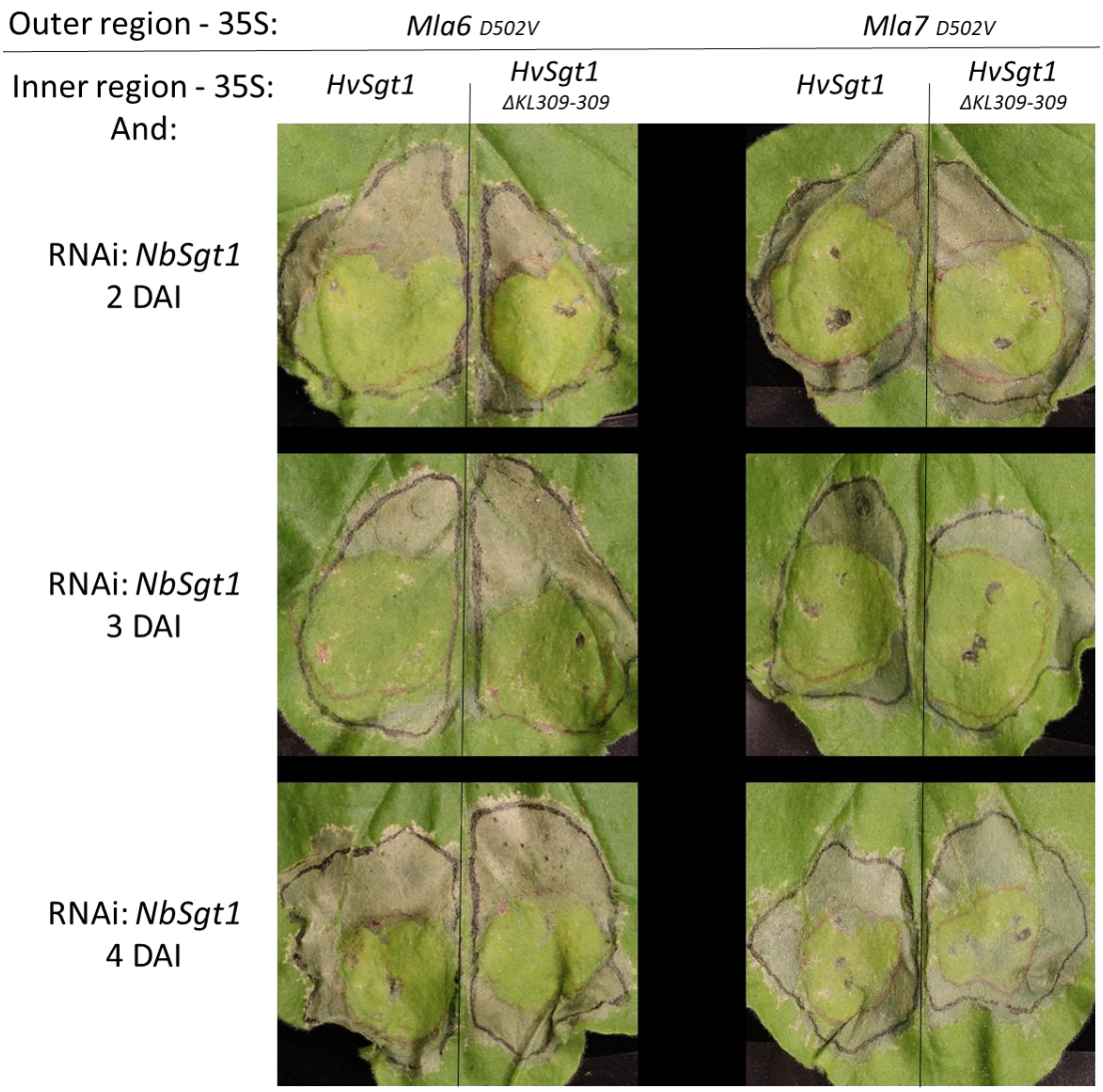

Figure 3-6. **Transient silencing of *NbSgt1* overlapped with overexpression of MLA cell death constructs**. In chronological order, the constructs expressing 35S:*HvSgt1* or 35S: *HvSgt1*$_{\Delta KL308\text{-}309}$ were infiltrated into the central red-bordered central regions. Two to four days after infiltration (DAI) of the *HvSgt1* constructs, RNAi: *NbSgt1* constructs were infiltrated into the same red-bordered central regions. Two days later, the full length 35S: *Mla6*$_{D502V}$ or 35S: *Mla7*$_{D502V}$ cell death constructs were infiltrated (black-bordered out region) overlapping the red-bordered central region. Leaves were taken, phenotyped, and photographed two days after the final infiltration. All infiltrations were performed with *Agrobacterium* strain EHA105.

To test this hypothesis, we utilized parallel reaction monitoring (PRM) mass spectrometry (MS) to measure the abundance of endogenous MLA6in the *Sgt1*$_{\Delta KL308\text{-}309}$ mutant line (Rauniyar, 2015, Bourmaud *et al.*, 2016). PRM involves targeting multiple predefined

precursor ions simultaneously by mass to charge ratio (m/z) before fragmentation and ion measurement. The specificity of the m/z allows for less noise and higher sensitivity than other methods, such as selected reaction monitoring (Peterson *et al.*, 2012).

To measure protein abundances in barley samples, we designed heavy versions of peptide candidates to calibrate. Three MLA- and two SGT1 peptide candidates were selected and synthesized (Thermo, Waltham, MA, **Table 3-2**). HvSGT1_pep1 had been previously detected in maize (Méchin *et al.*, 2007), which made it a promising candidate, whereas neither HvSGT1_pep2 nor any of the MLA peptides were identified previously. Of the MLA peptides, MLA6.9.13_pep2 and MLA6.7.12_pep3, were designed for targeting multiple alleles of MLA. MLA6.9.13_pep2 is unique to MLA, but is present in the MLA alleles MLA6, MLA9 and MLA13, whereas MLA6.7.12_pep3 targets MLA6, MLA7 and MLA12. The manufacturer also supplied a standard peptide, "ATLAS", which is not present in the barley proteome.

Table 3-2. **Synthetic peptides used in parallel reaction monitoring**. Parentheses surrounding a Leucine (L) indicate a heavy amino acid, [C(CAM)] indicates a Carbamidomethyl Cysteine.

Peptide Name	Sequence	MW	Location in sequence (AA)
MLA6_pep1	DPSH(L)SNLSDLVLPVK	1740.99	784-799
MLA6.9.13_pep2	S(L)[C(CAM)]NLHHIESLIIG[C(CAM)]NSR	2130.48	725-742
MLA6.7.12_pep3	WVPPVH(L)R	1010.22	757-764
HvSGT1_pep1	SFVESNGTV(L)STNWK	1675.83	337 -> 351
HvSGT1_pep2	(L)GSYTEAVADANK	1345.44	53 -> 65
Control Peptide ATLAS	HWYITTGPVREK	1486.70	

To test the quality and determine their fragment ion profile, we injected each synthetic peptide into the MS using our PRM settings at varying amounts (1 fm, 100 fm, and 1000 fm). From this survey, we could reliably detect the peptides ATLAS, MLA6.7.12_pep3 (hereafter designated MLA6 "WaVe"), and HvSGT1_pep2 (hereafter designated SGT1 "DANK") at both 100 and 1000 fm amounts. However, it should be noted that the amount of synthetic peptide injected does not correspond to the actual amount present due to the low quality, each of which contained a multitude of additional undesired peptides (Quality certificates, **Supplementary Data 1**). Therefore, it is only possible to determine the relative abundance as compared to the standard, and changes thereof. Once candidate peptides were chosen, complex CI 16151 samples were performed with 100 fm of MLA6 WaVe and SGT1 DANK synthetic peptides spiked in. Endogenous peptides were detected for both SGT1 DANK and MLA6 WaVe, eluting at ~55.5 minutes and ~77.5 minutes respectively (**Figure 3-6**). Therefore, we deemed our method suitable for quantification of MLA peptides in complex barley samples. For subsequent runs, the amount of synthetic peptide spiked in was adjusted so that their relative intensities were closer to the endogenous. We used 200 fm for SGT1 DANK, and 10 fm for MLA6 WaVe, as 10 fm seemed to be the lower boundary for confidence in detection of the heavy synthetic peptide.

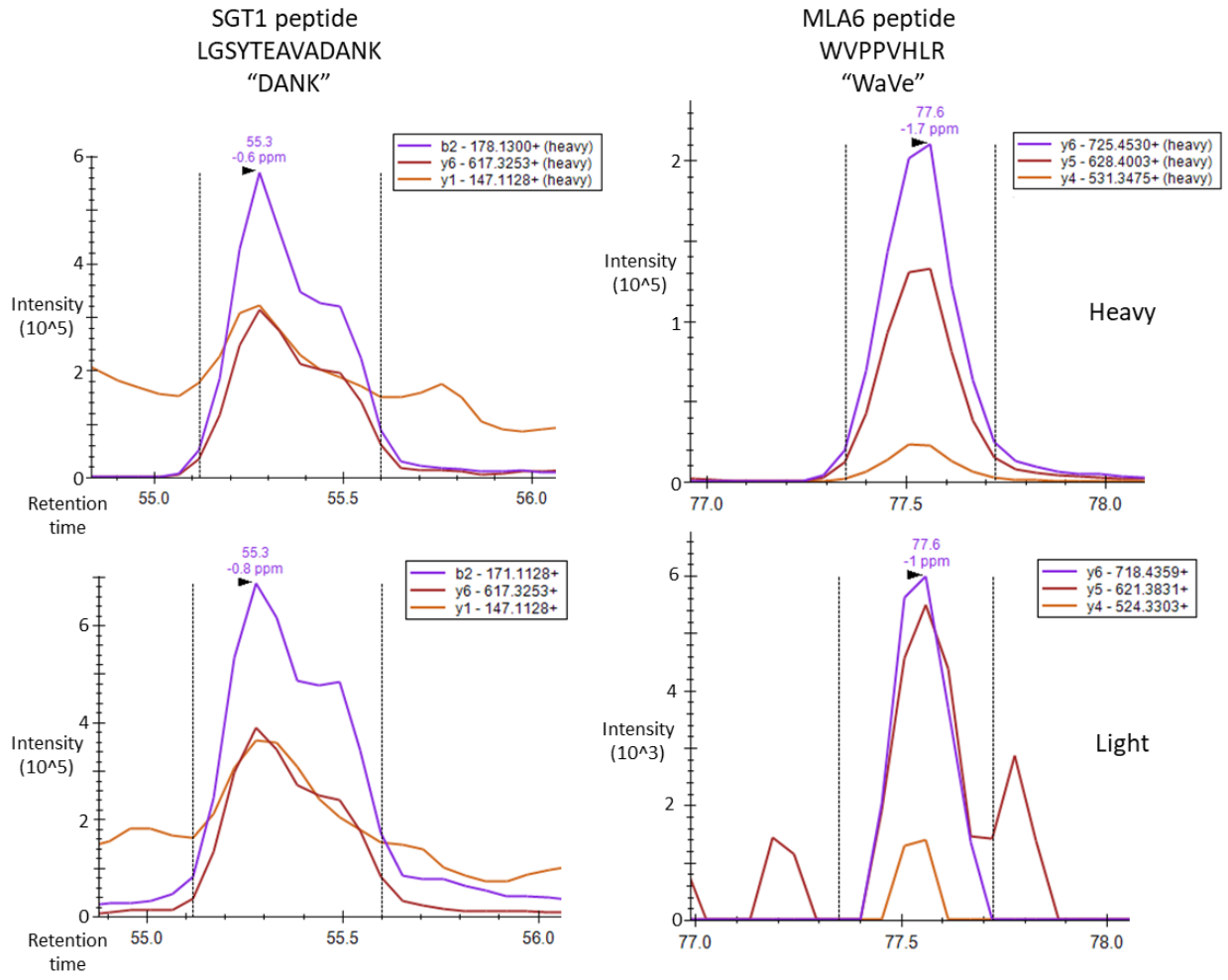

Figure 3-7. **PRM Chromatograms results.** Peak intensities for ions associated with the synthetic (top) or endogenous (bottom) versions of the SGT1 "DANK" peptide (left), or MLA6 "WaVe" peptide (right). 100 fm of synthetic peptide was spiked in to 1.25ug of complex barley samples. Values above peaks indicate retention time (minutes) and mass error (ppm). Exported from Skyline.

To examine whether the *Sgt1*$_{\Delta KL308\text{-}309}$ mutation reduced MLA6 abundance, we ran PRM on complex peptide samples isolated from CI 16151 (*Mla6*, *Sgt1*, *Rar1*), m18982 (*mla6*, *Sgt1*, *Rar1*), and m11526 (*Mla6*, *Sgt1*$_{\Delta KL308\text{-}309}$, *Rar1*) with heavy synthetic SGT1 DANK and MLA6 WaVe spiked in. As a comparison, we also included Sultan-5 (*Mla12*, *Sgt1*, *Rar1*) and m100 (Sultan-5 derived, *Mla12*, *Sgt1*, *rar1*) as the *rar1* mutation had been shown previously to reduce MLA accumulation (Bieri *et al.*, 2004), and the MLA6 WaVe peptide should be detectable in the

Sultan-5 (MLA12) background. The results were exported into Skyline, where the appropriate peaks were identified, peak boundaries were selected, and then quantified by computing the peak area.

When we examine the ratio of light/heavy MLA6 WaVe (**Figure 3-7**), we observe that the *mla6* deletion mutant, m18982, and *rar3 Sgt1*$_{\Delta KL308\text{-}309}$ mutant, m11526, both have significantly reduced levels of detected MLA6. In fact, m11526 has an almost half as much MLA6 abundance as CI 16151, whereas m18982 had a minor amount detected, though there should be none. For confidence in the isolation of the target MLA6 peptide, we require observation of all ions previously characterized for its profile, γ4, γ5, and γ6 (**Figure 3-6**). However, when we examine the chromatogram for the most abundant m18982 replicate (**Figure 3-S1**), we observe that only a single ion is observed, γ5. Additionally, if the abundance of MLA6 in m18982 was just below the lower boundary of detection, we would expect to observe the highest intensity ion first, which would be γ6, not γ5. Therefore, we believe it would be fair to argue that no MLA6 is detected in the *mla6* mutant, as would be expected from a knockout mutant. Examining the actual peak area for each biological replication, we observe consistency between the amount of heavy MLA6 WaVe detected, giving confidence to the ratio differences not being an artifact of varying synthetic amounts (**Figure 3-S2**).

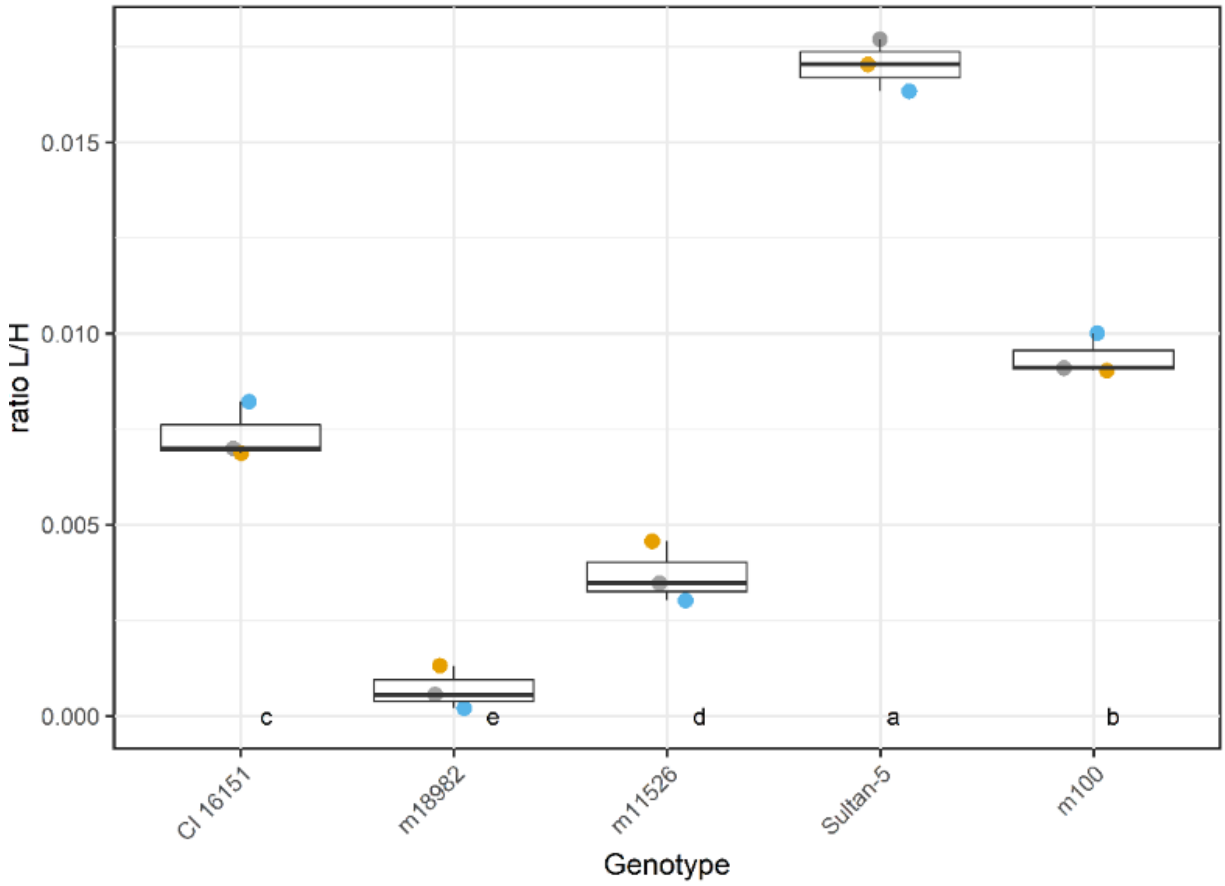

Figure 3-8. **Box plot diagram showing ratios of light endogenous MLA6 "WaVe" peptide to heavy synthetic peptide for each genotype**. CI 16151 (*Mla6, Sgt1, Rar1*), m18982 (*mla6, Sgt1, Rar1*), m11526 (*Mla6, Sgt1*$_{\Delta KL308\text{-}309}$*, Rar1*), Sultan-5 (*Mla12, Sgt1, Rar1*), m100 (*Mla12, Sgt1, rar1*). Letters indicate statistically significant groups at p<0.05, (**Table 3-S1**).

We observed that the *rar1* mutant m100 had significantly lower MLA6 WaVe abundance than its wildtype progenitor Sultan-5, which corresponds with previous data. Interestingly, we also observed that both Sultan-5 and m100 had significantly higher abundances of MLA6 WaVe than CI 16151. This may be due to the differences in genetic background between CI 16151 (Manchuria background) and Sultan-5. In contrast to MLA6, SGT1 does not appear to vary in its abundance between lines as there were no significant difference in the ratios observed in any genotype (**Figure 3-8**). However, unlike MLA6 WaVe, the ratios observed for SGT1 DANK do appear to vary significantly between lines.

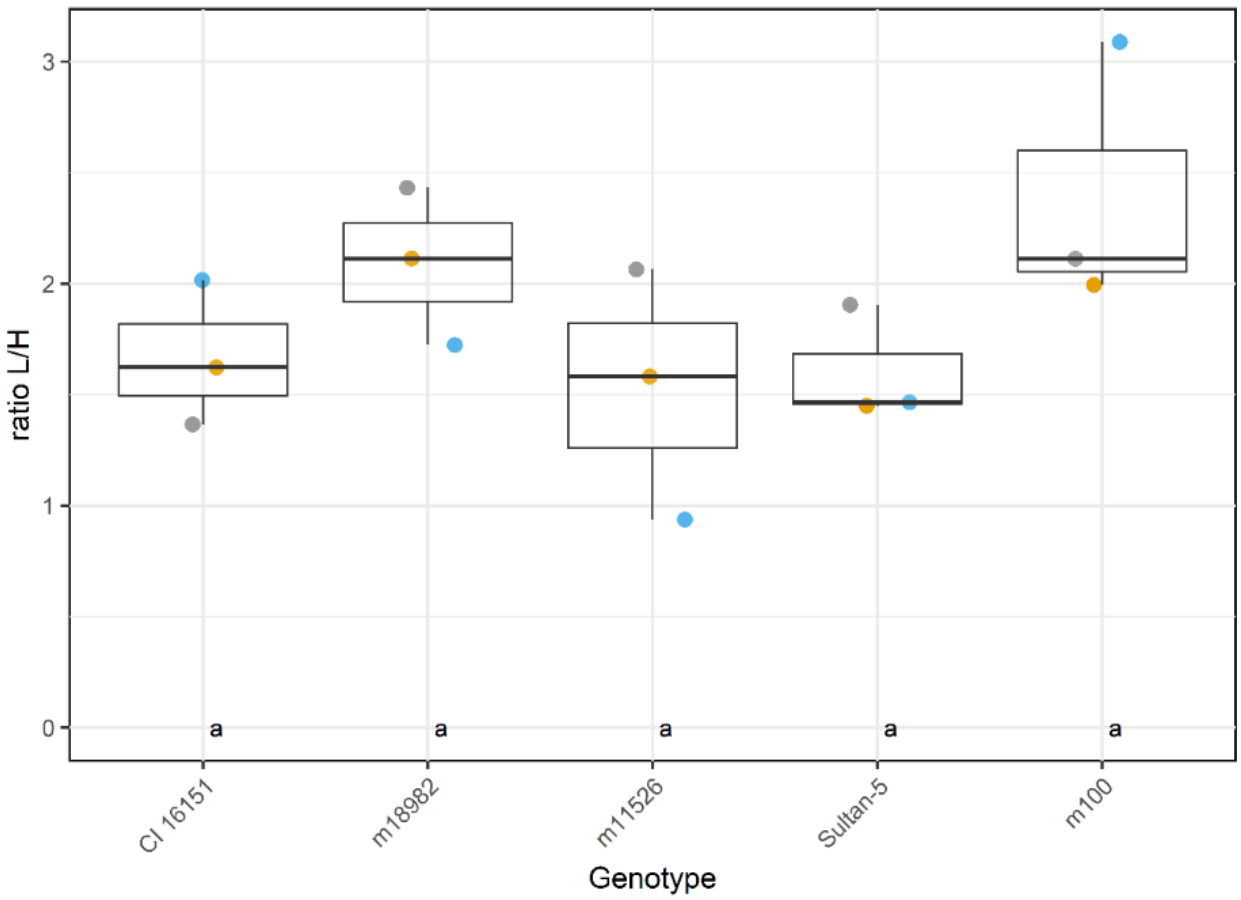

Figure 3-9. **Box plot diagram showing ratios of light endogenous SGT1 "DANK" peptide to heavy synthetic peptide for each genotype**. CI 16151 (*Mla6, Sgt1, Rar1*), m18982 (*mla6, Sgt1, Rar1*), m11526 (*Mla6, Sgt1*$_{\Delta KL308\text{-}309}$*, Rar1*), Sultan-5 (*Mla12, Sgt1, Rar1*), m100 (*Mla12, Sgt1, rar1*). Letters indicate statistically significant groups at p<0.05, (**Table 3-S1**).

Discussion

RAR1 and HSP90 facilitate interactions between SGT1 and MLA in Y2H systems

To investigate domains involved in SGT1–NLR interactions, we used yeast genome engineering to modify the contextual protein environment in the Y2H system to closer align to *in-planta* barley. Previously it was shown in yeast that MLA6 NLR does not interact with SGT1 whereas MLA1 does, even though *Mla6* function is disrupted by *Sgt1* silencing and *Mla1* is not (Bieri *et al.*, 2004, Azevedo *et al.*, 2006). However, it was also shown that *Mla6* requires *Rar1* and *Hsp90 in-planta* to function and the interaction itself may be ephemeral or dependent on

prior activation by the cognate effector (Maekawa *et al.*, 2012). Moreover, *rar1*-mutant lines show reduced MLA accumulation. Yeast does have its own HSP90 homologue (SGD: S000004798), with a 63% identity to HvHSP90, though we don't know whether they are functionally redundant. Therefore, the interaction between MLA6 and SGT1 may be missing at least two necessary components. We hypothesized that by reconstituting the barley HRS complex in the Y2H system, and thus restoring part of the *in-planta* context, we could use this to test interactions between MLA6 and SGT1.

Utilizing a Y8800 yeast strain with integrated *HvRar1* and *HvHsp90* (Y8800:*Rar1-cyc1-Hsp90-adh1*, Y-RcHa), we observed an increased interaction between SGT1 and MLA1 LRR fragments (**Figure 3-2**). However, we still were unable to detect interaction with MLA6 LRR or full-length versions, suggesting that the theoretical interaction was still below an observable threshold. NLRs exhibit auto-inhibition until they are activated (Ade *et al.*, 2007, Wang *et al.*, 2015b), therefore we hypothesized that using a full length autoactive mutant of MLA6 may strengthen the interaction with SGT1 to an observable level. With both the integrated HRS complex, and the autoactive mutant, we observed an interaction between MLA6 and SGT1. Moreover, this interaction was with a full-length NLR, not simply a fragment. When we tested this using the *N. benthamiana* heterologous system, we did not observe complementation of *NbSgt1* silencing with *HvSgt1* overexpression, which may suggest that these are not redundant, or that the expression system did not work. With this data, we show that integrating co-chaperones to reconstitute known complexes can be used to test interactions between proteins to be tested in Y2H systems. Moreover, it may be beneficial to revisit previous experiments while using autoactive NLRs in order to identify previously unobservable interactions.

To confirm the contribution of the modified Y-RcHa strain to improving the MLA-SGT1 interaction, we utilized multiple methods for detecting the presence and expression of the integrated genes. We did not use tagged versions of *HvRar1* or *HvHsp90* because we were concerned that the addition of tags may interfere with their function. Therefore, we used positive PCR results from the strains to see that each gene had been stably integrated, followed by amplification and sequencing of both genes from Y-RcHa genomic DNA. To see whether proteins were expressed, we extracted and purified peptides from diploids and performed a data-dependent acquisition mass-spectrometry method. We were able to detect HSP90 peptides from diploids derived from Y-RcHa and not from those derived from Y8800. However, we were unable to detect RAR1 peptides from Y-RcHa, suggesting that either the integrated *Rar1* is not expressed, is degraded, or it is too low to be detected.

The standard method for testing interactions using Y2H include using 3-AT (3-Amino-1,2,4-triazole), which is a competitive inhibitor of the product of *HIS3*. The addition of 3-AT to SC-LWH media increases the stringency of the system by requiring a higher level of *HIS3* function to overcome the inhibition (Dreze *et al.*, 2010). However, as we were examining an interaction that was potentially weak or ephemeral, even small concentrations of 3-AT would prevent discovery. There was some background growth observed in SC-LWH, but by comparing the growth of a diploid containing interactors of interest to the negative controls we could tell if there was an interaction that was not observed when 3-AT was used.

SGT1$_{\Delta KL308-309}$ disrupts interactions with MLA proteins

The recently discovered *Sgt1$_{\Delta KL308-309}$* mutation alters immunity conferred by a subset of *Mla* alleles. The *Sgt1$_{\Delta KL308-309}$* mutation is in the SGS domain, which has previously been shown to interact directly with the LRR domain of MLA1, human NOD1 and the F-Box protein TIR1 (Bieri *et al.*, 2004, da Silva Correia *et al.*, 2007, Wang *et al.*, 2015a). Furthermore, the deletion includes a lysine, which can be involved in protein-protein interactions through the formation of intermolecular salt bridges (Kumar and Nussinov, 2002). Therefore, the *Sgt1$_{\Delta KL308-309}$* mutation may cause a loss of an interaction site between SGT1 and MLA variants.

In previous literature, a point of issue has been regarding which MLA variants require SGT1 function, exemplified by MLA1 and MLA6. MLA1 is considered to not require SGT1 to function, as shown by its continued function when SGT1 is silenced (Azevedo *et al.*, 2002). However, it has also be shown to interact with SGT1 in the yeast–two-hybrid system (Bieri *et al.*, 2004). In contrast, MLA6 has been shown to require SGT1, as it stops functioning when SGT1 is silenced (Azevedo *et al.*, 2002). But prior to this study, it had not been shown to directly interact with SGT1 (Bieri *et al.*, 2004). This begs the question, why does the variant that does not require SGT1 interact with it, whereas the variant that does require SGT1, does not interact with it? Silencing experiments are inherently flawed as the reduction in expression of a gene does not necessarily mean there is no protein expressed or remaining before silencing. In fact, the reason why silencing of *Sgt1* is the norm for testing requirements is because *Sgt1* deletions are lethal (Azevedo *et al.*, 2006, Wang *et al.*, 2015a). Therefore, when *Sgt1* is silenced, there may be some protein still performing regular function to allow the individual to survive.

The answer to the discordant requirements and interactions of MLAs and SGT1 may be that all MLA require SGT1, and interact with it, but the strength of the interaction varies, and therefore so does their ability to function when SGT1 abundance is lowered. In fact, the silencing of *Sgt1* does have an effect on MLA1. When *Sgt*1 was silenced there was a small, but not insignificant, increase in susceptibility to *Bgh* in *Mla1*-containing barley lines (Azevedo *et al.*, 2006). Moreover, the loss of *Rar1*¸which MLA1 is considered not to require, reduces MLA1 protein accumulation (Bieri *et al.*, 2004). Thus, situations which lower the amount of SGT1 available (via silencing), or reduce the strength of the interaction (*rar1* and *rar3* mutations, or *rar1* silencing), would affect the function of those MLA variants with the weaker interactions (MLA6) before they affect those with the stronger (MLA1).

We previously observed a differential effect of the $Sgt1_{\Delta KL308\text{-}309}$ mutation on MLA alleles, which may be partially explained by our results herein (Chapman *et al.*, 2020). When we tested the interaction between MLA1 543-968 and SGT1 WT using Y8800 we found that it was relatively weak and it was difficult to see a significant difference between the interaction with SGT1 or $SGT1_{\Delta KL308\text{-}309}$. When Y-RcHa was used, the interaction between MLA1 and SGT1 WT was stronger, but we saw no obvious change in the strength of the interaction between MLA1 and $SGT1_{\Delta KL308\text{-}309}$. This suggests that the $SGT1_{\Delta KL308\text{-}309}$ mutation does interrupt the interaction between MLA1 and SGT1, to a comparable level as lacking RAR1 and/or HSP90. Moreover, when we used the autoactive mutant $MLA6_{D502V}$, which did interact with wildtype SGT1, we still did not observe an interaction with $SGT1_{\Delta KL308\text{-}309}$. Furthermore, we were able to disrupt this interaction further by using the $SGT1_{K308R}$ and $SGT1_{KL308AA}$ mutants, leading to complete loss of observable interaction with MLA1. Together, these suggest that the $Sgt1_{\Delta KL308\text{-}}$

309 mutation does not lead to complete loss of SGS function, but rather an abating of its function.

$SGT1_{\Delta KL308\text{-}309}$ could be tested for interactions with other proteins that interact with the SGS domain to test whether this weaker interaction is uniform or specific. There are a few possible outcomes of these tests; $SGT1_{\Delta KL308\text{-}309}$ may cause an altered interaction with only MLA, suggesting that this is a site specific to MLA interactions, or $SGT1_{\Delta KL308\text{-}309}$ may cause a weakened interaction with all NLR interactors but not with other types of interactors, which would suggest that this site is specific to disease resistance pathways. Another possibility is that $SGT1_{\Delta KL308\text{-}309}$ may disrupt interactions with all proteins that interact with the SGS domain, but it is a small reduction that we only see manifest in a subset. This last possibility is given credence by the fact that resistance pathways appear to exist in a heavily regulated equilibrium just below the threshold required for activation so that they are able to signal quickly upon detection of a pathogen, but do not cause rampant autoimmune responses (Bentele *et al.*, 2004, Bernoux *et al.*, 2016). Therefore, if $SGT1_{\Delta KL308\text{-}309}$ only slightly reduces interactions, it may significantly shift the equilibrium, causing a loss of action by the NLRs with the less robust interactions.

Y2H assays indicate $SGT1_{KL308\text{-}309}$ is important for SGT1-MLA interactions

We used SGT1 mutant constructs to investigate why the *Sgt1*$_{\Delta KL308\text{-}309}$ mutation affects its function in disease. We found that the *Sgt1*$_{\Delta KL308\text{-}309}$ mutation does appear to slightly alter its ability to interact with MLA1. However, the destabilization caused by the *Sgt1*$_{\Delta KL308\text{-}309}$ mutation is not as severe as the double alanine substitution or the K308R mutation (**Figure 3-3**). An interesting conundrum is that the SGS domain of SGT1 is able to interact with a multitude of

unrelated NLRs. Moreover, it interacts with the LRR domain, which is the most diverse part of the NLRs. For the SGS domain to interact with a multitude of varied LRRs, either; it must have extreme flexibility, there are shared LRR motifs that it interacts with, or linker proteins bridge the gap as suggested by (Kadota *et al.*, 2010). Considering the extreme disorder of the SGS domain, we hypothesize that the extreme flexibility is the most likely. It is possible that the SGS domain has the ability to interact with a multitude of proteins because it adopts different conformations, allowing its variable binding sites to interact with LRRs where possible. This is supported by our findings that the diminished interaction caused by the $Sgt1_{\Delta KL308\text{-}309}$ deletion, which arguably would increase disorder, was less severe than alanine mutations or the K308R mutation, which could decrease disorder.

We examined the structure of barley SGT1 to look for clues into why the $Sgt1_{\Delta KL308\text{-}309}$ deletion may affect its function (Taube *et al.*, 2014). The SGS domain consists of three coils and unstructured regions (**Figure 3-10**). In the SGS domain, almost 40% of the amino acids are either aspartate (D, ~11%), glutamate (E, ~11%), or lysine (K, ~17%), all of which can be involved in forming intermolecular salt-bridges. In coil 1, where the $Sgt1_{\Delta KL308\text{-}309}$ mutation is located, the proportions are even higher, D ~18%, E ~18%, and K ~32%, totaling almost 70% of the residues. Moreover, when these three residues are mapped onto the 3D structure, all the lysines appear on the same coil side (**Figure 3-10B**). This may indicate this side has potential to form multiple salt bridges with interacting proteins, perhaps with a domain with many surface aspartates and glutamates. Interestingly, there is a distinct lack of arginine both in the whole SGS domain (~3%) and coil 1 (0%), despite its function in forming salt-bridges, which suggests

that there may be some alternate characteristic which make its unsuitable for this domain. This negative selection may indicate why the K308R mutation has such a drastic affect.

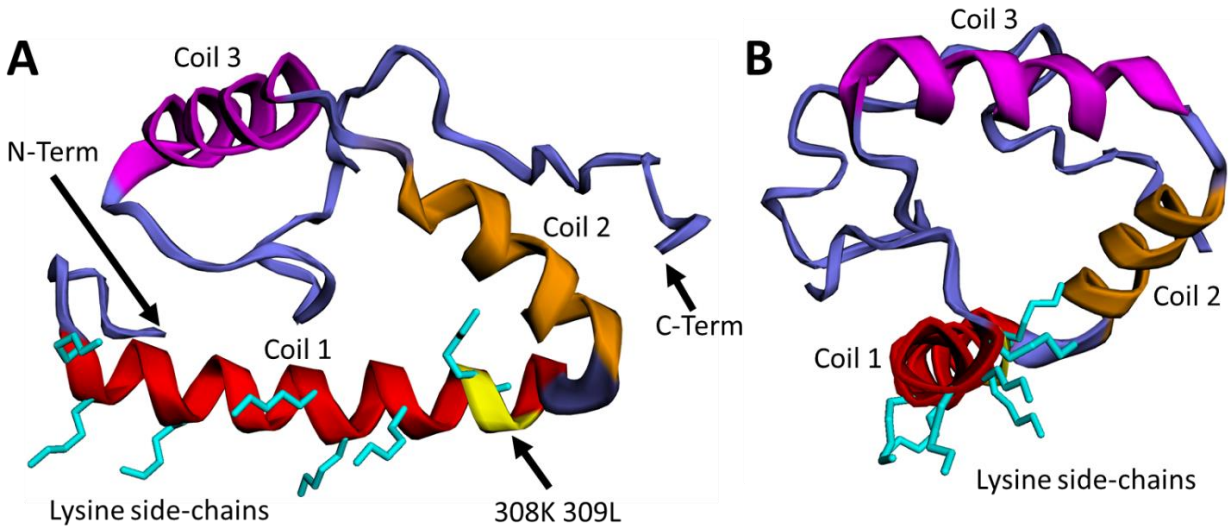

Figure 3-10. **Structure of HvSGT1 SGS domain.** Generated from data generously provided by (Taube *et al.*, 2014) and modeled in EZMol (v2.1, http://www.sbg.bio.ic.ac.uk/~ezmol/). **A**) The SGS domain spans from amino acid (AA) 285-373. Coil 1 (red) spans AA 290-311, Coil 2 (orange) spans AA 314-325, Coil 3 (fuchsia) spans AA 328-341, unstructured regions are shown in blue. The N-terminal connects to the VR2 domain, and the C-terminal is the terminus of the protein. Lysine side chains in Coil 1 are represented by stick models (teal). Positions K308 and L309 in Coil 1 are shown in yellow. **B**) Side view of the HvSGT1 SGS Coil 1 showing that all the lysine side chains in Coil 1 appear on one half of the coil.

A reduction in the strength of interaction with SGT1 correlates with a lower MLA abundance

The protein RAR1 is a co-chaperone of SGT1 that is required for the function of some MLA proteins, such as MLA6 and MLA12, but not for others, such as MLA1 and MLA7 (Halterman and Wise, 2004). Though it is considered to not be required for MLA1 function, loss of RAR1 has been shown to reduce the abundance of MLA1 and MLA6 (Bieri *et al.*, 2004). As m11526 has a similar phenotype to *rar1* mutants, we hypothesized that MLA abundances may be lowered as a result of the $Sgt1_{\Delta KL308\text{-}309}$ mutation. To pursue this, we utilized parallel reaction monitoring (PRM) mass spectrometry (MS) to assay MLA in native CI 16151 and

derived mutant plants. This method was selected as it displays higher sensitivity to low abundance peptides (Gallien *et al.*, 2012), and MLA6 peptides have not been detected using other MS methods (Lambertucci *et al.*, 2019).

Using an adapted PRM method, we were able to observe endogenous peptides for MLA6, MLA12, and SGT1 (**Figure 3-6**). We observed that in m11526 (*Mla6*, *Sgt1*$_{\Delta KL308\text{-}309}$, *Rar1*), the steady state levels of MLA6 were much lower than in the wildtype progenitor CI 16151 (*Mla6*, *Sgt1*, *Rar1*) (**Figure 3-7**). This is especially significant considering that the transcript accumulation of *Mla6* is not significantly different between m11526 and CI 16151 before or during infection (Chapman *et al.*, 2020). In contrast, there was no significant difference in the abundance of SGT1 in any line tested (**Figure 3-8**). This reduction of MLA6 abundance in m11526 does not equate to the complete loss of abundance in the phenotypically-similar *mla6* deletion mutant m18982 (*mla6*, *Sgt1*, *Rar1*). This lends credence to the hypothesis that resistance proteins have a threshold that is necessary for them to function. Interestingly, in the line Sultan-5 (*Mla12*, *Sgt1*, *Rar1*), MLA12 accumulated roughly twice as much as MLA6 in CI 16151. In contrast, in the *rar1* susceptible mutant m100 (*Mla12*, *Sgt1*, *rar1*), MLA12 abundance levels were much lower than Sultan-5, but still higher than in the resistant line MLA6. This may suggest that the thresholds for functionality differ greatly between different MLA variants, or that Sultan-5 has other factors that reduce the effectiveness of harbored MLA alleles. A higher abundance of MLA12 may be required to perform the same function as MLA6.

This data corresponds with previous that MLA1 accumulated to much higher levels than MLA6, even when these levels were greatly reduced by the *rar1* mutation (Bieri *et al.*, 2004). However, the MLA1 phenotype was unaffected by the large reduction of abundance, unlike the

susceptibility caused in m100 by the *rar1* mutation. Together, this data suggests that the *Sgt1*$_{\Delta KL308\text{-}309}$ mutation causes susceptibility in m11526 by reducing the abundance of MLA6 to a level below the threshold required for effective resistance.

A new cyclical model for MLA-HRS interactions

To generate a new model of MLA-HRS interactions, we combined our data with recent discoveries in NLRs. The NB domain of NLRs bind either ATP or ADP to act as an intramolecular switch, where the ADP bound state is inactive, and the ATP bound state is active (Williams *et al.*, 2011). Moreover, NLRs appear to naturally flit between these ATP and ADP bound forms outside of pathogen-recognition, in part due to inbuilt ATP-hydrolysis (Marquenet and Richet, 2007, Bernoux *et al.*, 2016). However, it has been shown that the active ATP-bound state is kept at a very low level, possibly to reduce autoactivation (Bernoux *et al.*, 2016). Interestingly, the flax L protein in the active ATP-bound state binds its matching effector stronger than the inactive version (Bernoux *et al.*, 2016), and similarly here we show that autoactive MLA proteins interact with SGT1 more strongly than respective wildtype variants. Moreover, there is recent evidence that the interaction between NLRs and ligands stabilizes the active conformations of NLRs (Yang *et al.*, 2018). As dimerization of CC domains are required for signaling (Maekawa *et al.*, 2011), and the HRS complex is predicted to allow docking of two NLRs simultaneously (Siligardi *et al.*, 2018), then the HRS may facilitate this dimerization. Therefore, the model proposed by (Bernoux *et al.*, 2016), which describes an NLR being locked in its active state by an effector, can be expanded to include the interaction with the HRS complex.

We propose that SGT1 may exist in a constant state of briefly interacting with ephemerally activated NLRs (**Figure 3-11A**). MLA, in its free/inactive ADP-bound state will

spontaneously swap ADP for ATP, this releases autoinhibition and “activates” the NLR. Once active, MLA can dock with the HRS. However, MLA may automatically hydrolyze the ATP into ADP, which will cause the MLA to form back into its autoinhibited state and eject from the HRS. This completes the active/inactive cycle. The small pool of ATP-bound NLR observed by (Bernoux *et al.*, 2016) suggests that the ATP bound state is very brief, which could indicate that the spontaneous activation of an NLR may occur relatively infrequently compared to the rest of the cycle. However, if all the NLR proteins are cycling between states, then it is likely that there is always a small pool of active and docked NLRs maintained.

If a pathogen introduces an effector into the cell during infection (**Figure 3-11B**), then during the brief window of MLA being active and docked with the HRS, the cognate effector can interact with the MLA LRR domain. This interaction stabilizes it in the active state by inhibiting ATP hydrolysis, preventing disassociation from the HRS. This provides the opportunity for another MLA unit to dock with the HRS and become stabilized. Once two MLAs are docked and stabilized, the CC domains are held in proximity, promoting homomeric dimerization and initiating the defense signaling cascade. This model is compatible with any NLR that requires the HRS complex and functions in a homo- or heteromeric pair. Therefore, for NLRs such as MLA, the MLA-HRS-Effector complex could be considered the “resistosome”. This is an alternative to the recently described resistosome complex for ZAR1, which does not require SGT1 or RAR1, and forms pentameric structures (Lewis *et al.*, 2010, Wang *et al.*, 2019a).

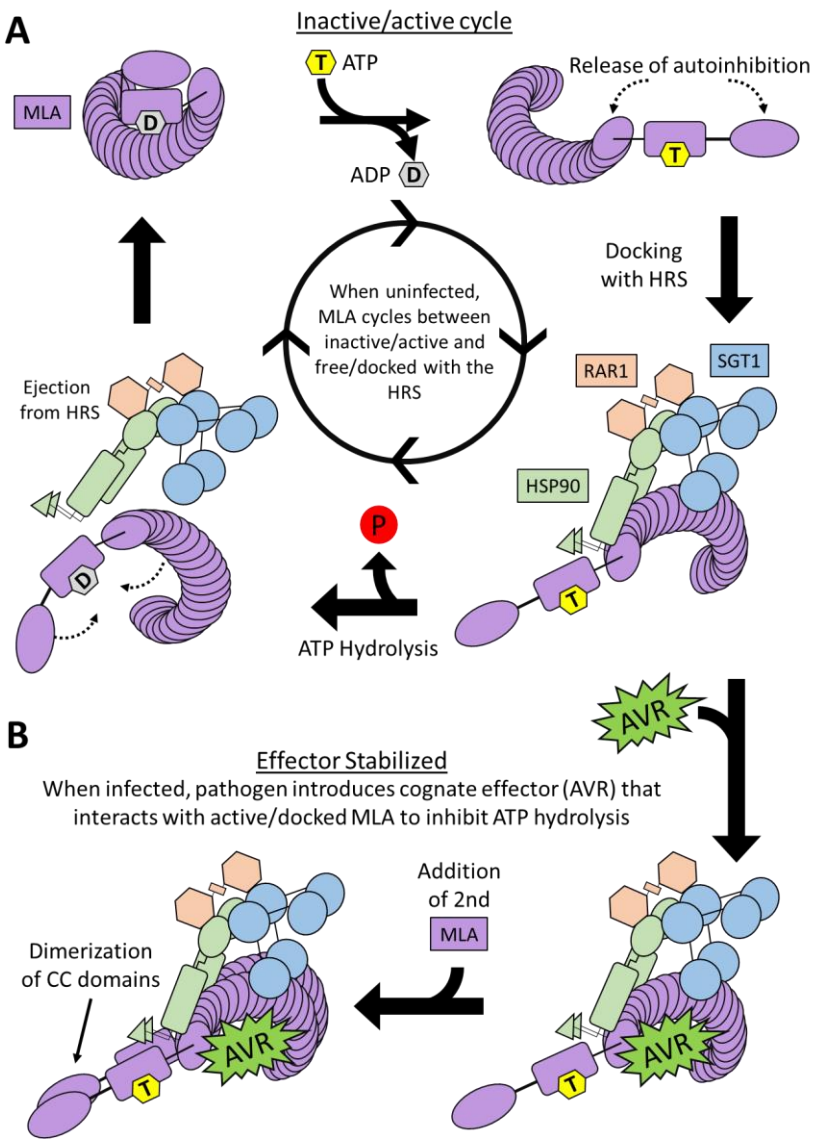

Figure 3-11. **MLA-HRS activation cycle model showing interactions between MLA, the HRS, and pathogen effectors**. **A**) The inactive/active cycle. MLA (Purple) primarily exists in an ADP-bound autoinhibited state. ADP is spontaneously swapped for ATP, which stops MLA autoinhibiting. Released from autoinhibition, MLA can dock and interact with the HRS, competing with other co-factors. Without the involvement of other factors, MLA will eventually hydrolyze the ATP into ADP, which causes it to eject from the HRS complex. Once freed, it reverts to its autoinhibited state. The smaller arrow for the swapping of ADP for ATP represents that this process likely happens slower than the rest of the model. **B**) Effector stabilized switch. When a pathogen introduces the cognate effector of the MLA (AVR, green), it will interact with the LRR domain of MLA and inhibit ATP hydrolysis, stabilizing the complex in the active conformation. This provides opportunity for another MLA to dock with the same HRS and also be stabilized by the effector. With two MLAs docked and stabilized with the HRS, the CC domains will be able to dimerize and initiate defense response signaling.

Conclusion

Our investigation of the *HvSgt1*$_{\Delta KL308\text{-}309}$ mutation challenges historic precedence set by previous studies. Due to being unable to make *Sgt1* knock-out mutants, the requirement of *Sgt1* for *R* genes to function has historically been performed by silencing experiments. However, not only are *Sgt1* silencing experiments in *N. benthamiana* called into question by recent studies (Yu *et al.*, 2019), but our results suggest that NLRs that are able to function despite the silencing of *Sgt1* may rather be those that interact with *Sgt1* the strongest.

The HRS complex is the core for many eukaryotic cell processes. However, Inter- and intra-molecular interactions for this complex are only partially understood. For instance, (Kadota and Shirasu, 2012) stated that for us to understand how RAR1 causes SGT1 to interact more strongly with NLRs, we need to understand how the SGT1 SGS domain interacts with the LRR domain of NLRs. Due to the lack of an interaction between MLA6 and SGT1, which MLA6 requires to function, it had been proposed that linker proteins may be involved, such as HSP70. However, by reconstituting the HRS complex in our Y2H system, and by using an autoactive full length MLA6, we provide evidence that MLA6 and SGT1 do directly interact.

Mutant MLA constructs, generated by examining correlations in amino acid sequence between groups either disrupted by the *Sgt1*$_{\Delta KL308\text{-}309}$ mutation or not, suggest that there are key positions in the LRR domain that are required for this interaction to occur. Moreover, the effect of mutant SGT1 constructs on interactions with MLA suggest that the exceptionally disordered nature of the SGT1 SGS domain may be important for its function by allowing it to adapt to the variety of protein interactors.

Though the *HvSgt1*$_{\Delta KL308\text{-}309}$ mutation disrupts the interaction between MLA and SGT1, the lethality or stunting that usually occurs when *Sgt1* is mutated or silenced is absent. This indicates that the abating still allows most cell processes to proceed as normal, while only disrupting the weakest interactors of *Sgt1*. This permits us to study *Sgt1* in disease resistance isolated from confounding factors. Reciprocal mutations made in other crops may answer similar questions regarding the requirement of *Sgt1* for NLRs to function. It is possible that *Sgt1* is required by every single CC-NLR, and thus is vitally important for studying further.

References

Ade, J., DeYoung, B.J., Golstein, C. and Innes, R.W. (2007) Indirect activation of a plant nucleotide binding site–leucine-rich repeat protein by a bacterial protease. *Proceedings of the National Academy of Sciences*, 104, 2531-2536.

Azevedo, C., Betsuyaku, S., Peart, J., Takahashi, A., Noël, L., Sadanandom, A., Casais, C., Parker, J. and Shirasu, K. (2006) Role of SGT1 in resistance protein accumulation in plant immunity. *The EMBO Journal*, 25, 2007-2016.

Azevedo, C., Sadanandom, A., Kitagawa, K., Freialdenhoven, A., Shirasu, K. and Schulze-Lefert, P. (2002) The RAR1 interactor SGT1, an essential component of R gene-triggered disease resistance. *Science*, 295, 2073-2076.

Bai, S., Liu, J., Chang, C., Zhang, L., Maekawa, T., Wang, Q., Xiao, W., Liu, Y., Chai, J., Takken, F.L., Schulze-Lefert, P. and Shen, Q.H. (2012) Structure-function analysis of barley NLR immune receptor MLA10 reveals its cell compartment specific activity in cell death and disease resistance. *PLoS Pathogens*, 8, e1002752.

Bentele, M., Lavrik, I., Ulrich, M., Stößer, S., Heermann, D.W., Kalthoff, H., Krammer, P.H. and Eils, R. (2004) Mathematical modeling reveals threshold mechanism in CD95-induced apoptosis. *Journal of Cell Biology*, 166, 839-851.

Bernoux, M., Burdett, H., Williams, S.J., Zhang, X., Chen, C., Newell, K., Lawrence, G.J., Kobe, B., Ellis, J.G., Anderson, P.A. and Dodds, P.N. (2016) Comparative analysis of the flax immune receptors L6 and L7 suggests an equilibrium-based switch activation model. *The Plant cell*, 28, 146-159.

Bhattarai, K.K., Li, Q., Liu, Y., Dinesh-Kumar, S.P. and Kaloshian, I. (2007) *Mi-1*-mediated pest resistance requires *Hsp90* and *Sgt1*. *Plant Physiology*, 144, 312-323.

Bieri, S., Mauch, S., Shen, Q.-H., Peart, J., Devoto, A., Casais, C., Ceron, F., Schulze, S., Steinbiss, H.-H., Shirasu, K. and Schulze-Lefert, P. (2004) RAR1 positively controls steady state levels of barley MLA resistance proteins and enables sufficient MLA6 accumulation for effective resistance. *The Plant Cell*, 16, 3480-3495.

Boter, M., Amigues, B., Peart, J., Breuer, C., Kadota, Y., Casais, C., Moore, G., Kleanthous, C., Ochsenbein, F., Shirasu, K. and Guerois, R. (2007) Structural and functional analysis of SGT1 reveals that its interaction with HSP90 is required for the accumulation of Rx, an R protein involved in plant immunity. *The Plant Cell*, 19, 3791-3804.

Bourmaud, A., Gallien, S. and Domon, B. (2016) Parallel reaction monitoring using quadrupole-Orbitrap mass spectrometer: Principle and applications. *PROTEOMICS*, 16, 2146-2159.

Burke, D., Dawson, D. and Stearns, T. (2000) Methods in Yeast Genetics: A Cold Spring Harbor Laboratory Course Manual (2000 Edition). *Plainview, NY: Cold Spring Harbor Laboratory Press.[Google Scholar]*.

Caldo, R.A., Nettleton, D. and Wise, R.P. (2004) Interaction-dependent gene expression in *Mla*-specified response to barley powdery mildew. *The Plant Cell*, 16, 2514-2528.

Carneiro, L.S., Martínez, L.C., Gonçalves, W.G., Santana, L.M. and Serrão, J.E. (2020) The fungicide iprodione affects midgut cells of non-target honey bee *Apis mellifera* workers. *Ecotoxicology and Environmental Safety*, 189, 109991.

Chang, C., Yu, D., Jiao, J., Jing, S., Schulze-Lefert, P. and Shen, Q.-H. (2013) Barley MLA immune receptors directly interfere with antagonistically acting transcription factors to initiate disease resistance signaling. *The Plant Cell*, 25, 1158-1173.

Chapman, A.V.E., Hunt, M., Surana, P., Velasquex-Zapata, V., Xu, w., Fuerst, G. and Wise, R.P. (2020) Disruption of immunity of barley to powdery mildew by a Lys-Leu in-frame deletion in the essential gene *Sgt1*. *GENETICS*, In press DOI: 10.1093/genetics/iyaa026.

Chen, J., Upadhyaya, N.M., Ortiz, D., Sperschneider, J., Li, F., Bouton, C., Breen, S., Dong, C., Xu, B., Zhang, X., Mago, R., Newell, K., Xia, X., Bernoux, M., Taylor, J.M., Steffenson, B., Jin, Y., Zhang, P., Kanyuka, K., Figueroa, M., Ellis, J.G., Park, R.F. and Dodds, P.N. (2017) Loss of *AvrSr50* by somatic exchange in stem rust leads to virulence for *Sr50* resistance in wheat. *Science*, 358, 1607-1610.

da Silva Correia, J., Miranda, Y., Leonard, N. and Ulevitch, R. (2007) SGT1 is essential for Nod1 activation. *PNAS*, 104, 6764-6769.

Draz, I.S., Esmail, S.M., Abou-Zeid, M.A.E.-H. and Essa, T.A.E.-M. (2019) Powdery mildew susceptibility of spring wheat cultivars as a major constraint on grain yield. *Annals of Agricultural Sciences*, 64, 39-45.

Dreze, M., Monachello, D., Lurin, C., Cusick, M.E., Hill, D.E., Vidal, M. and Braun, P. (2010) High-quality binary interactome mapping. In *Methods in Enzymology*: Academic Press, pp. 281-315.

Gallien, S., Duriez, E., Crone, C., Kellmann, M., Moehring, T. and Domon, B. (2012) Targeted proteomic quantification on quadrupole-orbitrap mass spectrometer. *Mol Cell Proteomics*, 11, 1709-1723.

Gietz, R.D. (2014) Yeast transformation by the LiAc/SS carrier DNA/PEG method. *Methods Mol Biol*, 1205, 1-12.

Godfrey, D., Zhang, Z., Saalbach, G. and Thordal-Christensen, H. (2009) A proteomics study of barley powdery mildew haustoria. *Proteomics*, 9, 3222-3232.

Graves, S., Piepho, H.-P., Selzer, L. and Dorai-Raj, S. (2019) multcompView: Visualizations of paired comparisons: R package version 0.1-8.

Halterman, D.A. and Wise, R.P. (2004) A single-amino acid substitution in the sixth leucine-rich repeat of barley MLA6 and MLA13 alleviates dependence on RAR1 for disease resistance signaling. *The Plant Journal*, 38, 215-226.

Helliwell, C. and Waterhouse, P. (2003) Constructs and methods for high-throughput gene silencing in plants. *Methods*, 30, 289-295.

Hothorn, T., Bretz, F. and Westfall, P. (2008) Simultaneous inference in general parametric models. *Biometrical Journal*, 50, 346-363.

Jaswal, R., Kiran, K., Rajarammohan, S., Dubey, H., Singh, P.K., Sharma, Y., Deshmukh, R., Sonah, H., Gupta, N. and Sharma, T.R. (2020) Effector biology of biotrophic plant fungal pathogens: Current advances and future prospects. *Microbiological Research*, 241, 126567.

Jorgensen, J.H. (1994) Genetics of powdery mildew resistance in barley. *Critical Reviews in Plant Science*, 13, 97-119.

Joseph, P.R.B., Sawant, K.V., Iwahara, J., Garofalo, R.P., Desai, U.R. and Rajarathnam, K. (2018) Lysines and Arginines play non-redundant roles in mediating chemokine-glycosaminoglycan interactions. *Scientific Reports*, 8, 12289.

Kadota, Y. and Shirasu, K. (2012) The HSP90 complex of plants. *Biochimica et Biophysica Acta*, 1823, 689-697.

Kadota, Y., Shirasu, K. and Guerois, R. (2010) NLR sensors meet at the SGT1–HSP90 crossroad. *Trends in Biochemical Sciences*, 35, 199-207.

Kitagawa, K., Skowyra, D., Elledge, S.J., Harper, J.W. and Hieter, P. (1999) SGT1 Encodes an essential component of the yeast kinetochore assembly pathway and a novel subunit of the SCF ubiquitin ligase complex. *Molecular Cell*, 4, 21-33.

Knebel, C., Heise, T., Zanger, U.M., Lampen, A., Marx-Stoelting, P. and Braeuning, A. (2019) The azole fungicide tebuconazole affects human *CYP1A1* and *CYP1A2* expression by an aryl hydrocarbon receptor-dependent pathway. *Food and Chemical Toxicology*, 123, 481-491.

Krattinger, S.G. and Keller, B. (2016) Molecular genetics and evolution of disease resistance in cereals. *New Phytologist*, 212, 320-332.

Kumar, S. and Nussinov, R. (2002) Close-range electrostatic interactions in proteins, pp. 604.

Lambertucci, S., Orman, K.M., Das Gupta, S., Fisher, J.P., Gazal, S., Williamson, R.J., Cramer, R. and Bindschedler, L.V. (2019) Analysis of barley leaf epidermis and extrahaustorial proteomes during powdery mildew infection reveals that the PR5 Thaumatin-Like Protein TLP5 is required for susceptibility towards *Blumeria graminis* f. sp. *hordei*. *Frontiers in Plant Science*, 10.

Lewis, J.D., Wu, R., Guttman, D.S. and Desveaux, D. (2010) Allele-specific virulence attenuation of the *Pseudomonas syringae* HopZ1a type III effector via the *Arabidopsis* ZAR1 resistance protein. *PLoS genetics*, 6, e1000894-e1000894.

Lo Presti, L., Lanver, D., Schweizer, G., Tanaka, S., Liang, L., Tollot, M., Zuccaro, A., Reissmann, S. and Kahmann, R. (2015) Fungal effectors and plant susceptibility. *Annu. Rev. Plant Biol.*, 66, 513-545.

Lu, X., Kracher, B., Saur, I.M.L., Bauer, S., Ellwood, S.R., Wise, R., Yaeno, T., Maekawa, T. and Schulze-Lefert, P. (2016) Allelic barley MLA immune receptors recognize sequence-unrelated avirulence effectors of the powdery mildew pathogen. *Proceedings of the National Academy of Sciences*, 113, E6486-E6495.

Lõoke, M., Kristjuhan, K. and Kristjuhan, A. (2011) Extraction of genomic DNA from yeasts for PCR-based applications. *BioTechniques*, 50, 325-328.

Maekawa, T., Cheng, W., Spiridon, L.N., Töller, A., Lukasik, E., Saijo, Y., Liu, P., Shen, Q.H., Micluta, M.A., Somssich, I.E., Takken, F.L.W., Petrescu, A.J., Chai, J. and Schulze-Lefert, P. (2011) Coiled-coil domain-dependent homodimerization of intracellular barley immune receptors defines a minimal functional module for triggering cell death. *Cell Host Microbe*, 9, 187-199.

Maekawa, T., Kracher, B., Vernaldi, S., Ver Loren van Themaat, E. and Schulze-Lefert, P. (2012) Conservation of NLR-triggered immunity across plant lineages. *PNAS*, 109, 20119-20123.

Marquenet, E. and Richet, E. (2007) How integration of positive and negative regulatory signals by a STAND signaling protein depends on ATP hydrolysis. *Molecular Cell*, 28, 187-199.

Martins, T., Maia, A.F., Steffensen, S. and Sunkel, C.E. (2009) Sgt1, a co-chaperone of Hsp90 stabilizes Polo and is required for centrosome organization. *The EMBO Journal*, 28, 234-247.

Meldau, S., Baldwin, I.T. and Wu, J. (2011) For security and stability: SGT1 in plant defense and development. *Plant Signaling & Behavior*, 6, 1479-1482.

Mestre, P. and Baulcombe, D.C. (2006) Elicitor-mediated oligomerization of the tobacco N disease resistance protein. *Plant Cell*, 18, 491-501.

Mikkelsen, M.D., Buron, L.D., Salomonsen, B., Olsen, C.E., Hansen, B.G., Mortensen, U.H. and Halkier, B.A. (2012) Microbial production of indolylglucosinolate through engineering of a multi-gene pathway in a versatile yeast expression platform. *Metabolic Engineering*, 14, 104-111.

Méchin, V., Thévenot, C., Le Guilloux, M., Prioul, J.L. and Damerval, C. (2007) Developmental analysis of maize endosperm proteome suggests a pivotal role for pyruvate orthophosphate dikinase. *Plant Physiol*, 143, 1203-1219.

Park, C.-J., Caddell, D. and Ronald, P. (2012) Protein phosphorylation in plant immunity: insights into the regulation of pattern recognition receptor-mediated signaling. *Frontiers in Plant Science*, 3.

Periyannan, S., Moore, J., Ayliffe, M., Bansal, U., Wang, X., Huang, L., Deal, K., Luo, M., Kong, X., Bariana, H., Mago, R., McIntosh, R., Dodds, P., Dvorak, J. and Lagudah, E. (2013) The gene *Sr33*, an ortholog of barley *Mla* genes, encodes resistance to wheat stem rust race Ug99. *Science*, 341, 786-788.

Peterson, A.C., Russell, J.D., Bailey, D.J., Westphall, M.S. and Coon, J.J. (2012) Parallel reaction monitoring for high resolution and high mass accuracy quantitative, targeted proteomics. *Molecular & Cellular Proteomics*, 11, 1475-1488.

Pinheiro, J., Bates, D., Debroy, S., Sarkar, D. and Team, R.C. (2020) nlme: Linear and nonlnear mixed effects models.

Pino, L.K., Searle, B.C., Bollinger, J.G., Nunn, B., MacLean, B. and MacCoss, M.J. (2020) The Skyline ecosystem: Informatics for quantitative mass spectrometry proteomics. *Mass Spectrom Rev*, 39, 229-244.

R Core Team (2019) R: A Language and Environment for Statistical Computing. Vienna, Austria: R Foundation for Statistical Computing.

Rauniyar, N. (2015) Parallel reaction monitoring: A targeted experiment performed using high resolution and high mass accuracy mass spectrometry. *International Journal of Molecular Sciences*, 16, 28566-28581.

Ridout, C.J., Skamnioti, P., Porritt, O., Sacristan, S., Jones, J.D.G. and Brown, J.K.M. (2006) Multiple avirulence paralogues in cereal powdery mildew fungi may contribute to parasite fitness and defeat of plant resistance. *The Plant Cell*, 18, 2402-2414.

Saur, I.M.L., Bauer, S., Kracher, B., Lu, X., Franzeskakis, L., Muller, M.C., Sabelleck, B., Kummel, F., Panstruga, R., Maekawa, T. and Schulze-Lefert, P. (2019) Multiple pairs of allelic MLA immune receptor-powdery mildew AVR_A effectors argue for a direct recognition mechanism. *eLife*, 8, e44471.

Savary, S., Willocquet, L., Pethybridge, S.J., Esker, P., McRoberts, N. and Nelson, A. (2019) The global burden of pathogens and pests on major food crops. *Nature Ecology & Evolution*, 3, 430-439.

Seeholzer, S., Tsuchimatsu, T., Jordan, T., Bieri, S., Pajonk, S., Yang, W., Jahoor, A., Shimizu, K.K., Keller, B. and Schulze-Lefert, P. (2010) Diversity at the *Mla* powdery mildew resistance locus from cultivated barley reveals sites of positive selection. *MPMI*, 23, 497-509.

Shen, Q.-H., Saijo, Y., Mauch, S., Biskup, C., Bieri, S., Keller, B., Seki, H., Ulker, B., Somssich, I.E. and Schulze-Lefert, P. (2007) Nuclear activity of MLA immune receptors links isolate-specific and basal disease-resistance responses. *Science*, 315, 1098-1103.

Shirasu, K. (2009) The HSP90-SGT1 chaperone complex for NLR immune sensors. *Annu. Rev. Plant Biol.*, 60, 139-164.

Siligardi, G., Zhang, M. and Prodromou, C. (2018) The stoichiometric interaction of the Hsp90-Sgt1-Rar1 complex by CD and SRCD spectroscopy. *Frontiers in Molecular Biosciences*, 4.

Sokalingam, S., Raghunathan, G., Soundrarajan, N. and Lee, S.-G. (2012) A Study on the Effect of Surface Lysine to Arginine Mutagenesis on Protein Stability and Structure Using Green Fluorescent Protein. *PLOS ONE*, 7, e40410.

Song, G., Hsu, P.Y. and Walley, J.W. (2018) Assessment and Refinement of Sample Preparation Methods for Deep and Quantitative Plant Proteome Profiling. *PROTEOMICS*, 18, 1800220.

Sun, Y., Zhu, Y.-X., Balint-Kurti, P.J. and Wang, G.-F. (2020) Fine-tuning immunity: Players and regulators for plant NLRs. *Trends in Plant Science*, 25, 695-713.

Tameling, W.I.L., Vossen, J.H., Albrecht, M., Lengauer, T., Berden, J.A., Haring, M.A., Cornelissen, B.J.C. and Takken, F.L.W. (2006) Mutations in the NB-ARC domain of I-2 that impair ATP hydrolysis cause autoactivation. *Plant Physiology*, 140, 1233-1245.

Taube, M., Pieńkowska, J.R., Jarmołowski, A., Kozak, M. and Silman, I. (2014) Low-resolution structure of the full-length barley (*Hordeum vulgare*) SGT1 protein in solution, obtained using small-angle X-ray scattering. *PLOS ONE*, 9, e93313.

Thao, N.P., Chen, L., Nakashima, A., Hara, S.-i., Umemura, K., Takahashi, A., Shirasu, K., Kawasaki, T. and Shimamoto, K. (2007) RAR1 and HSP90 form a complex with Rac/Rop GTPase and function in innate-immune responses in rice. *The Plant Cell*, 19, 4035-4045.

van Wersch, S., Tian, L., Hoy, R. and Li, X. (2020) Plant NLRs: The whistleblowers of plant immunity. *Plant Communications*, 1, 100016.

Wang, G.-F., Fan, R., Wang, X., Wang, D. and Zhang, X. (2015a) TaRAR1 and TaSGT1 associate with TaHSP90 to function in bread wheat (*Triticum aestivum* L.) seedling growth and stripe rust resistance. *Plant Molecular Biology*, 87, 577-589.

Wang, G.F., Ji, J., El-Kasmi, F., Dangl, J.L., Johal, G. and Balint-Kurti, P.J. (2015b) Molecular and functional analyses of a maize autoactive NB-LRR protein identify precise structural requirements for activity. *PLoS Pathogens*, 11, e1004674.

Wang, J., Hu, M., Wang, J., Qi, J., Han, Z., Wang, G., Qi, Y., Wang, H.-W., Zhou, J.-M. and Chai, J. (2019a) Reconstitution and structure of a plant NLR resistosome conferring immunity. *Science*, 364, eaav5870.

Wang, J., Wang, J., Hu, M., Wu, S., Qi, J., Wang, G., Han, Z., Qi, Y., Gao, N., Wang, H.-W., Zhou, J.-M. and Chai, J. (2019b) Ligand-triggered allosteric ADP release primes a plant NLR complex. *Science*, 364, eaav5868.

Wei, F., Wing, R.A. and Wise, R.P. (2002) Genome dynamics and evolution of the *Mla* (powdery mildew) resistance locus in barley. *Plant Cell*, 14, 1903-1917.

Wickham, H. (2016) *ggplot2: Elegant graphics for data analysis* New York: Springer-Verlag.

Williams, S.J., Sornaraj, P., deCourcy-Ireland, E., Menz, R.I., Kobe, B., Ellis, J.G., Dodds, P.N. and Anderson, P.A. (2011) An autoactive mutant of the M flax rust resistance protein has a preference for binding ATP, whereas wild-type M protein binds ADP. *Molecular Plant-Microbe Interactions*, 24, 897-906.

Yamaoka, N., Matsumoto, I. and Nishiguchi, M. (2006) The role of primary germ tubes (PGT) in the life cycle of *Blumeria graminis*: The stopping of PGT elongation is necessary for the triggering of appressorial germ tube (AGT) emergence. *Physiological and Molecular Plant Pathology*, 69, 153-159.

Yang, X., Yang, F., Wang, W., Lin, G., Hu, Z., Han, Z., Qi, Y., Zhang, L., Wang, J., Sui, S.-F. and Chai, J. (2018) Structural basis for specific flagellin recognition by the NLR protein NAIP5. *Cell Research*, 28, 35-47.

Yu, G., Xian, L., Sang, Y. and Macho, A.P. (2019) Cautionary notes on the use of *Agrobacterium*-mediated transient gene expression upon SGT1 silencing in *Nicotiana benthamiana*. *New Phytologist*, 222, 14-17.

Zhang, J., Coaker, G., Zhou, J.-M. and Dong, X. (2020) Plant immune mechanisms: from reductionistic to holistic points of view. *Molecular Plant*, 13, 1358-1378.

Appendix. Supplemental Tables and Figures

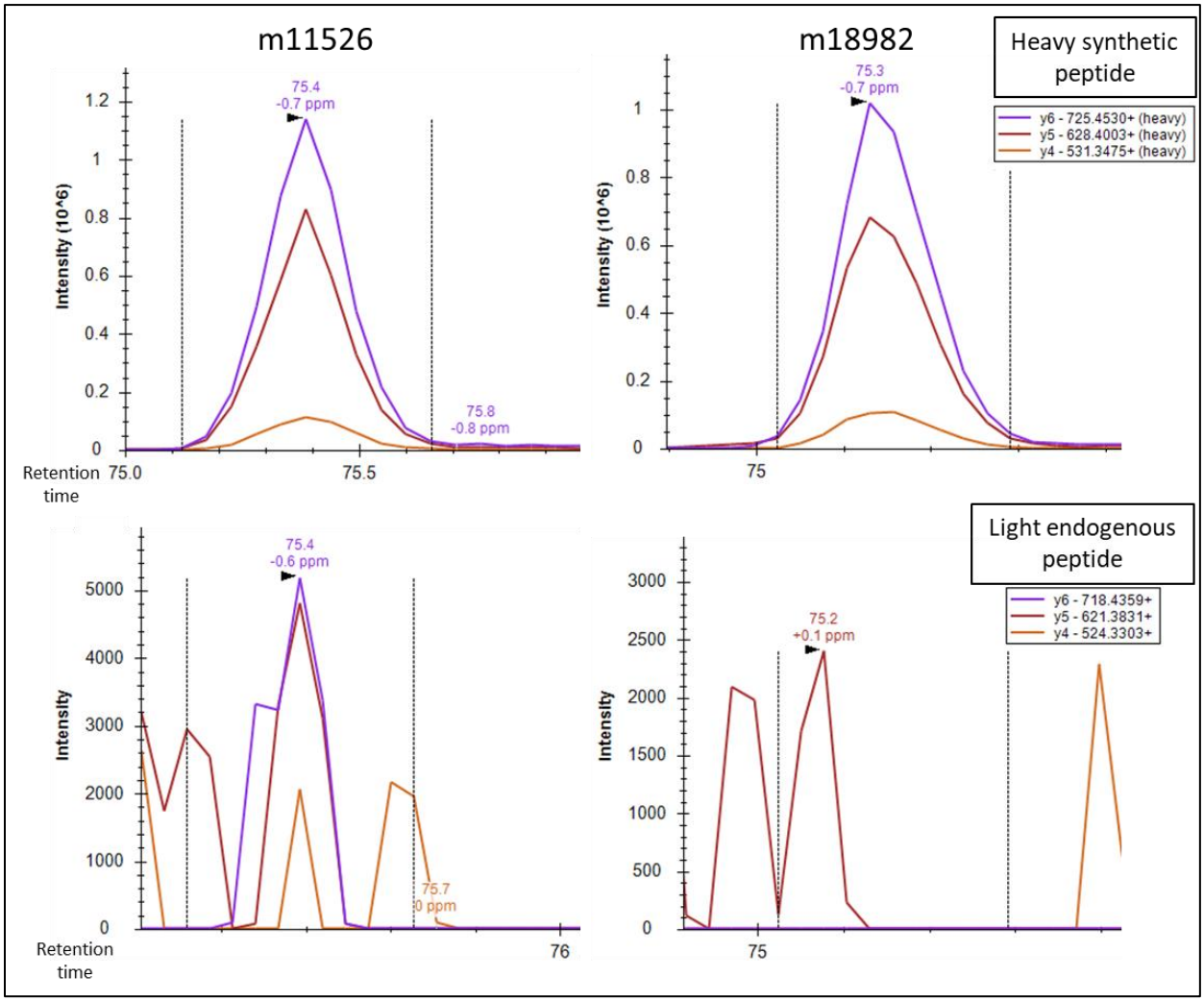

Figure 3-S1. Chromatograms of results for the MLA6 peptide WaVe in m11526 and m18982. Top = heavy synthetic peptide, bottom = light endogenous peptide, left = m11526 (*Mla6, Sgt1*$_{\Delta KL308\text{-}309}$), right = m18982 (*mla6, Sgt1*). Values above peaks indicate retention time (minutes) and mass error (ppm). Exported from Skyline.

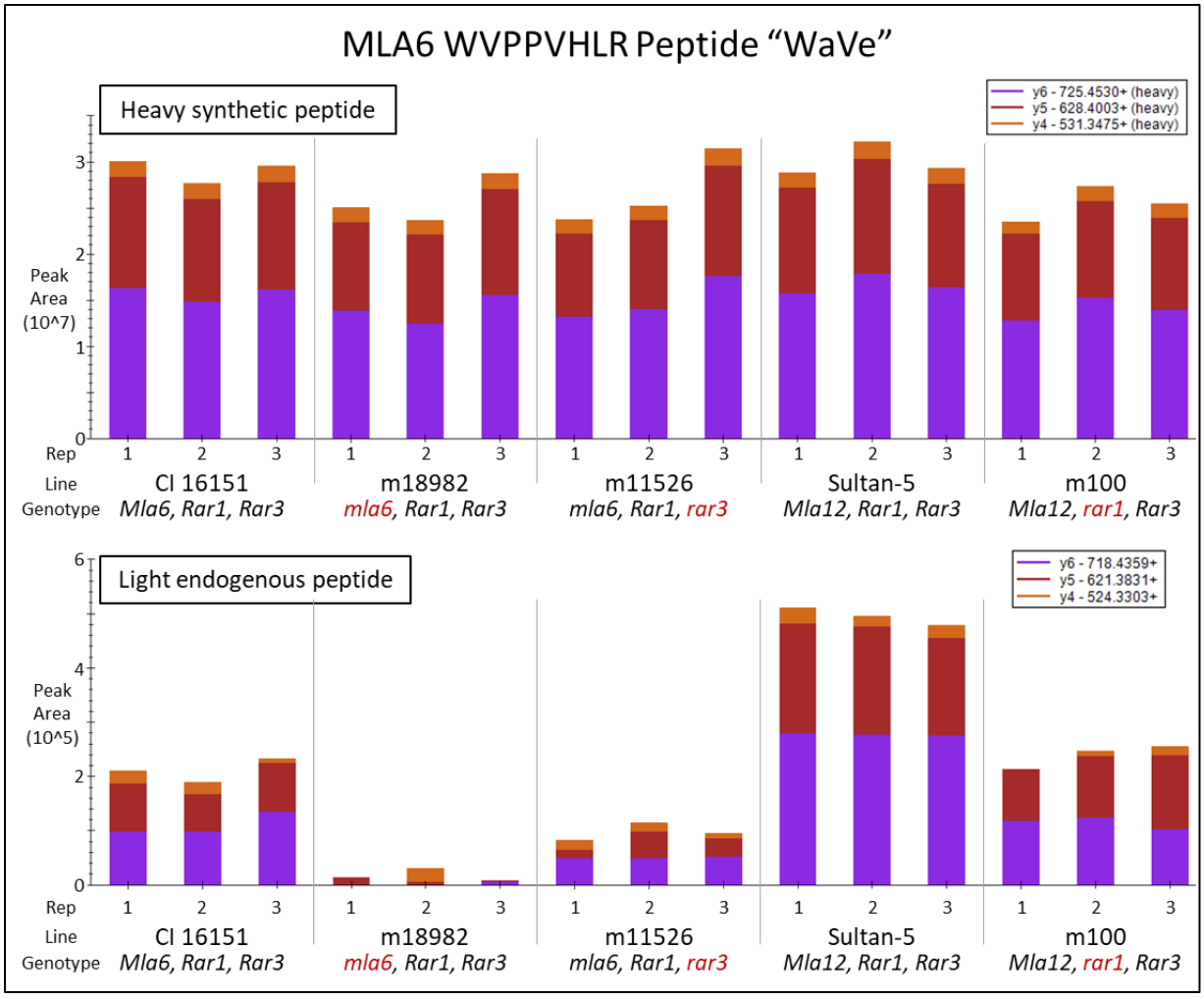

Figure 3-S2. Peak area of MLA6 peptide WaVe detected for each genotype. Top = heavy synthetic peptide, bottom = light endogenous peptide. Exported from Skyline.

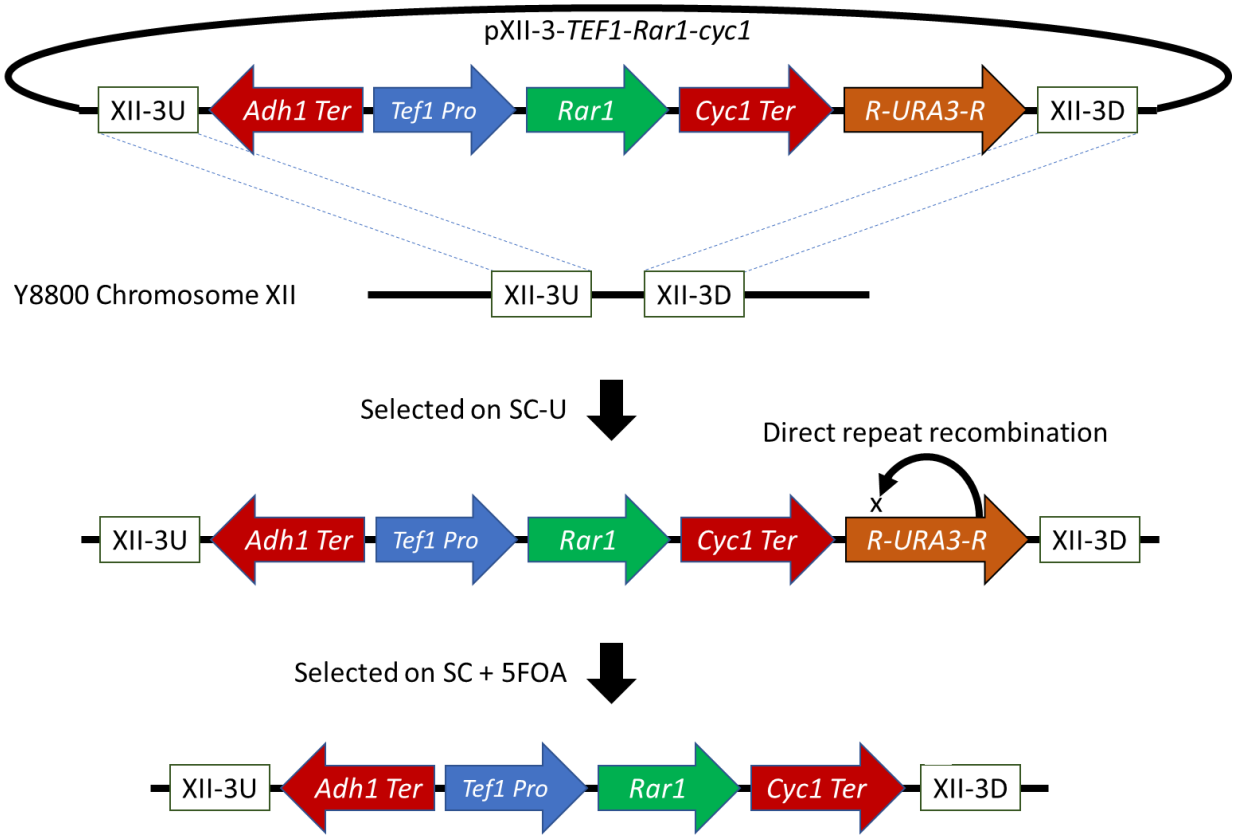

Figure 3-S3. Stable introgression of genes into yeast followed by marker recycling. Plasmid pXII-3-*TEF1-Rar1-cyc1* was generated by inserting the *TEF1* promoter amplified from Y8800 into plasmid pXII-3 according to (Mikkelsen *et al.*, 2012). An *AsiSi* restriction site was added to the end of the *TEF1* promoter that allowed for the restriction enzyme-based insertion of *HvRar1* to generate the final construct. pXII-3-*TEF1-Rar1-cyc1* was transformed into yeast strain Y8800 and selected on media lacking uracil (SC-U) for integration of the insert by homologous recombination. Colonies that grew on SC-U were then selected on SC + F-Fluoroorotic acid (5FOA) for excision of *Ura3* gene. This process was repeated with pXI-5-*TEF1-Hsp90-adh1* to generate the strain Y8800-*Rar1-cyc1-Hsp90-adh1*, aka Y-RcHa. Insertion was confirmed by PCR and sequencing from gDNA. Expression of *HvHsp90* was confirmed by detection of HSP90 peptides in Y-RcHa derived diploids.

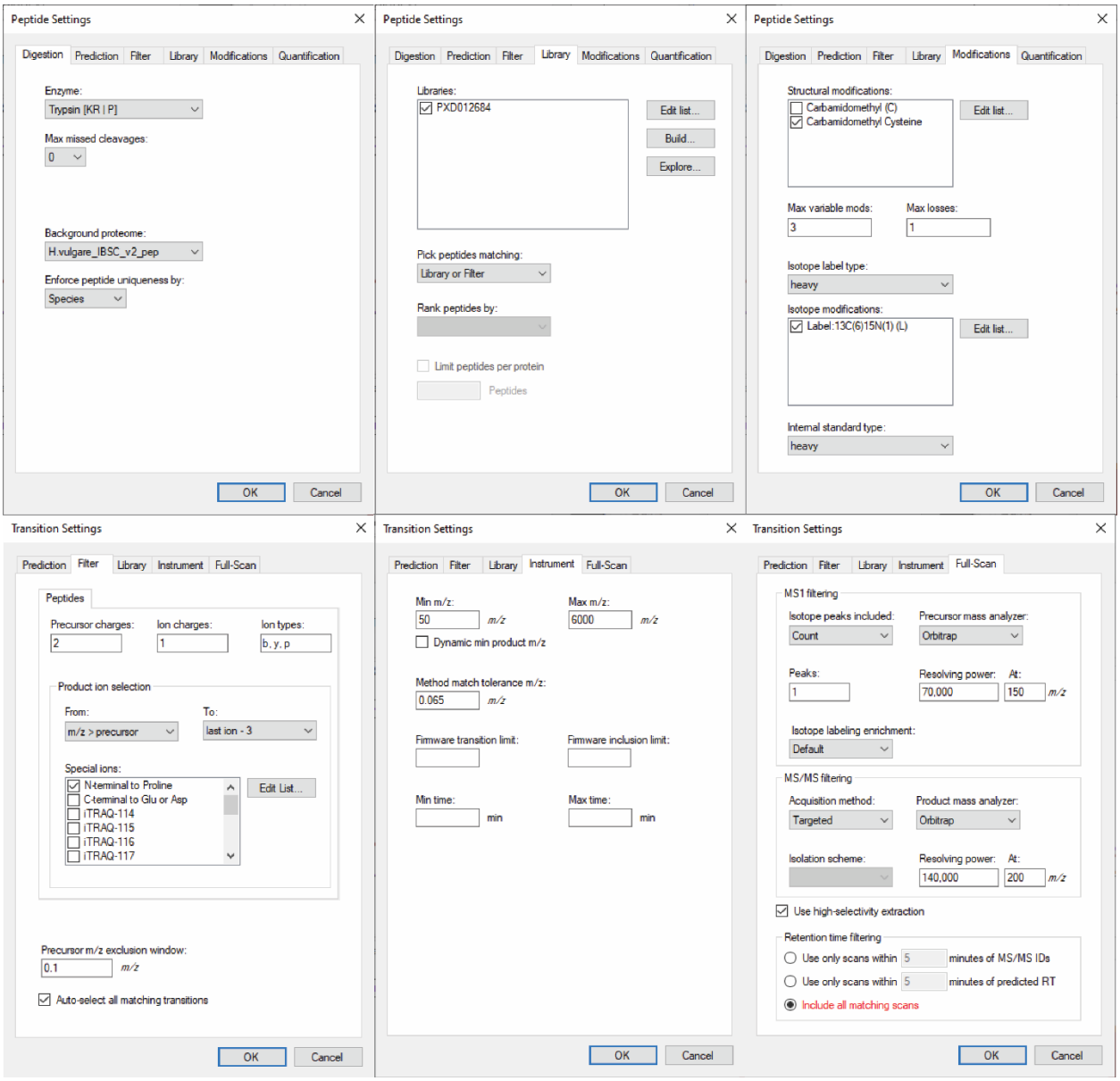

Figure 3-S4. Settings for Skyline program for PRM detection of MLA6 and SGT1 peptides. (Exported directly from Skyline).

Table 3-S1. Table displaying results of the ANOVA tests. SE = Standard error, DF = Degrees of freedom.

MLA6 WAVE ANOVA results

Contrast	Estimate	SE	DF	t.ratio	p.value
CI 16151 - m100	-0.00202	0.000551	8	-3.665	0.0376
CI 16151 - m11526	0.00368	0.000551	8	6.673	0.0011
CI 16151 - m18982	0.00667	0.000551	8	12.106	<.0001
CI 16151 - (Sultan-5)	-0.00966	0.000551	8	-17.54	<.0001
m100 - m11526	0.00569	0.000551	8	10.337	<.0001
m100 - m18982	0.00869	0.000551	8	15.77	<.0001
m100 - (Sultan-5)	-0.00764	0.000551	8	-13.876	<.0001
m11526 - m18982	0.00299	0.000551	8	5.433	0.0041
m11526 - (Sultan-5)	-0.01334	0.000551	8	-24.213	<.0001
m18982 - (Sultan-5)	-0.01633	0.000551	8	-29.646	<.0001

SGT1 DANK ANOVA results

Contrast	Estimate	SE	DF	t.ratio	p.value
CI 16151 - m100	-0.7302	0.361	8	-2.021	0.3366
CI 16151 - m11526	0.1403	0.361	8	0.388	0.9942
CI 16151 - m18982	-0.4215	0.361	8	-1.166	0.7693
CI 16151 - (Sultan-5)	0.0618	0.361	8	0.171	0.9998
m100 - m11526	0.8705	0.361	8	2.409	0.2063
m100 - m18982	0.3087	0.361	8	0.854	0.9057
m100 - (Sultan-5)	0.792	0.361	8	2.192	0.2727
m11526 - m18982	-0.5618	0.361	8	-1.555	0.5597
m11526 - (Sultan-5)	-0.0785	0.361	8	-0.217	0.9994
m18982 - (Sultan-5)	0.4833	0.361	8	1.338	0.6784

Table 3-S2. Primers used in this study.

Primer	Sequence (5' to 3')	Notes
HvHSP90 Start F	ATGGCGACGGAGACCGAGAC	
HvHSP90 Stop R	TTAGTCGACCTCCTCCATCTTG	
HvRar1 Start F	ATGTCGGCGGAGACGGAGA	
HvRar1 Stop R	TCACACAGCATCAGCATTGTGCC	
HvSGT1 Start F	ATGGCCGCCGCCGCC	
HvSGT1 Stop R	TAATACTCCCACTTCTTGAGCT	
Mla1 543 F	AATGAAGATCATCAAGCC	
Mla1 555 F	AAGAGTATGTCACGAGTGAGGT	
Mla1 562 F	TCAATTACTATCTTTCCATCTGCT	
Mla1 -797S F	CCGAGTTAATCCTCTCAGTGAAGGACGT	Deletion of 3bp between red bases
Mla1 -797S R	ACGTCCTTCACTGAGAGGATTAACTCGG	Deletion of 3bp between red bases
Mla1 D708E F	TGAGGGTGCTTGAGATTTGCTTCAG	Red indicates changed base
Mla1 D708E R	CTGAAGCAAATCTCAAGCACCCTCA	Red indicates changed base
Mla1 S798P F	TAATCCTCTCGCCAGTGAAGGACGT	Red indicates changed base
Mla1 S798P R	ACGTCCTTCACTGGCGAGAGGATTA	Red indicates changed base
Mla1 Stop R	TCAGTTCTCCTCCTCGTCCTCAC	
Mla6 543 F	AATGAAGATCATCAAGTCAGGCC	
Mla6 D502V F	TGCTTGCCGTGTACATGTTATGGTTCTGGACCTTA	Red indicates changed base
Mla6 D502V R	TAAGGTCCAGAACCATAACATGTACACGGCAAGCA	Red indicates changed base
Mla6 G721D F	AGTTTGGATTTGTATGAAGATTTCGTGAAGTCTCTTTGC	Red indicates changed base
Mla6 G721D R	GCAAAGAGACTTCACGAAATCTTCATACAAATCCAAACT	Red indicates changed base
Mla6 Start F	ATGGATATTGTCACCGGTGCCA	
Mla6 Stop R	AGGGCGAGGAGGAGAACTAA	
TEF1 End R	gaaagcatagcaatctaatctaaggcgatcgc	AsiSI restriction site on 3' end (red)
TEF1 Start F	catagcttcaaaatgtttctactcc	

CHAPTER 4. GENERAL CONCLUSION

In this dissertation, I identified and investigated a mutant gene that selectively disrupted effector-specific immunity of barley to the fungal pathogen *Blumeria graminis* f. sp. *hordei*. In Chapter 2, we utilized a fast-neutron mutagenesis screen of a resistant barley line to identify a susceptible mutant line, m11526. Through the use of classic genetic crosses, I showed that the susceptibility-causing mutation in m11526 impaired the function of *Mla6*, *Mla7*, and *Mla12*, but did not overtly affect the function of *Mla1*, *Mla9*, *Mla10*, or *Mla13*. To map the causal mutation, I performed bulk-segregant exome-capture of two F2 populations, which indicated that the mutation lay in a low-recombination region on chromosome 3H. I delineated the causal mutation using molecular markers on a large F2 mapping population, to an in-frame 6-bp deletion in the essential gene *Sgt1* that removed only the Lys and Leu amino acids, $Sgt1_{\Delta KL308\text{-}309}$. Though *Sgt1* is already known to function in the *Mla* pathway, the identification of a resistance-impaired *Sgt1* mutant without the lethality or stunted growth associated with genetic knock-outs or silencing is unprecedented in plants with only one copy of *Sgt1*. This suggested that the $Sgt1_{\Delta KL308\text{-}309}$ mutation represents a golden opportunity to reinvigorate research into *Sgt1* by separating disease resistance from other cellular functions.

In Chapter 3, to aid in the research of the $Sgt1_{\Delta KL308\text{-}309}$ mutation, I developed multiple innovations and utilized these to uncover new details in the intermolecular interactions between MLA and SGT1. Using a synthetic biology approach, I engineered a yeast strain from a Y2H system to stably express co-chaperones known to be required for the function of *Mla6 in-planta*, HvRAR1 and HvHSP90. I utilized this yeast strain, Y-RcHa (Y8800-XII-3-*Rar1*-*CYC1*-XI-5-

Hsp90-ADH1, pronounced “Y archer”), which facilitated the interaction between MLA1 and SGT1, to show that the *Sgt1*$_{\Delta KL308\text{-}309}$ interaction with MLA1 was weaker. Moreover, with site-directed mutagenesis I developed autoactive MLA6 constructs which lack the autoinhibition that has prevented the use of full-length MLA in previous Y2H studies. The autoactive MLA6 interacted with SGT1 when tested using Y-RcHa yeast, but no interaction was observed with the SGT1$_{\Delta KL308\text{-}309}$. As the function of *Mla6* is disrupted by the *Sgt1*$_{\Delta KL308\text{-}309}$ mutation, whereas *Mla1* is not, the mutation appears to disproportionately affect MLA variants with inherently weaker interactions with SGT1. If function of MLA is linked to the strength of the interaction with SGT1, then MLA alleles which have been considered not to require *Sgt1*, such as *Mla1*, may be those with a strong enough interaction to compensate for *Sgt1* silencing. Based on my findings, utilizing Y2H systems with integrated co-chaperones and autoactive NLR’s may uncover molecular mechanisms or interactors that were previously undetectable.

As SGT1 is involved in the stability of NLRs, I utilized parallel reaction monitoring (PRM) mass spectrometry (MS) to investigate whether the *Sgt1*$_{\Delta KL308\text{-}309}$ mutation affected the abundance of MLA. Standard data-dependent acquisition methods have previously been unable to detect MLA peptides in complex samples, perhaps due to their ephemeral nature. I adapted a PRM protocol to allow for the detection of MLA peptides and compare their abundances. Using this method, I showed that the abundance of MLA6 is significantly lower, but still detectable, in the *Sgt1*$_{\Delta KL308\text{-}309}$ mutant. The reduction was equitable to that previously observed in the *rar1* mutant line, m100. This suggests that the abundance of MLA6 in the m11526 is below a critical threshold required for effective resistance. Thus, PRM can be used

to detect and quantify low abundance endogenous NLRs *in-planta*, without the need for tags or antibodies.

To uncover specific molecular mechanisms behind their interactions, I used site-directed mutagenesis to generate specific MLA1, MLA6, and SGT1 mutant constructs and tested these in our Y2H system. I found that two specific sites in MLA1, when mutated to the MLA6 residues at the same aligned position, abolished interaction between MLA1 and SGT1. However, the reciprocal mutations did not confer an equal gain of interaction to MLA6. Moreover, I show that the $Sgt1_{\Delta KL308\text{-}309}$ mutation disrupts the interaction with MLA to a lesser degree than a double alanine or single arginine substitution at the same sites, which may indicate that the disorder of the SGS domain is paramount for its function. This correlated with a prominent lack of arginine in the SGS domain, despite the overabundance of other residues capable of forming intermolecular salt-bridges.

Combining my data, that MLA interacts more strongly with SGT1 when autoactivated, with recent observations that another CC-NLR interacted stronger with its effector when autoactivated, I propose a cyclical model of the MLA-HRS resistosome function and interactions. In this model, NLRs that spontaneously flit between active/ATP-bound and inactive/ADP-bound conformations will competitively dock with the HRS, and eventually undock in an uninfected situation as they hydrolyze their ATP. However, if the cognate effector of the NLR is present, interaction between the effector and the NLR LRR domain will inhibit hydrolysis. This locks the NLR into the active, docked conformation, providing opportunity for a matching second NLR to dock with the HRS and be stabilized. These two NLRs will dimerize their CC domains and initiate defense signaling.

Future Directions

My work herein illustrates that the role of SGT1 in MLA-dependent disease resistance may be more complicated than previously thought. To disseminate further the role of SGT1 with NLRs, future work could include mimicking the *Sgt1*$_{\Delta KL308\text{-}309}$ mutation in other model plant systems via CRISPR mutagenesis, to test whether it inhibits the function of other NLRs. This would determine if SGT1$_{KL308\text{-}309}$ represents a unique MLA-interaction site, one shared by a subset of NLRs, or common to all.

Our data suggests that there is more than a single interaction site between SGT1 and MLA. Combining a quantitative system to measure the interaction between SGT1, NLRs, and their mutants, it would be possible to determine the interaction strength of each NLR with SGT1. Then, this data could be correlated with resultant NLR protein abundance, and their capability for conferring effective resistance, to determine the functional threshold of each NLR. This could be used to determine key sites on NLRs and SGT1 that improve or weaken their interactions. Extrapolating these results, the relative interaction strength of NLRs could be predicted, and therefore their requirement for certain co-chaperones. Considering the capability of the SGT1 SGS domain to interact with divergent LRR domains, mapping sites of interaction for each NLR may determine if the SGS interacts with common LRR features. However, it may instead utilize its inherent disorder to contort its multiple potential interaction sites into a conformation unique to each LRR ligand.

As no single MLA6 mutant was conferred MLA1-equivilent interaction with SGT1, it would be beneficial to test double, or even triple mutants for their strength of interaction. Moreover, MLA$_{D721}$, that confers *Rar1*-independence, could be combined with other mutations

we generated to test our hypothesis that it improves the interaction with SGT1 sufficiently to compensate for loss of RAR1. Additionally, interaction tests that had been previously performed with single domains of NLRs, due to autoinhibition, could be replaced by, or supplemented with, tests with autoactive full-length versions. This may reveal simultaneous interactions with multiple NLR domains or complexes that previously went unnoticed.

Two sites in MLA1 destroyed the interaction with SGT1 when they were mutated to the equivalent MLA6 residues. As both of these residues in MLA1 were serine, it is possible that their function is linked to their phosphorylation capability, though no phosphorylation of CC-NLRs has been published as of yet. Therefore, mutants could be generated with residues at these sites that mimicked a phosphorylated serine, also known as phosphomimetic residues, such as aspartate or glutamate. If these mutants displayed loss-of-function, then this would indicate that the function of these particular serine residues was not associated with phosphorylation.

The involvement of the HRS complex in disease resistance makes it a target that is too good for pathogens to pass up. Recent work has identified multiple pathogen effectors that subvert host defenses by targeting HSP90 and SGT1 specifically, and we can expect many more to be discovered. Uncovering these mechanisms may allow for us to engineer NLRs that are able to outcompete effectors for the same sites. Additionally, it could be possible to engineer SGT1 that lack effector interaction sites but maintain NLR interaction sites, or design decoy SGT1-NLR constructs that specifically keep these effector interaction sites. Understanding the complex interactions between the HRS and NLRs is paramount if we are to be prepared for the next disastrous crop pathogen, and may even provide the key to those we already face.